Master's thesis

NTNU
Norwegian University of Science and Technology
Faculty of Medicine and Health Sciences
Department of Clinical and Molecular Medicine

Ulrik Horn

Investigating iPSC derived macrophages as a model to study Mtb infection compared to alveolar macrophages, monocyte derived macrophages and THP-1 macrophages

Master's thesis in Molecular Medicine
Supervisor: Yashwanth Subbannayya
Co-supervisor: Marit Bugge
June 2022

NTNU
Norwegian University of Science and Technology

Ulrik Horn

Investigating iPSC derived macrophages as a model to study Mtb infection compared to alveolar macrophages, monocyte derived macrophages and THP-1 macrophages

Master's thesis in Molecular Medicine
Supervisor: Yashwanth Subbannayya
Co-supervisor: Marit Bugge
June 2022

Norwegian University of Science and Technology
Faculty of Medicine and Health Sciences
Department of Clinical and Molecular Medicine

NTNU
Norwegian University of
Science and Technology

Abstract

Mycobacterium tuberculosis (Mtb) remains a major public health issue for a large part of the developing world, causing more than 1.5 million deaths annually. However, many aspects of the host pathogen interactions remain elusive and poorly understood. This is partially due to the pathogen's relationship with the alveolar macrophage, which provides an early replicative niche, allowing immune evasion and the establishment of latent disease which is believed to affect a quarter of the world's population today. The unique characteristics of the alveolar macrophage and milieu in which it is specific for, hampers our understanding of the early interactions as *in vitro* models of this environment are difficult to simulate. However, recent advances in stem cell based technologies are providing a range of new cell types for research purposes that can theoretically adopt any cell fate, including the elusive alveolar macrophage. iPSC derived macrophages (iMAC) have recently been applied to tuberculosis related research, however, their Mtb induced immune response and potential role as a model cell line for alveolar macrophages has not been evaluated in house. Therefore, this thesis has compared iMACs with alveolar macrophages, monocyte derived macrophages and the established TB model cell line, THP1 macrophages, to characterize their role as a tool for tuberculosis research. To provide a broad overview of the Mtb induced immune responses from all four macrophage types, mRNA sequencing was performed to compare the gene expression of untreated and Mtb treated cells. mRNA sequencing is an effective tool for an initial exploration and provides data on a range of biological processes, which is useful when trying to establish an overview of a cell's immune response.

The data analyzed in this thesis shows that Mtb induced changes in the gene expression of iMACs is highly comparable to AMs and MDMs in aspects such as the inflammatory response, receptor expression and antigen presentation processes. Several key differences are also observed, including a much stronger type 1 interferon response and in the expression of proteins that may affect the cell fate of T-cells interacting with iMACs. Although MDMs display a closer relationship with AMs, iMACs offer advantages such as homogeneity, reproducibility and ease of manipulation, previously only offered by other secondary cell lines such as THP1. Furthermore, this thesis provides evidence that iMACs are better suited for AM (and MDM) emulation than THP1 cells which, although a well-established cell type for tuberculosis research, present themselves as an outlier when compared to the other cells.

Although, a limited number of specific conclusions can be drawn from mRNA expression data, the observations made in this thesis serve as an initial guide for researchers at CEMIR in determining the specific applications of iMACs. Furthermore, the data highlights characteristics that may affect observations in future iMAC based experiments. Hopefully, this thesis can contribute to further improvements aimed at making iMACs an accurate model cell line, a much-needed asset in the field of tuberculosis research.

Sammendrag

Mycobacterium tuberculosis (Mtb) er fortsatt et omfattende folkehelseproblem for en stor del av verdens utviklingsland, og forårsaker mer enn 1,5 millioner dødsfall årlig. Imidlertid forblir mange aspekter av interaksjonene i vertspatogenet flyktige og vanskelige å forstå. Dette er delvis på grunn av patogenets relasjon til den alveolære makrofagen, som gir en tidlig replikativ nisje. Dette legger til rette for immununnvikelse og etablering av den latente sykdommen som antas å påvirke en fjerdedel av dagens verdensbefolkning. De unike egenskapene til den alveolære makrofagen og miljøet den er spesifikk for, hemmer vår forståelse av de tidlige interaksjonene ettersom in vitro-modeller av dette miljøet er vanskelige å simulere. Nyere fremskritt innen stamcellebaserte teknologier gir imidlertid en rekke nye celletyper for forskningsformål som, i teorien, kan imitere enhver celleskjebne, inkludert den flyktige alveolære makrofagen. iPSC-avledede makrofager (iMAC) har nylig blitt brukt til tuberkuloserelatert forskning, men deres Mtb-induserte immunrespons og potensielle rolle som en modellcellelinje for alveolære makrofager har ikke blitt evaluert. Derfor har denne oppgaven sammenlignet iMAC-er med alveolære makrofager, monocyttavledede makrofager og den etablerte TB- modellcellelinjen, THP1-makrofager, for å analysere deres egnethet som et verktøy for tuberkuloseforskning. For å gi en bred oversikt over de Mtb-induserte immunresponsene, ble mRNA-sekvensering utført for å sammenligne genuttrykket til ubehandlede og Mtb-behandlede celler. mRNA-sekvensering er et effektivt verktøy for en innledende granskning og gir data om en rekke biologiske prosesser. Dette er nyttig når man prøver å etablere oversikt over en celles immunrespons.

Dataene som er analysert i denne oppgaven viser at Mtb-induserte endringer i genuttrykket til iMAC-er er svært sammenlignbare med AM-er og MDM-er i aspekter som inflammatorisk respons, reseptoruttrykk og antigenpresentasjonsprosesser. Flere viktige forskjeller er også observert, inkludert en mye sterkere type 1 interferonrespons og i uttrykket av proteiner som kan påvirke celleskjebnen til T-celler som samhandler med iMAC-er. Selv om MDM-er viser et nærmere forhold til AM-er, har iMAC-er fordeler som homogenitet, reproduserbarhet og enkel manipulering, tidligere bare funnet i andre sekundære cellelinjer som THP1. Videre viser denne oppgaven at iMAC-er er bedre egnet for AM- (og MDM)-emulering enn THP1-celler, som, selv om de er en veletablert celletype for tuberkuloseforskning, viser seg som en avviker sammenlignet med de andre cellene.

Selv om det kan trekkes en begrenset mengde spesifikke konklusjoner fra mRNA-uttrykksdata, tjener observasjonene som er gjort i denne oppgaven som en guide for forskere i å bestemme de spesifikke anvendelsene av iMAC-er. Videre fremhever dataene egenskaper som kan påvirke observasjoner i fremtidige iMAC-baserte eksperimenter. Forhåpentligvis kan denne oppgaven bidra til ytterligere forbedringer rettet mot å gjøre iMAC-er til en nøyaktig modellcellelinje, en sårt tiltrengt ressurs innen tuberkuloseforskning.

Preface

This master thesis was written in partnership with the Molecular Mechanisms of Mycobacterial and Viral Infections research group at the Centre of Molecular Inflammation Research (CEMIR), Faculty of Medicine and Health Sciences, at the Norwegian University of Science and Technology (NTNU).

When I started my master's degree, I elected not to choose a thesis project from the list we were handed, rather seeking out my own project as I wanted to work with bioinformatics and preferably tuberculosis. In a stroke of luck, I met Trude Flo who proposed a project that covered both my desired topics to which I am very grateful. However, during the long and arduous journey that is writing a master thesis I have grown to understand that in my naiveté I greatly overestimated my skills in method development as well as immunological and bioinformatic understanding. I now have a greater respect for the work that goes into planning and executing a research project. Although I sometimes longed for a more structured and traditional master thesis project where I could work directly beneath a supervisor for whom I generated results, I would not alter my decision to seek out my own project. Through my many mistakes, I have learned much about bioinformatics, immunology, and not least, how little I really know.

I would like to thank Marit, Yashwanth and Tuva for their support, feedback and proofreading. I would also like to thank Trude Flo and the Mycovir research group for challenging me with difficult questions that helped me find the right direction of this thesis.

Ulrik Horn

Table of contents

Figures

Tables

Acronyms

AIM2	Absent in myeloma 2
AM	Alveolar Macrophages
AMP	Adenosine monophosphate
ALR	AIM2- like receptor
ASC	Apoptosis-associated Speck like protein
BALF	Bronchoalveolar Lavage Fluid
BCG	Bacillus Calmette-Guérin
bp	Base pair
BMP-4	Bone morphogenic protein 4
cAIP1/2	Cellular inhibitor of apoptosis
CARD9	Caspase Recruitment Domain
CASP	Caspase
cFLIP	CASP8 And FADD Like Apoptosis Regulator
cGAS	Cyclic GMP-AMP synthase
CISH	Cytokine Inducible SH2 Containing Protein
CIITA	Class II Major Histocompatibility Complex Transactivator
CLR	C-Type Lectin Receptor
CD	Cluster of differentiation
CPM	Counts per million
CO2	Carbon dioxide
CR	Complement receptor
CSF2	Colony stimulating factor 2
CTSS	Cathepsin S
CXCL	C-X-C motif chemokine ligand
DAMP	Damage Associated Molecular Pattern
DE	Differentially Expressed
DMSO	Dimethyl sulfoxide
DNA	Deoxyribonucleic Acid
DPBS	Dulbecco’s Phosphate Buffered Saline
EB	Embryoid Body
FADD	FAS associated death domain
FCS	Fetal Calf Serum
GFC	Genomics Core Facility
GM-CSF	Granulocyte-macrophage colony-stimulating factor
GO	Gene Ontology
GPX4	Glutathione Peroxidase-4
GS	Gene Significance
GSS	GSH Synthase
GSDMD	Gasdermin D
GSH	Glutathione
HBSS	Hank's Balanced Salt Solution
HIV	Human Immunodeficiency Virus

IDO1	Indoleamine 2,3-Dioxygenase 1
IFN	Interferon
IFNAR	Interferon-alpha receptor
IL	Interleukin
iMAC	Induced pluripotent stem cell derived macrophage
iMos	Monocyte-like cells
iPSC	Induced pluripotent stem cell
IRAK	Interleukin 1 Receptor Associated Kinase
K+	Potassium ion
KEGG	Kyoto Encyclopedia of Genes and Genomes
LDH	Lactate dehydrogenase
LPS	Lipopolysaccharide
LXR	Liver X receptor
M-CSF	Macrophage colony-stimulating factor
M1	Classically activated macrophages
M2	Alternately activated macrophages
MDM	Monocyte derived macrophage
MDR	Multi-drug resistant
MHC	Major histocompatibility complex
MLKL	Mixed Lineage Kinase Domain Like Pseudokinase
MOI	Mixed Lineage Kinase Domain Like Pseudokinase
mRNA	Messenger Ribonucleic Acid
MS	Mass spectrometry
Mtb	Mycobacterium tuberculosis
MYD88	Myeloid Differentiation Primary Response Gene 88
NLRP3	Nucleotide-Binding Oligomerization Domain, Leucine Rich Repeat And Pyrin Domain Containing 3
NFkB	Nuclear factor kappa B
NOD	nucleotide-binding oligomerization
OADC	Oleic Albumin Dextrose Catalase
P/S	Penicillin-Streptomycin
PAMP	Pathogen associated molecular pattern
PBMC	Peripheral blood mononuclear cell
PBS	Phosphate buffered saline
PCA	Principle component analysis
PCR	Polymerase Chain Reaction
PEG	Polyethylene Glycol
PMA	Phorbol Myristate Acetate
PRR	Patter recognition receptor
QC	Quality control
RIPK	Receptor Interacting Protein kinase
RIN	RNA Integrity Number
RNA	Ribonucleic acid
RNI	Reactive nitrogen species
ROS	Reactive oxygenated species
RT-PCR	Reverse transcription PCR

RPMI	Roswell Park Memorial Institute Medium
RSL-3	RAS-selective lethal 3
SDEG	Significantly differentially expressed gene
SH2	Src Homology 2
SOCS	Suppressor of cytokine signaling
STAT	Signal transducer and activator of transcription
STING	Stimulator of interferon genes
TB	Tuberculosis
TGFB	Transforming growth factor beta
Th	T-helper
TLR	Toll-like receptor
TMM	Trimmed Mean of M
TNF	Tumor necrosis factor
TNFR	Tumor necrosis factor receptor
TRADD	TNFR associated death domain
TRAF	TNFR associated factor
V-AT-Pase	Vacuolar-type ATPase
VEGF	Vascular endothelial growth factor
WGCNA	Weighted gene correlation network analysis
XDR	Extensively drug-resistant
ZBP	Z-DNA Binding Protein 1

1 Introduction

1.1 Tuberculosis

Mycobacterium tuberculosis (Mtb) one of the major human pathogens that have plagued humanity for thousands of years. Even with the development of antibiotics, Mtb still causes 1.5 million deaths annually, making it one of the leading causes of death from a single infectious agent, only behind SARS-CoV-2 [3]. Today the burden of tuberculosis (TB) falls primarily on the poor as the 30 countries that contribute to more than 80% of cases are almost exclusively located in low- to middle-income countries in Asia and Africa [3]. The WHO estimates that around a quarter of the world's population is currently infected with Mtb. However, only around 5-10% of these will develop active tuberculosis during their lifetime. Mtb transmits from person to person via inhaled droplets but can cause disease in a range of organs (extrapulmonary TB) in addition to the lungs (pulmonary TB). Once inhaled, the aerosolized particles deposit the bacteria in the respiratory tract where they can infect a number of cell types in the upper and lower respiratory tract such as neutrophils, endothelial cells and macrophages [4]. Most Mtb are deposited in the lower respiratory alveoli where they encounter alveolar endothelial cells, dendritic cells and alveolar macrophages (AM). AMs play a key role in TB pathogeneses as they are among the first cells to be infected and provide a reservoir for bacterial replication [4]. Usually, the immune system effectively contains the bacteria in the alveoli and surrounding tissue, by forming a granuloma around the infected cells, preventing dissemination and progression to active disease [5]. However, the bacteria are not cleared and are rather pushed into a dormant state remaining in the granuloma, possibly for the rest of the host's life as a latent tuberculosis infection [6]. The state of the bacteria inside the granuloma, as well as the factors that lead to the reactivation of TB are poorly understood, but it is generally accepted that immunosuppression as a result of undernutrition, alcohol abuse, diabetes and secondary infections such as human immunodeficiency virus (HIV) are contributing factors [7].

Active TB can be diagnosed in several ways such as microscopy of lung sputum, chest X-ray and polymerase chain reaction (PCR) techniques. Microscopy and x-ray are most widespread in lower-income countries; however, the sensitivity of microscopy is highly variable (20-80%) [8] and x-ray alone cannot differentiate between active and latent TB [9]. Further exacerbating the skewed burden of TB is the early detection of drug-resistant Mtb offered by PCR-based diagnostic techniques [9] that are unavailable in rural areas and low-income countries. The emergence of multi-drug resistant (MDR) and extensively drug-resistant (XDR) Mtb is a major public health concern that is increasing globally [10,11]. The increase of drug resistance in Mtb is perpetuated by factors such as poor adherence to the long treatment regiment (>9 months) [12], the length of which only increases with mycobacterial resistance [10].

The obvious solution to drug resistance is vaccination, however, the efficacy of the Bacillus Calmette-Guérin (BCG) vaccine, being the only approved TB vaccine, is varies greatly, showing either no protection or a protective rate of up to 80% [13]. This is a major area of research and the M72/AS01E subunit vaccine is currently finishing the phase 2 trials, which indicate a protective efficacy of 54% [14].

1.2 The Alveolar Macrophage

AMs play a major role in tuberculosis induced activation of both innate and adaptive immune responses. Mtb has been shown to be unable to establish an effective infection in mice lacking AMs [15], highlighting the importance of understanding the AM-Mtb interactions. Due to the difficulties associated with human AMs acquisition, other more easily accessible macrophages such as monocyte-derived macrophages (MDM) and THP-1 macrophages as well as murine AMs have been used to understand the complex interactions between the macrophage and pathogen. However, AMs represent a type of macrophage that does not fit into the commonly used categories of classically activated (M1) and alternately activated (M2) macrophages as they display markers found on both phenotypes [16,17]. M1 and M2 can be characterized as pro-inflammatory and regenerative macrophages respectively, however, AM show a complex balance of immunoregulatory and inflammatory processes as well as receptor expression seen in both macrophage phenotypes (see Figure 1-1).

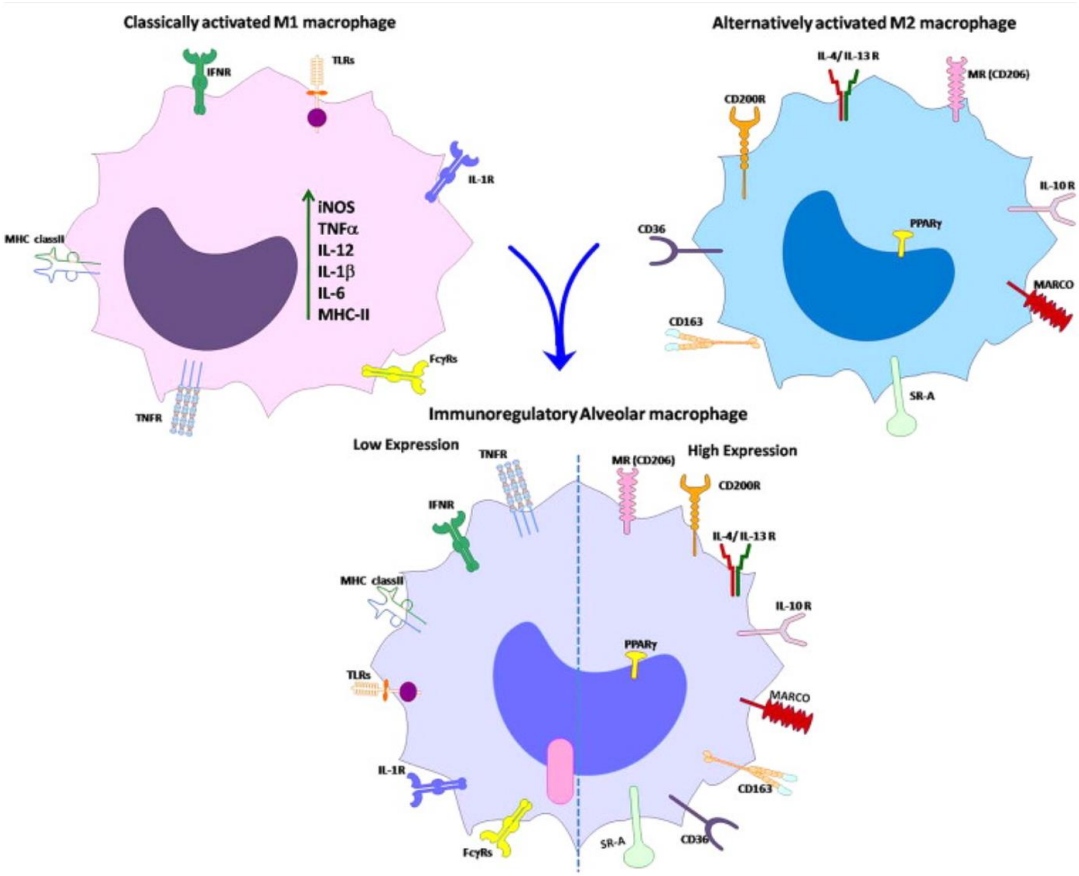

Figure 1-1. Comparison of classically alternatively and alveolar macrophages. The pattern recognition receptors of classically and alternatively activated macrophages as well as alveolar macrophages are visualized and compared based on their relative expression. The figure is adapted from [17].

MDMs from the blood stream are differentiated into a M1 or M2 polarization based on a cocktail of cytokines, interferons (IFN) and colony-stimulating factors (CSF) at the site of infection [18,19]. In contrast, AMs are embryonically derived and therefore do not have a monocyte intermediary stage, which likely contributes to their unorthodox characteristics [20]. Studies have shown that AMs are kept in a quiescent state, displaying poor phagocytic properties and producing little pro-inflammatory cytokines to prevent inflammatory responses against the foreign antigens they are constantly exposed to from the air we

breathe [21]. The anti-inflammatory state is perpetuated through close adherence to alveolar epithelial cells that express integrin beta 6, a surface receptor that activates AM secreted transforming growth factor (TGFB), an anti-inflammatory growth factor that suppresses phagocytosis and cytokine production. Once AM toll-like receptors (TLR) are activated, the adherence is lost, and TGFB is no longer activated, allowing the AMs to become more active and pro-inflammatory [22]. This close interaction between the cells of the alveoli is one of the factors that makes AMs unique and consequently difficult to study in vitro.

1.2.1 The macrophage inflammatory response to Mtb

Mycobacterial antigens are recognized by macrophage surface receptors such as Fcγ receptors, complement receptors (CR) [23], TLR2/4 and several C-type lectins (CLR) such as DC-SIGN, dectin-1, mannose receptors and mincle [24], leading to the phagocytosis of the bacteria and activation of inflammatory responses.

Once inside the cell, bacterial products can also be recognized by cytosolic receptors such as TLR9, nucleotide-binding oligomerization domain containing 2 (NOD2) and NOD-, LRR- and pyrin domain-containing protein 3 (NLRP3). The wide range of receptors that recognize Mtb indicates redundancy and studies with TLR and CLR deficient mice show no change in Mtb lethality, while the deletion of MYD88 and CARD9 receptor adaptor molecules resulted in accelerated host death [25,26].

TLR2 has been shown to be one of the central pattern recognition receptors (PRR) responsible for inducing an early inflammatory response and activating pathways that are critical in controlling the Mtb infection [27]. TLR2, together with the adaptor protein MYD88, activates the NFkB cascade leading to the expression and secretion of tumor necrosis factor (TNF) -alpha, interleukin (IL)-1B and IFN-gamma, all central pro-inflammatory mediators in tuberculosis [28]. TNF-alpha plays a major role in the recruitment and activation of lymphocytes, inducing the production of reactive nitrogen species (RNI) [29] as well as the formation of the granuloma [30]. TNF-alpha and IFN-gamma work synergistically to activate macrophages in a paracrine and autocrine manner, increasing their capability to phagocytose and kill Mtb, as well as stimulating apoptosis, depriving the bacteria of their replicative niche [31]. IFN-gamma also stimulates Major histocompatibility complex (MHC) class 1 and 2 antigen presentation in infected cells, and is therefore a critical factor in T-cell activation promoting a T-helper (Th) 1 differentiation of naïve CD4+ lymphocytes [32]. Macrophage activity is also regulated by IL-1B, which has been shown to induce the production of nitric oxide, which has anti-mycobacterial properties [33] as well as promoting phagosome maturation [30].

However, AMs also suppress the inflammatory response to TB by decreasing antigen presentation, limiting the production of oxidants, and downregulating inflammatory cytokines. These functions are mediated by the release of anti-inflammatory cytokines such as IL-10, TGFB and type 1 interferon, regulatory molecules like interleukin 1 Receptor Associated Kinase 3 (IRAK-M), and suppressor of cytokine signaling (SOCS) proteins as well as transcription factors like PARPy and liver X receptor (LXR) [17,28].

Suppression of inflammatory responses can be triggered by several receptors. Bacterial entry through the mannose receptor (MR) has been shown to decrease the fusion of lysosomes to the phagosome and is therefore vital for the Mtb survival inside the cell [34]. Furthermore, activation of the CD206 leads to the increased expression of PARPy, a transcriptional regulator that has anti-inflammatory properties, likely inhibiting the NFkB pathway and subsequently suppressing the production of TNF, IL-6 and IL-1B [17,35].

IL-10 is one of the major immunoregulatory cytokines expressed by AMs in response to Mtb and has been shown to inhibit CD4+ T-cell IFN-gamma production and proliferation [36,37], phagosome maturation [38] as well as nuclear translocation and DNA binding activity of NFkB [39]. The role of IL-10 and the factors responsible for balancing the immunoregulatory effect of the cytokine, are not fully understood. Murine studies show variable results regarding the protective and detrimental role of IL-10 expression [17]. Similar to, and working synergistically with IL-10, TGFB also limits inflammatory responses, downregulating co-stimulatory receptors and de-activating macrophages [30,40]. Furthermore, TGFB production by macrophages affects T-cell proliferation and function indirectly through the induction of anti-inflammatory cytokines.

Type 1 interferon is another major regulator of the inflammatory response elicited by Mtb recognition of mostly cytosolic PRRs, and has been shown to inhibit IFN-gamma signaling and nitric oxide, IL-1 and IL-12 production while simultaneously inducing expression of IL-10 and IL-1 receptor antagonists [17,41]. Type 1 interferon activation is induced by viral or bacterial DNA in the cytosol and is thought to be mediated by the mycobacterial secretion system ESX-1 [42]. Although type 1 interferons have protective properties, the concentration of type 1 interferons in the blood has been shown to correlate with TB severity [43].

1.2.2 T-cell activation

CD4+ T-cells, specifically Th1 and Th17 phenotypes have been shown to be a vital part of Mtb protection [44]. Naïve CD4+ cells are recruited to the site of infection primarily through CXCL10 secretion by macrophages [45]. They are activated by interacting with antigen-presenting cells, like AMs, displaying Mtb antigens on MHC class 2 molecules and secreting a cocktail of cytokines. Naïve CD4+ T-cells are differentiated into Th1 cells by the presence of IL-12 and IFN-gamma while a Th17 specification is induced by TGFB, IL-1B, IL-6, IL-21 and IL-23 [44]. The primary role of Th1 cells is to activate macrophages through IFN-gamma signaling, inducing pro-inflammatory responses, antigen presentation and phagosome maturation [46]. Th17 protection is believed to be primarily mediated through IL-17 induced neutrophil recruitment [47], and local proinflammatory responses. However, the pro-inflammatory role of Th17 cells might also have pathological consequences and its regulation and precise role in Mtb infection have not been fully determined [44].

1.2.3 Mtb survival in the phagosome

Although phagocytized by the macrophages, the bacteria can survive in the cell and undergo colony expansion in the phagosome [48,49], or free in the cytosol [50]. Studies have shown that an increased availability of Mtb antigen-specific CD4 T-cells did not affect bacterial growth or survival during the first week, suggesting that Mtb is located in a niche that offers resistance or prevents recognition by adaptive immune cells [51]. The methods of environment modulation and the cellular location of the bacteria is therefore an area of significant interest with differing views as to what actually occurs *in vivo*. However, there is strong evidence that Mtb can be located both in the cytosol and in phagosomes or other membrane-bound compartments [52].

Bacterial survival in the phagosome is proposed to occur by preventing phagolysosome maturation and acidification. Mtb secreted protein PtpA has been shown to bind directly to macrophage vacuolar-H+-ATPase (V-ATPase), a protein that pumps H+ into the early phagosome to decrease pH, inhibiting acidification [53-55]. Furthermore, phagocytosis of Mtb induces granulocyte-macrophage (GM)-CSF secretion, leading to the expression of

cytokine-inducible Src homology 2 (SH2) containing (CISH) protein which can ubiquitinate V-ATPase leading to its degradation [56].

Escape from the phagosome has been proposed to be facilitated through the Mtb ESX-1 secretion system can then disrupt the phagosome membrane resulting in the release of the bacteria, however the mechanisms are still unclear [57]. The damaged or disrupted phagosome membrane allows the release of bacterial products into the cytosol triggering the cytosolic surveillance pathways leading to an interferon type 1 response and IL-1B release [58].

1.2.4 Antigen presentation

The adaptive immune response to Mtb is characterized by a long delay compared to other pathogens. A mouse study showed that the transportation of the bacteria took 8-10 days [59] in comparison to the transportation of influenzae which takes approximately 20 hours [60]. Several virulence factors contribute to limit the effectiveness of adaptive immune responses, including interference with MHC class II antigen presentation [61], and resistance to macrophage activation by T-cell secreted IFN-gamma [62]. Furthermore, it has been shown that AMs fail to provide an adequate B7 costimulatory signal that interacts with T-cell CD28 surface receptors in conjunction with antigen-loaded MHC class 2 molecules, to activate the lymphocytes [63]. Recently, it has also been shown that dendritic cell transportation of live bacteria to the lung lymph nodes is required for proper T-cell activation. Mtb regulates this transportation to allow early proliferation in the absence of activated lymphocytes [64]. The downregulation of MHC class 2 molecules and B7 costimulatory signal, and the need to transport live bacteria to the lymph nodes for T-cell activation combine to protect the alveoli form immunopathology, while simultaneously allowing Mtb proliferation [17].

1.2.5 Cell death

Mtb has been shown to activate and regulate a range of cell death pathways in host cells. The induced cell death pathway is dependent on the host cell type, mycobacterial strain and other conditions of the infections that are poorly understood [65]. Apoptosis is a key defense mechanism against intracellular pathogens, as the bacteria or virus lose their replicative niche and are prevented from being released into the extracellular space [66]. TNF has been shown to be one of the main drivers of apoptosis in AMs in response to Mtb, and is believed to work in an autocrine and paracrine manner by activating the caspase cascade responsible for initiating apoptosis [67]. The caspase cascade leads to a careful deconstruction of the cell, packaging all the cytosolic components into apoptotic bodies, which can be engulfed by other phagocytic cells through efferocytosis. Studies have shown that the efferocytosis of infected apoptotic bodies by uninfected macrophages effectively eliminates the pathogen when the bacteria escaped phagocytosis mediated killing in the first cell [65,68]. Furthermore, this process increased both MHC class 1 and 2 presentation of Mtb antigens [65,69]. However, researchers discovered that apoptosis was induced more often in attenuated Mtb strains, while virulent strains resulted in a higher degree of necrotic cell death in macrophages [70]. The inverse relationship of apoptosis and virulence lead to the discovery that apoptosis inhibitions are Mtb-mediated virulence factor. Mtb have been shown to secrete secA2 and by making a secA2 Mtb mutant Hinchey et al. showed that apoptosis was induced at a much higher rate in mice and guineapigs than when infected with wild type Mtb, and furthermore, that T-cell activation and pathogen control was increased, however the mechanism remains unknown [71]. Several mechanisms have been proposed to contribute to Mtb mediated apoptosis inhibition, and it is likely that it is a

combination of several factors that leads to inflammatory cell death. These mechanisms include inhibition of membrane repair, Mtb mediated damage of the mitochondrial membrane, and impairing the formation of the apoptotic envelope [70].

Several forms of programmed necrotic cell death have been identified in the context of tuberculosis such as necroptosis, pyroptosis and ferroptosis [72-74]. The mixed lineage kinase domain-like pseudokinase (MLKL) mediated necroptosis pathway has been identified to be prevalent during Mtb infection [75]. Similar to apoptosis, MLKL mediated necroptosis is activated by TNF binding to its respective receptor TNFR1, forming a complex with receptor-interacting protein kinases (RIPK) 1, RIKP3 and caspase-8 that can initiate both pathways. In apoptosis the RIP proteins are cleaved by caspase-8 leading to caspase-3 activation. However, the inhibition of caspase-8 leads the complex to phosphorylate MLKL which can oligomerize on the cell membrane disrupting the membrane integrity and resulting in necrotic cell death [76]. This is characterized by the induction of a robust immune response as the cytosolic contents of the cell are released into the extracellular space and recognized by other immune cells as damage-associated molecular patterns (DAMPs) [77].

Ferroptosis is another type of regulated necrotic cell death that has been shown to occur in macrophages when challenged with Mtb [73]. Infection with Mtb has been shown to be associated with increased an intracellular concentration of free iron and experiments affecting the Mtb availability of iron have been shown to reduce virulence [78]. This is important as ferroptosis is triggered by iron-mediated lipid peroxidation, which disrupts the plasma membrane [79]. During homeostatic conditions glutathione peroxidase–4 (GPX4) prevents lipid peroxidation, however, this mechanisms is proposed to be inhibited by Mtb by limiting glutathione availability and reducing GPX4 expression [73].

Pyroptosis is initiated by the activation of an inflammasome consisting of oligomerized NLRP3 or absent in myeloma 2 (AIM2)-like receptors (ALRs), apoptosis-associated speck-like protein (ASC) and caspase-1. The AIM2 inflammasome is activated by double-stranded DNA in the cytosol [80] however, direct NLRP3 agonists are still unknown [81]. Two processes are believed to be required for NLRP3 activation, the increased expression of IL-1B and the components of the NLRP3 inflammasome and a secondary signal caused by damaged cells, such as K+ and CL- efflux, mitochondrial dysfunction or lysosomal damage [82-84]. The inflammasome cleaves proteins such as pro-IL-1B and IL-18 as well as the pore forming molecule gasdermin D (GSDMD), and can lead to pyroptotic cell death [85]. Pyroptosis has been proposed to be induced in THP1 cells by Mtb mediated plasma membrane damage [72], leading to an efflux of K+ which is associated with NLRP3 activation [82]. However, previous studies have also shown that Mtb induced necrotic cell death is caspase-1 independent, arguing against pyroptosis activation[86].

The role of necrotic cell death in tuberculosis is complex and difficult to define, but it is generally accepted that the release of intracellular components as a result of Mtb mediated inhibition of apoptosis facilitates immune evasion, bacterial dissemination[87,88], immunopathology and reduced antigen presentation [65,69]. Further research is therefore needed to understand the effects of the different cell death pathways on TB outcome.

1.3 Studying Mtb

Researchers use model systems ranging from primary and secondary cell lines and zebrafish, to non-human primates such as macaque to study tuberculosis [89]. Animal models are used to understand clinical manifestations, drug and vaccine efficacy and virulence at a systemic level. However, as tuberculosis is a human disease, several key factors that make translating animal model research into inferences about the human body difficult, such as the amount of nitric oxide produced by the immune cells [90] and different transcriptional responses induced by the activation of pattern recognition receptors [91].

For basic science research on the establishment of disease, Mtb virulence factors and host immune response, *in vitro* cultured macrophages have been used extensively. These cultured macrophages can either be primary cell lines obtained from a donor like MDMs, or secondary cell lines, like THP1, obtained by sub-culturing primary cells and immortalizing them, thus making it possible to passage the cells for an indefinite number of times. There are several advantages and disadvantages of primary and secondary cell lines with the main difference being their heterogenous and homogenous nature respectively. Cells derived from different donors reflect the host genotype, increasing variability for better or worse, while secondary cell lines are essentially clones, making experiments easier to reproduce but offering little in the way of capturing the heterogeneity of real life. Furthermore, cell lines like THP1 that have undergone passaging for a long time often display abnormal characteristics in processes such as cell division, phagocytosis and adherence [89]. In contrast, MDMs are physiological relevant and more likely reflect *in vivo* interactions occurring between Mtb and recruited macrophages. However, as a model cell line for tissue resident AMs, their usefulness is more unclear. Primary cell lines are also difficult to produce in large quantities, and therefore limit the scope of the experiments they are used in.

Induced pluripotent stem cells (iPSCs) are another type of secondary cell line that are reprogrammed, using Yamanaka factors (master transcriptional regulators), to stem cells that can adopt any cell fate. As these cells can undergo cell proliferation and passaging, they are susceptible to genetic manipulation, and can therefore be used for techniques such as gene knock-out/in as well as other genotype manipulations [92]. Recently, a protocol for generating iPSC derived macrophages (iMAC) was published [93], and their use in research is increasing. The Centre of Molecular Inflammation Research (CEMIR) is one of the groups aiming to incorporate iMACs into several areas of research, including TB.

1.4 Aims and Research question

The need for improved model systems in tuberculosis research is highlighted by the unique characteristics of the alveolar macrophage, and the importance of its early encounter with *mycobacterium tuberculosis* in shaping the innate and adaptive immune response. The complexity of tuberculosis, the gaps in early host-pathogen knowledge, the emerging threat of drug-resistant Mtb and the lack of an effective vaccine highlight the need for an accurate model system. An immortalized, tailor-made cell line, that is simple to culture and manipulate would present researchers with a valuable basic science tool that can lay the foundation of the clinical research that can change disease outcome and prevalence. iMACs have the potential to combine all these characteristics. However, if they are to be used as a model system, it is important to properly characterize them and compare them against existing model cell lines.

Recently, Trude Flo's research group performed mRNA sequencing on AMs, iMACs, MDMs and THP1 cells challenged with Mtb in parallel with untreated cells. Using the mRNA sequencing data provided by Trude Flo's research group, this thesis aims to evaluate iMACs as a new model cell line in tuberculosis research and its eligibility to replace or supplement the previously established MDM and THP1 model systems.

Goals:

- Use mRNA sequencing data to explore and characterized the differences in Mtb elicited immune responses displayed by the four cell types.
- Evaluate the possible causes and downstream effects of these differences using the current literature.

2 Materials and Methods

Tackling the scope of the data analysis and selecting the biological processes that are evaluated and compared in this thesis is an important part answering the research question as mRNA sequencing produces a vast amount of data that can be explored in an unlimited number of ways. Therefore, this thesis attempts to combine a data and theory driven approach to extract the most important processes that can be evaluated using mRNA sequencing. First, exploratory methods such as WGCNA, enrichment analysis and hierarchical clustering were used to find biological processes and gene clusters that change as a result of the Mtb infection and differ between cell types.

Then, the literature was used to choose important immunological events or processes (both host and pathogen mediated) that might affect the overall immunological response of the macrophages. Furthermore, the importance of the observations made by the exploratory analyses was evaluated, and central genes were defined by reviewing the current literature. The aim of this combined approach was to provide a picture of differences highlighted by both the bioinformatical exploratory methods, and the literature to ensure that the most important cellular functions were compared.

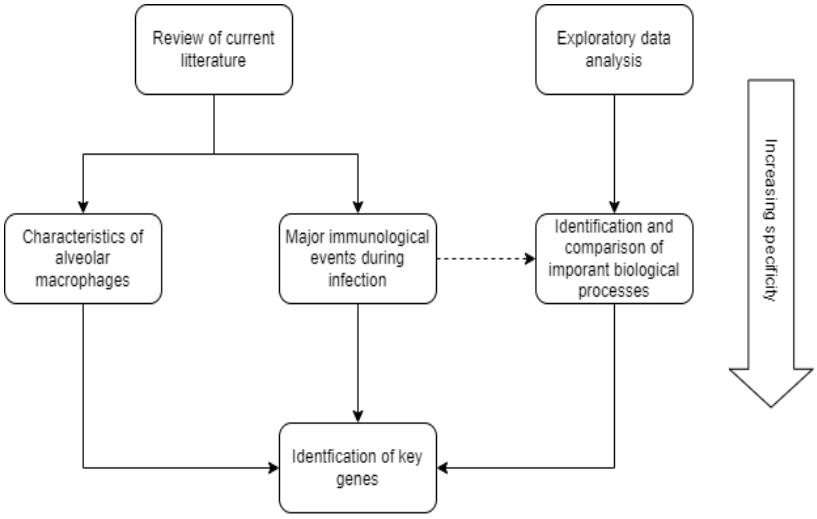

Figure 2-1. Flow diagram of the thesis approach.

2.1 RNA-seq infection experiment

The RNA sequencing infection experiment was performed by Trude Flo's lab in 2021, while the author of this thesis was tasked with analyzing the resulting data. Thus, section 2.1, detailing the principals and procedure of the infection experiment is included here to provide background information about the cells and experimental conditions which the mRNA sequencing data was obtained from. Sections 2.1.3.4 (for the cell death pathway assay), 2.2 and 2.3 were performed by the author of this thesis.

2.1.1 Principles

An early exploratory comparison of cell types subject to different conditions can be done using mRNA sequencing to capture the complete expression profiles of the cells. The sequencing data can be used to perform a range of analysis that provide insights into the global expression patters such as principal component analysis, and spearman's correlation matrix as well as insights into specific genes and pathways such as differential expression, pathway enrichment and co-expression analysis.

2.1.2 Procedure

An infection experiment was performed on AMs, iMACs, MDMs and THP1 cells in order to capture their gene expression response to Mtb infection using lipopolysaccharide (LPS) as a positive control. All cell types were treated with Mtb and LPS parallel to an untreated sample, and after 20 hours the cells were lysed, and their mRNA extracted. The mRNA was then sent to the NTNU Genomics Core Facility (GCF) for high-throughput sequencing and the data was analyzed by the author of this thesis.

Table 2-1. RNA-seq infection experiment metadata.

Sample_ID	Cell type	Treatment
1iMACUntreated	iMACs	Untreated
2iMACUntreated	iMACs	Untreated
3iMACUntreated	iMACs	Untreated
4iMACMtbAUX	iMACs	MtbAUX
5iMACMtbAUX	iMACs	MtbAUX
6iMACMtbAUX	iMACs	MtbAUX
7iMACLPS	iMACs	LPS
8MDMUntreated	MDM	Untreated
9MDMUntreated	MDM	Untreated
10MDMUntreated	MDM	Untreated
11MDMMtbAUX	MDM	MtbAUX
12MDMMtbAUX	MDM	MtbAUX
13MDMMtbAUX	MDM	MtbAUX
14MDMLPS	MDM	LPS
15AMUntreated	AM	Untreated
18AMMtbAUX	AM	MtbAUX
21AMLPS	AM	LPS
22THP1Untreated	THP1	Untreated
23THP1LPS	THP1	LPS
24THP1MtbAUX	THP1	MtbAUX

2.1.3 Production of Human Macrophages from Pluripotent Stem Cells (iMACs)

Generation of macrophages from iPSCs consist of a multi-step process that includes: 1) IPSC culturing; 2) Generation of embryoid bodies (EBs); 3) Myeloid expansion and 4) Macrophage maturation. Step 1-3 requires considerable skill and experience and was therefore performed by Dr. Marit Bugge, while differentiation from Monocyte-like to Macrophages (step 4) was performed by the thesis author.

2.1.3.1 iPSC culturing:

iPSCs were obtained from the European Bank for induced pluripotent Stem Cells (EBiSC, https://ebisc.org/about/bank), distributed by the European Cell Culture Collection of Public Health England (Department of Health, UK). The iPSCs were cultured in Vitronectin XF (StemCell Technologies, 7180) coated plates with mTeSR™ Plus medium (StemCell Technologies), which was changed daily. Growth medium was removed for passaging and the

cells were treated with 1x ReLeSR™ (StemCell Technologies, 5826) to break up iPSC colonies, before being re-plated at 1:6 density in mTeSRplus media.

2.1.3.2 Generation of embryoid bodies (EBs)

The formation of EB and myeloid differentiation of iPSCs is described in a protocol made by former NTNU postdoc Eugenia Meiler, current a researcher at GSK Madrid, based on the methods published by Van Wilgenburg et al. in 2013 [93]. Brief description of the protocol: A single-cell suspension of the iPSCs was obtained by treating the cells with Versene (Gibco-Thermo Fisher, 15040066) for 5 minutes. Cells were then counted before being resuspended in EB media at a concentration of 10 000 cells/ 50 µL. EB media is composed of mTeSR™ Plus medium (StemCell Technologies, 5826) supplemented with 50 ng/mL bone morphogenic protein 4 (BMP-4) (R&D, 315-BP-010), 20 ng/mL SCF (R&D, 255-SC-050) and 50 ng/mL vascular endothelial growth factor (VEGF) (R&D, 293-VE-050) to differentiate iPSCs towards mesodermal induction and hematopoietic specification (see Figure 2-2). Rock inhibitor, Y-27632 (StemCell Technologies 72304) was added to increase cell survival. Cell suspension (50 ul/well) was added into a 384-well Spheroid Microplate (Corning. 3830). followed by centrifugation at 1000 RPM for 3 minutes and incubated for 4 days at 37 degrees, 5%CO2. Fresh EB media without rock inhibitor (50 ul) was added at day 2.

2.1.3.3 Myeloid expansion

After 4 days the EBs were harvested and seeded onto gelatine coated T175 flask in X-VIVO-15 (Lonza) media containing 100 ng/mL macrophage CSF (M-CSF) (Prepotech, 300-25), 25 ng/mL IL-3 (Prepotech, 200-03), 2 mM glutamax (Gibco-Thermo Fisher, 35050061), and 0.055 mM β-mercaptoethanol (Gibco-Thermo Fisher, 31350010). Cytokines IL-3 and M-CSF (Prepotech, 300-25) further promotes a myeloid expansion and differentiation into monocyte-like cells (iMos). Media was then changed every week and the EB culture was renewed after 3-4 months. The resulting monocytes were checked routinely using a flow cytometry panel defined for expected surface markers.

2.1.3.4 Macrophage maturation

The harvested monocytes were differentiated into macrophages by removing them from an IL-3 environment and culturing them in roswell Park Memorial Institute medium (RPMI) 1640 (Gibco-Thermo Fisher, 61870044) with 10% fetal calf serum (Gibco) and 100 ng/mL M-CSF (Prepotech, 300-25) for 5-7 days.

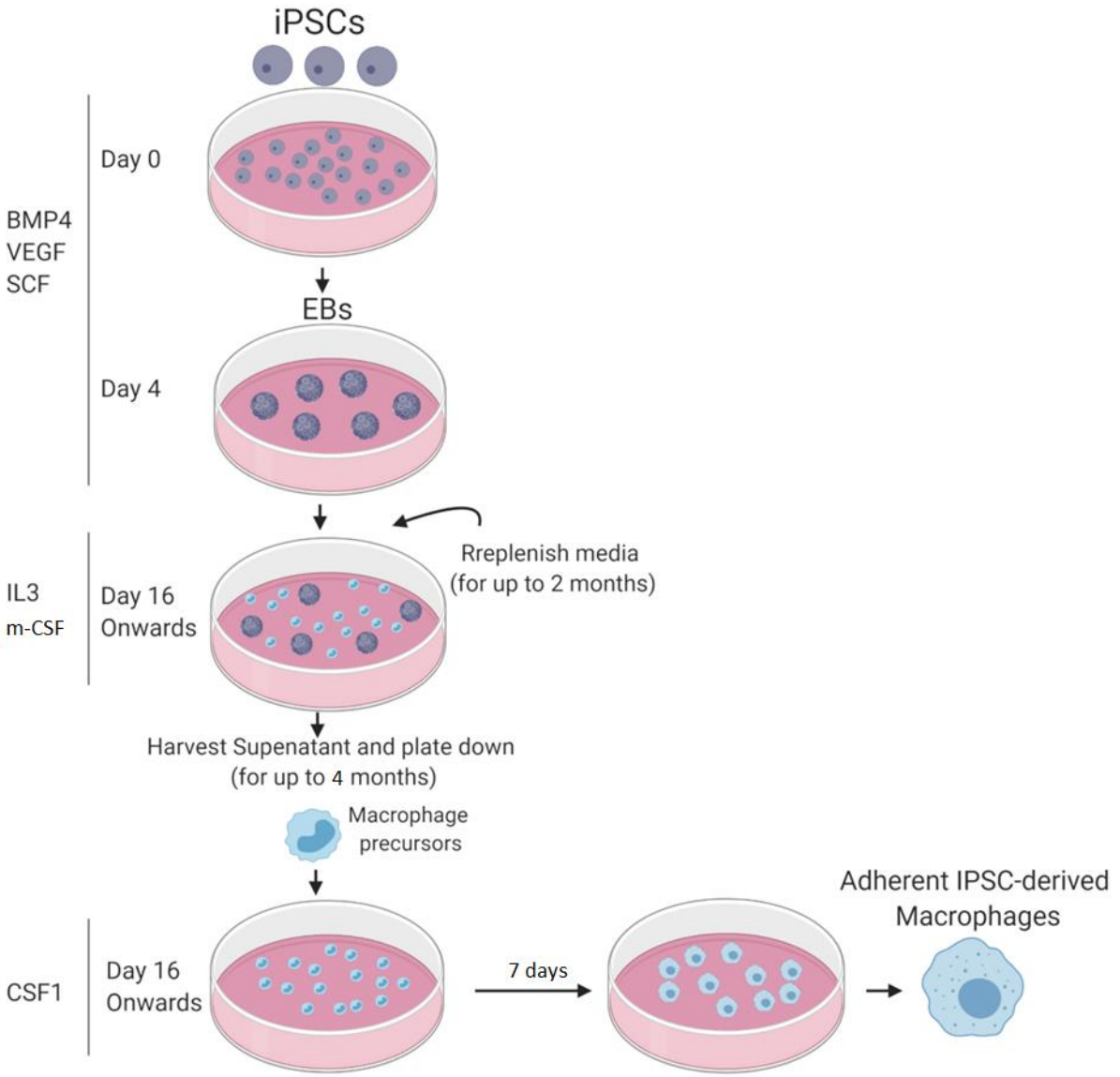

Figure 2-2. Differentiation of iPSC derived macrophages. The timeline and reagents used to differentiate stem cells to macrophages. Figure adapted from [1]

2.1.4 MDM isolation and culture

MDM isolation and culture was performed by Håvard Haukaas and Anne Marstad in 2021 and is included in this thesis to provide adequate background information about the cells.

2.1.4.1 Peripheral blood mononuclear cells (PBMC) isolation from whole blood

Pooled serum and buffy coats were acquired from the St. Olavs Hospital blood bank (Trondheim, Norway), obtained from healthy donors after informed consent, with approval from the Regional Committee for Medical and Health Research Ethics (No. 2009/2245). PBMCs were separated using the density gradient medium Lymphoprep™ (StemCell Technologies, 07801) and centrifugation according to the manufacturer's protocol. The buffy coat was mixed with 100ml of PBS and 14ml lymphoprep was added to 30 ml of the blood-PBS mixture and centrifuged at 1800 rpm for 20 minutes at room temperature. The middle

layer of PBMCs was harvested using a serological pipette. The PBMC solution was centrifuged at 2000 rpm for 10 minutes and the supernatant was discarded. The cells were then washed 3 times by adding 20ml of phosphate-buffered saline (PBS) and centrifuging at 800 rpm for 8 minutes. A drop of ZAP-OGLOBIN II Lytic Reagent (Beckman Coulter, Cat #NC0098316) was added to lyse any remaining red blood cells and the PBMCs were counted using a Z2 Coulter counter (Beckman Coulter). The cells were then washed a final time with 20ml PBS and resuspended in RPMI + 10% human serum.

2.1.4.2 Monocyte isolation from PBMC and differentiation into macrophages

MDM media was prepared by adding M-CSF (Prepotech, 300-25) to RPMI (Gibco-Thermo Fisher, 61870044) + 10% human serum for a final concentration of 25ng/ml. Monocytes were isolated by adding the PBMC solution to a culture flask at a density of 730000 cells/cm^3 and incubated at 37°C for 1 hour to facilitate adherence. Non-adherent cells were removed by washing 3 times with HBSS (Sigma, H9394) before the MDM media was added. The monocytes were then incubated for 5-7 days to allow differentiation into MDMs with a media change on day 3.

2.1.5 THP1 culture

THP1 preparation and culture was performed by Anne Marstad. Briefly, THP1 cells were differentiated into THP1 macrophages (THP-1M) by culturing them for a minimum of 3 days in RPMI 1640 medium with 3.4% L-glutamine (Gibco-Thermo Fisher, G8540) and 1% HEPES buffer (Sigma, H0887) supplemented with 10% Fetal calf serum (FCS)(Gibco) and 100ng/ml phorbol 12-myristate 13- acetate (PMA).

2.1.6 AM acquisition and culture

AMs were isolated using adherence from Bronchoalveolar Lavage Fluid (BALF) obtained from 3 donors undergoing bronchoscopy at St. Olavs hospital. Donors were selected by Dr. MD Anders Tøndell, Senior consultant in respiratory medicine, Department of Thoracic medicine at St. Olavs University Hospital, with a focus on choosing patients that were healthy. Attachment media was prepared using RPMI 1640 (Gibco-Thermo Fisher, 61870044) medium with 3.4% L-glutamine (Gibco-Thermo Fisher, G8540) and 1% HEPES buffer (Sigma, H0887) supplemented with 1% Penicillin-Streptomycin (P/S) (Gibco-Thermo Fisher, 15140122) and 10% A+ human serum.

BALF was collected immediately after bronchoscopy and centrifuged at 500x g for 10 minutes, and supernatant was removed. The pellet was then resuspended in ice cold DPBS (Gibco-Thermo Fisher, 14190250) and centrifuged at 300x g for 5 minutes, a process that was repeated 3 times before being resuspended in the attachment media. The cells were then incubated at a density of 87000 cells/cm^2 for 2 hours in 37°C to facilitate adherence before non-adherent cells were removed by washing 3 times with Hanks' balanced salt solution (HBSS).

AM media was prepared using RPMI 1640 medium with 3.4% L-glutamine and 1% HEPES buffer supplemented with 10% A+ human serum which was added to the adherent cells and incubated for 1 hour before experiments were performed.

2.1.7 Stimuli suspensions

2.1.7.1 Mtb culture

The leucine and pantothenate auxotroph strain Mtb mc^2 6206 was used to create the Mtb infection solution. Growth media was prepared using Middlebrook 7H9 broth (BD

Biosciences, 00382902713104) supplemented with 10% Oleic Albumin Dextrose Catalase (OADC), 0.05% Tween-80, 24 g/ml D-pantothenate and 50 g/ml L-leucine. The Mtb was cultured in a shaking incubator at 37°C with weekly splits that included addition of glycerol (final concentration of 0.2%) to ensure exponential growth.

2.1.7.2 Mtb infection suspension

The infection suspension was creating by taking four aliquots of 5ml of Mtb mc2 6206 culture and spinning it down at 4754xg. The remaining pellets were resuspended in the same media the 4 cell types were cultured in and sonicated 1 minute in an ultrasonic cleaner bath (VWR) at maximum power. The suspensions were then vortexed and centrifuged at 300x g for 4 minutes to make a pellet of the largest aggregations of bacteria. The supernatant was harvested and OD_{600} was measured and diluted to make a Mtb suspension of multiplicity of infection (MOI) 2.

2.1.7.3 LPS suspension

Solutions of LPS in cell specific media was made with a final concentration of 10ng/ml.

2.1.8 Cell stimulation

AM (87000 cells/well), MDM (73000 cells/well), and iMACs (73000 cells/well) were plated in triplicates for the untreated and Mtb stimulated samples while one sample was stimulated with LPS. THP-1M had only one replicate per sample for all stimuli types. All cells were then stimulated for 20 hours with Mtb at an MOI of 2 and LPS at a final concentration of 10ng/ml before the experiment was ended and RNA extracted.

2.1.9 RNA isolation

After 20 hours the cells were washed once with DPBS and lysed with RTL buffer (Qiagen, 79216) and store at -80°C. Later, the lysate was thawed on ice and RNA was isolated using Qiagen RNeasy® Mini Kit (Qiagen, 74106) as per manufacturer's protocol. RNA was then eluted and stored in RNAse free water and the concentration was measured using a NanoDrop™ 1000 (ThermoFischer).

2.1.10 Sequence alignment

RNA from the infection experiment was sent to the Genomics core facility (GCF) at NTNU for library preparation and sequencing. The RNA integrity number (RIN) of all samples passed the quality control (QC) threshold of RIN >= 7. Libraries from the 24 samples were prepared using Lexogen SENSE mRNA kit, and the RNA was sequenced using Illumina NS500, 1x high output flow cell with 75bp single end reads. Pseudo gene alignment was performed with Salmon [94] and aggregation of transcripts to genes was done using tximport [95].

2.2 Data analysis

All data analysis was performed in RStudio [96] using the raw read counts obtained from the NTNU GCF. An identical approach was used on the sequencing data generated by Bernard et al. [2], with count data obtained from Gene Expression Omnibus (accession number GSE132283) in February 2022 (https://www.ncbi.nlm.nih.gov/geo/query/acc.cgi?acc=GSE132283). The Rmarkdown documents containing the scripts used to generate the results and corresponding visualizations are all available in (gitbub link) and can be reproduced by following the instructions in the README file.

2.2.1 Selection of samples

Two of the AM samples showed signs of pre-activation prior to being stimulated with Mtb and LPS, most likely a result of the extraction process or due to lung inflammation in the donors (see Appendix Figure 1). A decision was therefore made to discard the two activated samples from the analysis in order to be able to identify genes that are differentially expressed between untreated and stimulated samples.

The removal of replicates results in lower statistical power and a loss of significantly differentially expressed genes, however, this was determined to be less detrimental than the masking effect the stimulated untreated samples would have on the differential expression analysis.

2.2.2 Data Normalization

2.2.2.1 Principles

Following the sequencing process the number of reads mapped to specific genes do not represent the actual expression of that gene in the cell. For the raw count data to reflect the number of transcripts within a cell, the data has to be normalized for gene length, library composition and library size. Furthermore, accuracy and statistical power is increased by removing genes with very low read counts. Genes with very few mRNA transcripts are generally not translated into protein at a biologically significant level, if translated at all, and are therefore removed before differential expression analysis occurs. Furthermore, these genes unlikely to provide the statistical power to classify them as differentially expressed and can therefore be removed with minimal loss of information, while simultaneously improving the accuracy of the differential expression analysis [97].

The illumina sequencing process requires relatively short DNA fragments and transcripts are therefore cut at regular intervals (50-350 bp) meaning the length of the gene will determine the number of fragments created per mRNA transcript and therefore affect the number of reads aligned to the gene. Furthermore, when comparing different cell types some genes will be highly expressed in some cells while not being expressed in others. As there is a limited number of total reads per sample, highly expressed genes will result in less reads for the rest of the genes and therefore needs to be accounted for [98]. The total number of reads in the sample will also affect the number of reads mapped to genes, and as the library size of each sample will vary as a result of the amplification process, raw counts are usually converted to counts per million.

2.2.2.2 Procedure

The R code for the following procedure can be found in the rawdata_normalization.rmd file (gitbub link). To ensure identical normalization and filtering steps for all downstream analysis, the rawdata_normalization.rmd is rendered from the individual scripts that require the normalized data using the source_rmd() function.

The DGElist function (edgeR package, version 3.36.0) [99] was used to create an object containing the raw gene counts from GCF, metadata and gene information. Using this object, the raw data was filtered for genes with low counts using the filterByExpr function (edgeR package, version 3.36.0) [99]. The filterByExpr function removes genes that have less than 10 counts per million in n samples (n is determined by smallest group of samples, in this case 1) and less than 15 counts across all samples reducing the total number of represented genes from 60271 to 18117. Normalization factors were calculated with the calcNormFactor() function (edgeR package, version 3.36.0) [99] using the trimmed mean of

M values (TMM) method [100], which takes into account gene length, library composition and library size. To apply the normalization factors to the counts the cpm() function (edgeR package, version 3.36.0) [99] was used. This returns the log2(counts per million) values that will be referred to as normalized counts for the remainder of this thesis. Z-scores were calculated for each gene (*i*) observed in a sample (j) based on the average expression of that gene (G) across all samples.

$$Z_{ij} = \frac{G_{ij} - \bar{G}_i}{\sigma_{G_i}}$$

Equation 1.

The Z-score values represents the how many standard deviations an observation is from the mean expression of that gene and is therefore useful in visualizations comparing between cell relative expression of a large number of highly variable gene with heatmaps.

2.2.3 Principal component and Correlation analysis

The R code for the following procedure can be found in the PCA_and_corr.rmd file (https://github.com/ulrikhorn/MasterThesis). The principal component was performed on the z-transformed normalized count data using the prcomp() (stats package, version 4.1.3) [96]. The sample spearman correlations were calculated using the cor() function (stats package, version 4.1.3) [96].

2.2.4 Hierarchical clustering

2.2.4.1 Principals

Hierarchical clustering groups samples together according to the correlation of the observations between samples or genes. All observations are first treated as separate clusters, and the clusters with the smallest distance between them are merged into a larger cluster. This bottom-up approach results in a set of clusters containing objects that are broadly similar.

2.2.4.2 Procedure

The R code for the following procedure can be found in the h_clustering.rmd file (https://github.com/ulrikhorn/MasterThesis). Z- transfomed normalized count data (log2(CPM) was filtered for all differentially expressed genes across samples, and the euclidian distance between both genes and samples were calculated using the dist() function (Stats package version 4.1.3) [96]. Complete hierarchal clustering was then performed using the hclust() function (Stats package version 4.1.3) [96] and the resulting dendrograms were cut to create 4 sample clusters and 7 gene clusters using the cuttree() function (Stats package version 4.1.3) [96]. The resulting dendrograms revealed that THP1 clustered separately from the other samples (see Figure 3-3) and as such should be treated as an outlier. THP1 affected the analysis due to a high number of highly expressed genes related to cell cycle and developmental biological processes and as such reduced the information on immunological processes. With THP1 samples removed the clusters were analysed for enriched GO terms using the enrichgo() function (clusterProfiler package, version 4.2.2) [101] and a summary of the biological processes for each cluster was plotted together with the expression values in a heatmap using the heatmap() function (ComplexHeatmaps package, version 2.10.0) [102] and clustered according to the previously created dendrograms.

Hierarchical clustering was also used when generating gene specific heatmaps. These dendrograms show the similarity of expression with regards to the selected genes as well as indicate weather the changes in expression are a result of the simuli. If the gene expression patterns are affected by the stimuli, the samples will cluster according to the treatment group rather than the cell type, which by default is most similar. Therefore, if the samples cluster according to cell type, this indicates that the treatment has little to no effect on the observed expression patterns.

2.2.5 Differential expression analysis

2.2.5.1 Principles

The normalized and filtered expression data obtained from mRNA sequencing can be used to find differentially expressed (DE) genes. Differential expression analysis is a useful way of comparing the expression profiles and identifying key genes in cells under different conditions by quantifying the magnitude differential expression and estimating the significance of the difference. Differential expression analysis estimates the difference in gene expression using regression-based models and then estimates significance using a statistical test based on a null hypothesis that expression is the same for all conditions.

2.2.5.2 Procedure

The R code for the following procedure can be found in the deg_analysis.rmd file (https://github.com/ulrikhorn/MasterThesis). The normalized counts were used to fit each gene to a linear model using the lmFit() function (Limma package, version 3.50.1) [103], and then fit to the defined contrast matrix using the contrast.fit() function (Limma package, version 3.50.1) [103]. Empirical bayes statistics were then calculated using the eBayes() function (Limma package, version 3.50.1) [103] resulting in a data frame of differential expression data and the corresponding statistics. Genes with an absolute log2 fold change of more than 1 and a p-value of less than 0.05 were filtered from the results and will be referred to as significantly differentially expressed genes for the remainder of this thesis.

2.2.6 Weighted gene correlation network analysis

2.2.6.1 Principles

Weighted correlation network analysis (WGCNA) is used to describe correlation patterns across RNA-seq or microarray gene expression data. WGCNA uses expression values to find clusters or modules of highly correlated co-expressed genes and the relationship between such modules and experimental traits. Correlation networks are constructed from a matrix where, in the case of expression data, the row indices correspond to the samples of different experimental conditions and the column indices correspond to the genes to which the expression was measured. The module trait relationship is calculated by finding the correlation between a module and treatment groups in the experiment.

2.2.6.2 Procedure

The R code for the following procedure can be found in the wgcna.rmd file (https://github.com/ulrikhorn/MasterThesis). The blockwiseModules function (WGCNA package, version 1.71) [104] was used to create a signed pearson correlation network with a soft threshold power value of 12 based on the pickSoftThreshold() function (WGCNA package, version 1.71) [104]. The categorical variables (untreated, MtbAUX and LPS) were binarized using the binarizeCatagoricalVariable() function (WGCNA package, version 1.71)[104] and the pearson correlation between the modules and treatment was calculated

using the cor() function (Stats package version 4.1.3) [96]. Modules significantly (p-value < 0.05) associated with the Mtb stimuli were then investigated further by analyzing for enriched GO terms using the enrichgo() function (clusterProfiler version 4.2.2) [101].

2.2.7 Gene ontology enrichment analysis

2.2.7.1 Principles

The gene ontology (GO) platform is a database of terms describing molecular functions, biological processes and cellular components. Within each GO term is a list of genes associated to the process described, curated from published peer reviewed literature. Using a list of all genes obtained from a differential expression analysis, together with a list of significantly differentially expressed genes ($p<0.05$), over-represented processes that are affected by treatment or regulated differently between cell types can be identified.

2.2.7.2 Procedure

The R code for the following procedure can be found in the enrichment_analysis.rmd file (https://github.com/ulrikhorn/MasterThesis). The GO enrichment analysis was performed using the enrichGO() function (clusterProfiler version 4.2.2) on the data frame containing the log2Fold change and p-values of all gene transcripts collected alongside the list of significantly differentially expressed genes ($p<0.05$). The search was limited to GO terms describing molecular function and the maxGSSize was set to 100, increasing the specificity of the GO terms included as more generalized terms with a large number of genes are excluded. The GO term descriptions, gene ratios (percentage of total DE genes in GO term) and p-adjusted values of the over-representation was plotted using the dotplot() function (Enrichplot package, version 1.14.2)[105].

2.2.8 Pathview

The R code for the following procedure can be found in the enrichment_analysis.rmd file (https://github.com/ulrikhorn/MasterThesis). Pathview images were generated using the log2 fold change (MtbAUX vs untreated) and overlaid on Kyoto encyclopedia of genes and genomes (KEGG) pathway images (KEGG PATHWAY Database (genome.jp), images obtained march 2022) using the pathview() function (Pathview package, version 1.34.0) [106].

2.3 Cell death pathway assay

2.3.1 Principles

To identify the cell death pathways that are active in the iMACs, a cell death experiment aimed at triggering apoptosis, necroptosis, pyroptosis and ferroptosis (see Table 2-2) in the presence of a range of reagents (see Table 2-3) was performed. The reagents target biological processes involved in the different cell death pathways, some specific for a single pathway while others affect more than one. These reagents were added to verify what components of the different cell death pathways that were active, and to see the effects of the reagents on lactate dehydrogenase (LDH) release.

Table 2-2. iMAC cell death stimuli. The cell death pathway assay used four types of stimuli, aimed at activating pyroptosis, ferroptosis, apoptosis and necroptosis in order to investigate the ability of the iMACs to activate different cell death pathways.

Stimuli	Cell death pathway
LPS + Nigericin	Pyroptosis
RSL-3	Ferroptosis
Venetoclax	Apoptosis
TNF + zVAD	Necroptosis

The samples stimulated with Venetoclax (Tocris, 6960) and TNF (Peprotech, 300-01A) + zVAD were prepared the day before the other samples were stimulated due to previous experience indicating that a longer incubation time was needed for these reagents to have the desired effect. An additional negative control was then included to show the cytotoxicity of the inhibitors over 18 hours.

Table 2-3. Inhibitors of cell death processes. The known effects of the reagents used to inhibit specific cell death signaling molecules or cellular processes. These were added to investigate the activity of central effector proteins as well as to investigate the reagents effects on the LDH release.

Reagent	Function
MCC950	NLRP3 inhibition
Disulfiram	GSDMD and TNF inhibition
PEG 8000	Stabilization of osmotic swelling caused by plasma membrane pores
Glycine	Inhibition of necrotic cell death

2.3.2 Procedure

iMACs were harvested after myeloid expansion (see section 2.1.3.3) and plated in a 96 well glass bottom plate (Cellvis p96-1.5-H-N) at a concentration of 30000 cells/well in RPMI 1640 (Gibco-Thermo Fisher, 61870044) with 10% fetal calf serum and 100 ng/mL M-CSF (Peprotech, 315-02) for 7 days.

The inhibitors were solubilized in RPMI 1640 (Gibco-Thermo Fisher, 61870044) with 3.4% L-glutamine (Gibco-Thermo Fisher, G8540), 1% fetal calf serum and 1:1800 DRAQ7. Disulfiram and MCC950 were first solubilized in dimethyl sulfoxide (DMSO), while polyethylene glycol (PEG)-8000 (VWR, 97061-102) and glycine (Merck, 1042010100) were dissolved directly into the culture medium. DMSO was also added to one of the columns at the same concentration as the disulfiram and MCC950, to measure the cytotoxicity of DMSO alone.

10mM PEG-8000, 50mM glycine, 30uM disulfiram and 10uM MCC950 was added to the wells that were to be stimulated by venetoclax (Tocris, 6960) and TNF-alpha (Peprotech, 300-01A) + zVAD as well as the 18 hour no stimuli control and incubated for 30 minutes before 25uM venetoclax (Tocris, 6960) and 10ng/ml TNF-alpha (Peprotech, 300-01A) + 20uM zVAD was added to their respective wells.

The cells where then incubated at 37°C., 5% CO2 for 18 hours. After 18 hours new inhibitor solutions were made and added to the remaining wells, and incubated 30 minutes

before 200ng/ml LPS, and 4uM RAS-selective lethal (RSL)-3 was added. After 3 hours 20uM nigericin (Sigma N7143) was added to the wells stimulated with LPS. After 4 hours 10X LDH lysis buffer (CyQuant, cat# C20300) was added to 3 control wells to measure max LDH release and 50ul of supernatant was harvested and added to an ELISA 96 well plate and 50ul of LDH reaction mixture (CyQuant, cat# C20300) was added. The ELISA plate absorbance was read after 30 minutes at 490nm and 655nm.

3 Results

3.1 Expression profile comparisons between AMs, MDMs, iMACs and THP1

3.1.1 Global expression profiles reveal a high degree of AM and MDM similarity

Visualizing the overall similarities between cell types and treatment groups, is an important initial step in comparing the macrophages. Therefore, the global transcriptional profiles of the query cells were used to generate a principal component analysis (PCA) plot. This analysis shows the relative similarity of the samples based on the principal components (PC) that represent the most variance between samples, PC1 and PC2.

As expected, the samples primarily cluster according to cell type. iMACs showed the largest difference between treatment groups followed by THP1. MDMs and AMs however show little to no difference between treatment groups (see Figure 3-1). Furthermore, the PCA plot suggests that the iMACs correlate more with AMs and MDMs in PC1, while THP1 are closer to the primary cell lines in PC2.

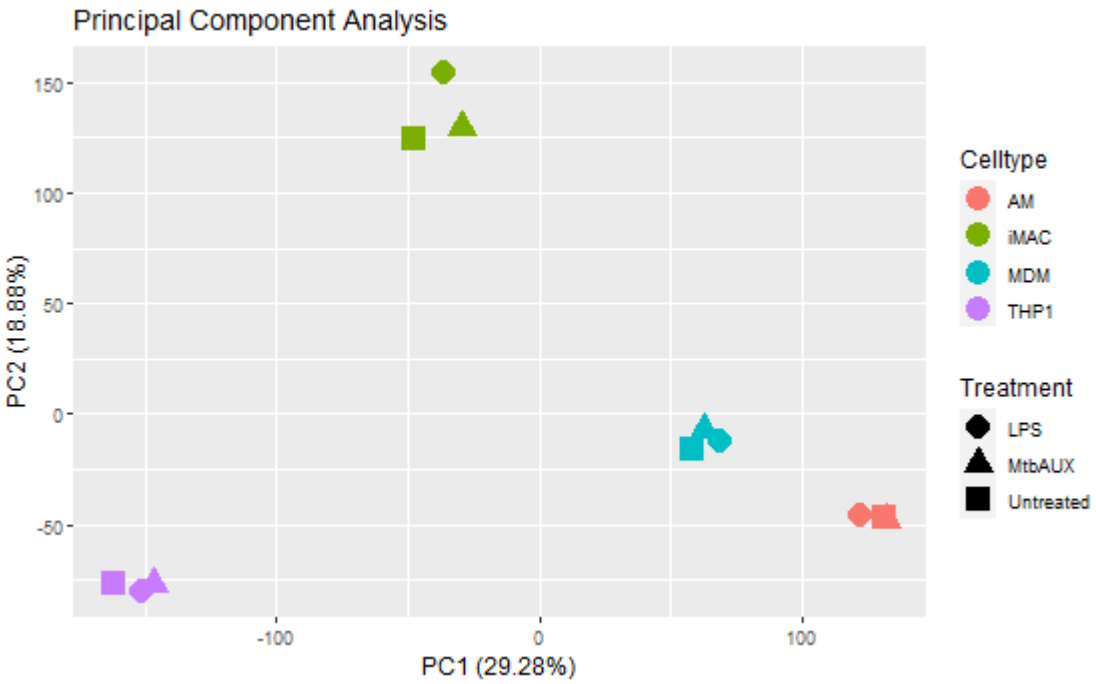

Figure 3-1. AMs and MDMs show the highest degree of similarity. Principal component analysis of the global expression patterns of the samples averaged for replicates treated with the same stimuli. The axis shows the variance attributed to principal component (PC) 1 (x-axis) and PC2 (y-axis), where PC1 represents the most variance. The cell types are differentiated by color while the sample treatment is denoted by the point shape.

The global transcriptional profiles were further investigated using a spearman correlation analysis to make a heatmap of sample similarity. In accordance with the PCA plot, this heatmap reveals a high degree of correlation within cell type. iMACs and THP1 also show

some clustering according to treatment group, however, this is not discernable in MDMs and AMs (see Figure 3-2). The correlation between the cell types based on their global transcriptional profiles provides an early indication of the applicability of iMACs, as they seem to have a slightly higher degree of similarity with AMs than THP1. However, to discern more about the differences in immune response, the correlation of genes affected by Mtb needs to be investigated.

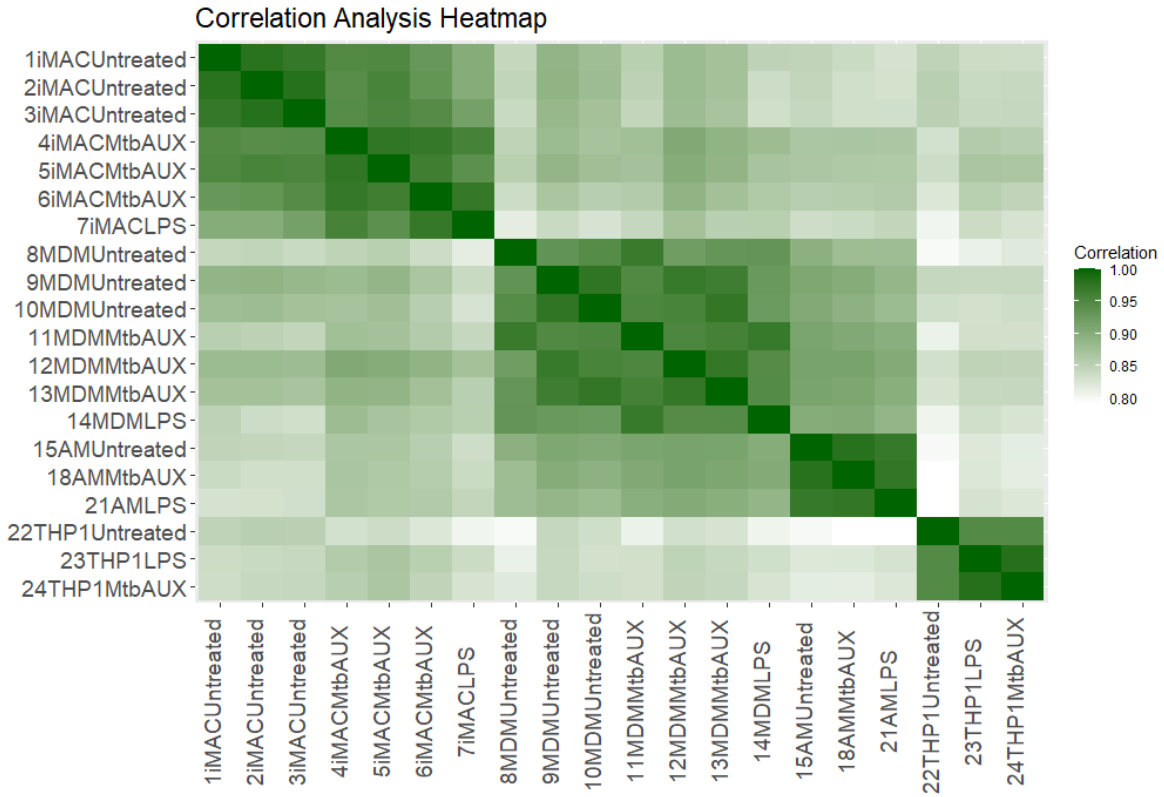

Figure 3-2. iMACs display a higher degree of correlation with AMs than THP1. The correlation between iMACs, MDMs, AMs and THP1 with and without Mtb infection is visualized based on their global transcription profiles. The spearman correlation coefficient is visualized by the gradient color intensity of the heatmap tiles, from 0.8 (white) to 1 (darkgreen).

3.1.2 Hierarchical clustering indicates a strong type 1 interferon response in iMACs

To investigate the similarity between samples based on genes affected by Mtb infection, hierarchical clustering was performed based on all observed significantly differentially expressed genes (MtbAUX vs untreated, total of 3,320 genes). This generates a dendrogram visualizing the hierarchical clustering of the Euclidian distances, a metric of similarity, between the samples.

The cluster dendrogram displays two major clusters consisting of AMs, iMACs and MDMs in one, and THP1 in the other (see Figure 3-3). Again, the MDMs and AMs cluster most closely, indicating a similarity in the expression of Mtb stimulated genes as well as in the global expression patterns (see Figure 3-1 and Figure 3-2). The Euclidean distance between the treatment groups of the iMACs was higher than in the other cells forming two distinct clusters, indicating a strong response to the stimuli that had a large impact on gene expression. The clustering according to treatment was also seen in MDMs and THP1

cells, however, this was not evident in the AMs, indicating little differential expression in response to Mtb and LPS.

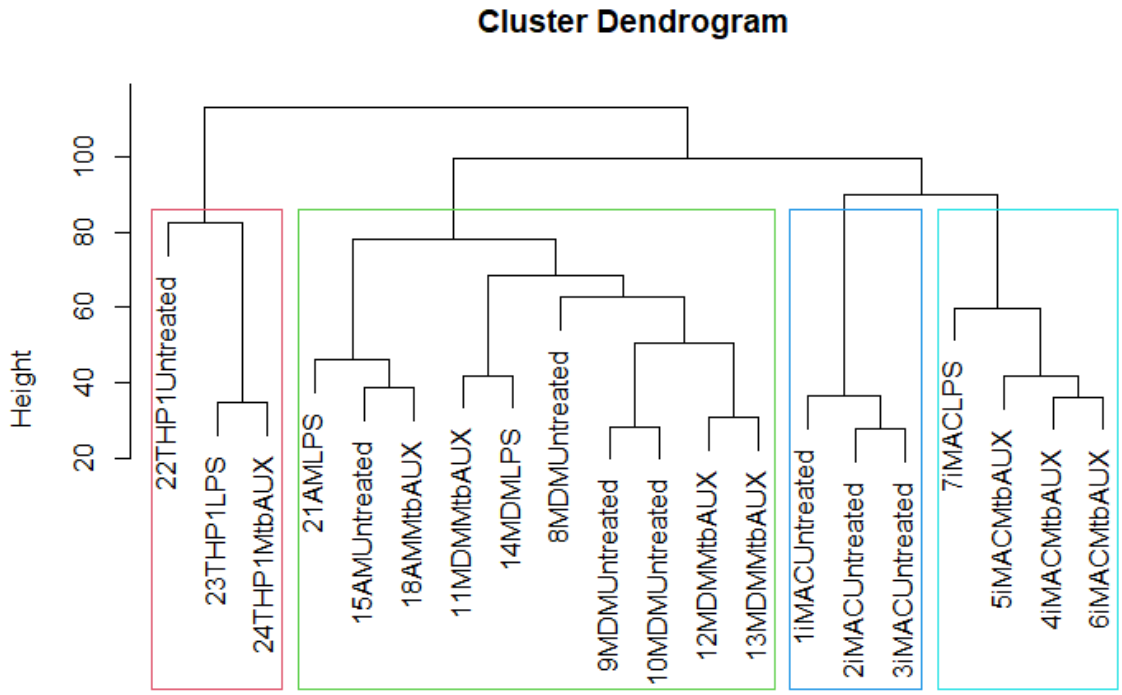

Figure 3-3. THP1 cells differ from iMACs, MDMs and AMs in expression of Mtb affected genes. The hierarchal clustering of AM, MDM, iMAC and THP1 samples generated from the Euclidean distances between the samples based on expression of all Mtb vs Untreated significantly differentially expressed genes (-1 > log2FoldChang > 1 and p-value < 0.05).

Using the same technique, large clusters of genes, that were similarly expressed were identified. These clusters could then be compared between cell types and treatment groups, by visualizing the relative gene expressions in a heatmap (see Figure 6). Furthermore, using enrichment analysis, the major biological functions that the identified clusters, could be defined. As the THP1 samples clustered as an outlier (see Figure 3-3), they were excluded from the following analysis to improve the resolution of the of differences in immune-related gene expression.

Clusters 1, 2 and 3 are composed of genes related to expected immunological processes such as IFN-gamma, IL-1, chemokine and type 1 interferon signaling, while clusters 4 and 5 represents nuclear DNA replication and tissue biomineralization (see Figure 3-4).

The hierarchical clustering heatmap reveals several cell type specific expression trends of note. First, the similarity between the Mtb and untreated AM samples indicate that the stimuli had a low impact on the expression of the selected genes. Second, and in contrast to the AMs, iMACs show a more obvious pattern of expression according to treatment. Lastly, the MDMs display a trend of subdued differential expression of the selected genes.

Cluster 3, representing inflammatory drivers, is similarly expressed in Mtb infected iMACs and AMs, and although being showing an upregulating trend this change is more moderated in MDMs (see Figure 3-4, cluster 3). Interestingly, cluster 2 is highly upregulated in iMACs and slightly upregulated in MDMs, while AMs display a consistently low expression of these type 1 interferon related genes.

The hierarchical clustering heatmap shows that MDMs and AMs have the most closely related overall expression profiles of the differentially expressed genes (see Figure 3-3). However, the upregulation of the proinflammatory related genes (see Figure 3-4, gene cluster 3) seems to be somewhat more similar between iMACs and MDM.

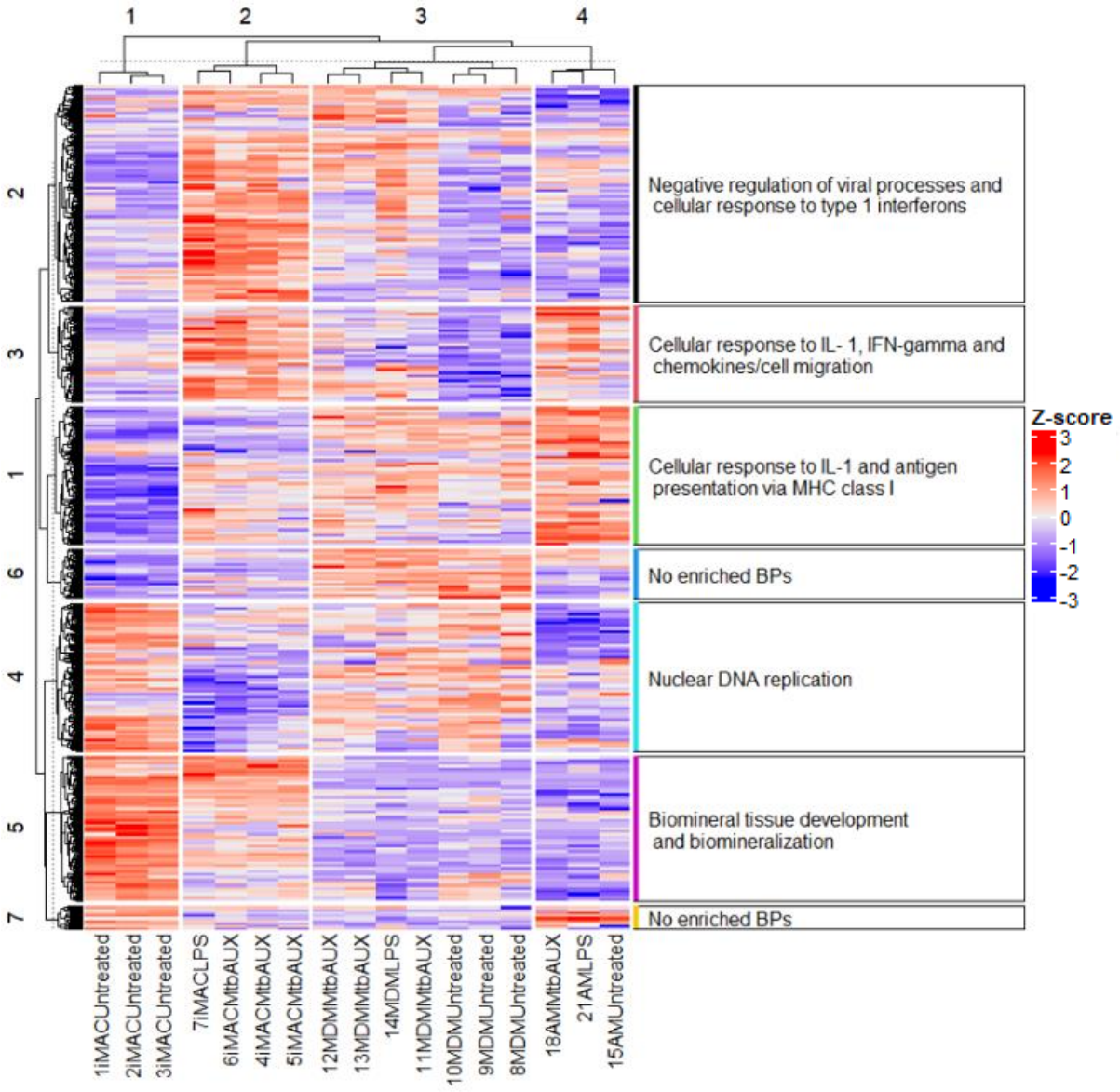

Figure 3-4. Hierarchical clustering reveals a modest MDM inflammatory response and a strong type 1 interferon response in iMACs. Z-transformed relative gene expression heatmap of all Mtb vs Untreated significantly differentially expressed genes (-1 > log2FoldChang > 1 and p-value < 0.05) clustered according to the euclidean distances between samples (columns) and genes (rows). The biological processes represented by the clusters were identified using GO enrichment analysis on the genes in their respective clusters (1-7). The GO terms specified are the top significantly enriched (Benjamini-Hochberg adjusted p-value < 0.05).

3.2 All macrophage cell lines are enriched for inflammatory processes

To determine the main biological functions affected in response to the Mtb challenge, gene ontology enrichment analysis was run on the Mtb vs untreated significantly differentially expressed (log2 fold change > 1 or < -1 and P-value < 0.05).

As expected, the most significantly enriched terms are almost exclusively related to an immune response, confirming that the majority of the differentially expressed genes are a result of the Mtb infection. Many similarities in the enriched biological processes can be observed, such as cellular response to interleukin-1 and INF-gamma as well as processes related to chemokine signaling (see Figure 7). iMACs and THP1 cells are also highly enriched for negative regulation of viral processes which correlates with the findings of the

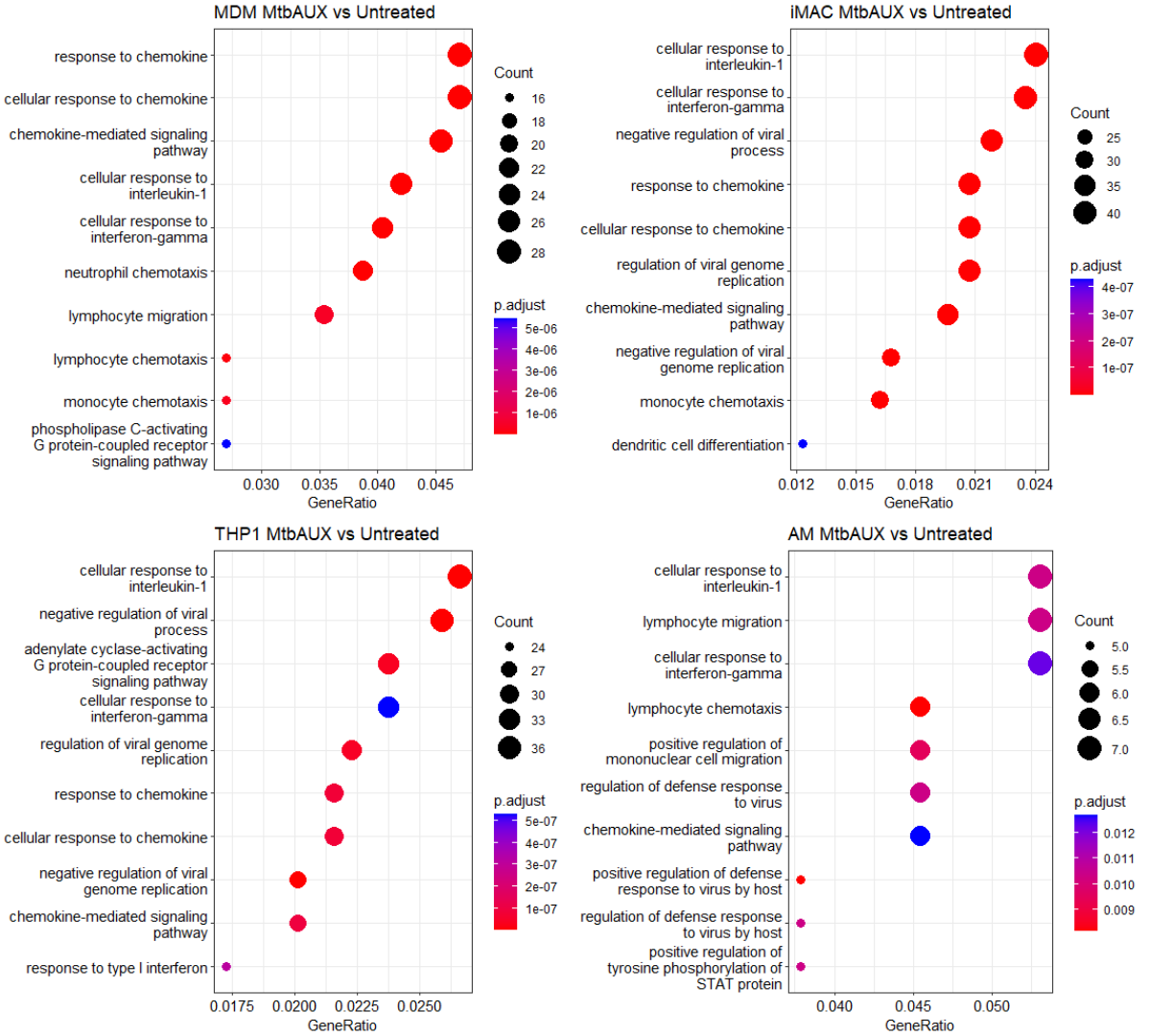

Figure 3-5 iMACs, AMs, MDMs and THP1 are all enriched for cellular response to IL-1 and IFN-gamma. The dotplot of enriched GO terms in MDMs, iMACs, THP1 and AMs, was generated based on the Mtb vs Untreated significantly differentially expressed genes (-1 > log2FoldChang > 1 and p-value < 0.05) displaying the top 10 significantly (adjusted P-value < 0.05) enriched biological processes. The x-axis displays the geneRatio (ratio of input genes that are annotated in the given GO term), while the size of the dot indicates the number of genes that conformed to the respective GO term. The color of the dot indicates the Benjamini-Hochberg adjusted P-value.

WGCNA observations (see Figure 3-8). MDMs are most significantly enriched for biological processes related to chemokines and chemotaxis, which, although represented, is not as prominently featured in the other macrophages. Interestingly, although the cellular response to IFN-gamma features prominently, no IFN-gamma mRNA was detected in any of the query cells. This analysis shows that IL-1 and IFN-gamma are main inflammatory drivers activated by Mtb and that chemokines affect cellular signaling in all macrophage phenotypes.

3.3 Weighted gene correlation network analysis

In order to investigate similarities and differences in the expression of clusters of co-expressed genes, weighted gene correlation network analysis was employed. 49 modules were identified (see Appendix Figure 2) and the correlation between module and sample was visualized in a heatmap (see Figure 3-6). The linear modeling was then employed to identify three modules that were significantly (adjusted P-value < 0.05) upregulated in response to Mtb.

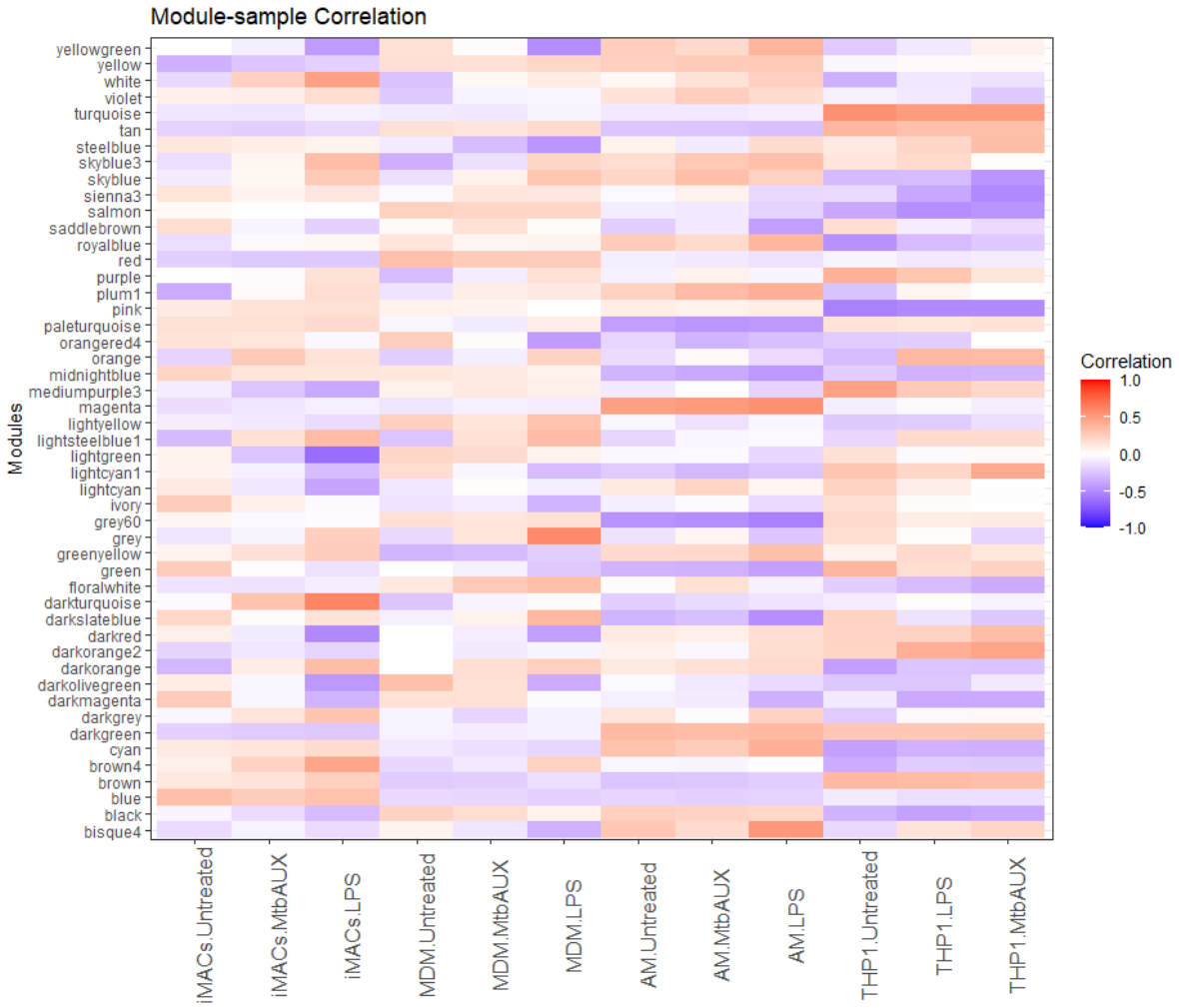

Figure 3-6. Three modules of co-expressed genes are significantly associated with Mtb infection of macrophages. Heatmap showing the association between the modules of co-expressed genes (y-axis) identified by the WGCNA analysis, and the samples, averaged for replicates (x-axis). Modules lightsteelblue1, orange and white were identified to be significantly (adjusted P-value < 0.05) differentially expressed between Mtb- and untreated cells using linear modeling. The correlation value is expressed as a color from -1 (blue) to 1 (red).

The degree to which the modules of genes were upregulated in response to Mtb differed between the cell types with the AMs consistently showing the least amount of differential expression, and iMACs showing the most (see Figure 3-8). Module 41 (lightsteelblue1) showed highest correlation with the change in expression between untreated and Mtb treated samples. This module consisted of 68 genes that are enriched for biological processes related to regulation of T-cell activation, type 1 interferon production and cellular responses to interleukin-1 and interferon-gamma. Furthermore, the strong correlation between module membership (MM) and gene significance (GS) (r =0.75, p-value = 1.8e-13) indicates that the hub genes in the module are significant in the cellular response to Mtb (see Figure 3-7). The main three hub genes in this module are indoleamine 2,3-dioxygenase 1 (IDO1), aconitate decarboxylase 1 (ACOD1) and intercellular adhesion molecule 1 (ICAM1).

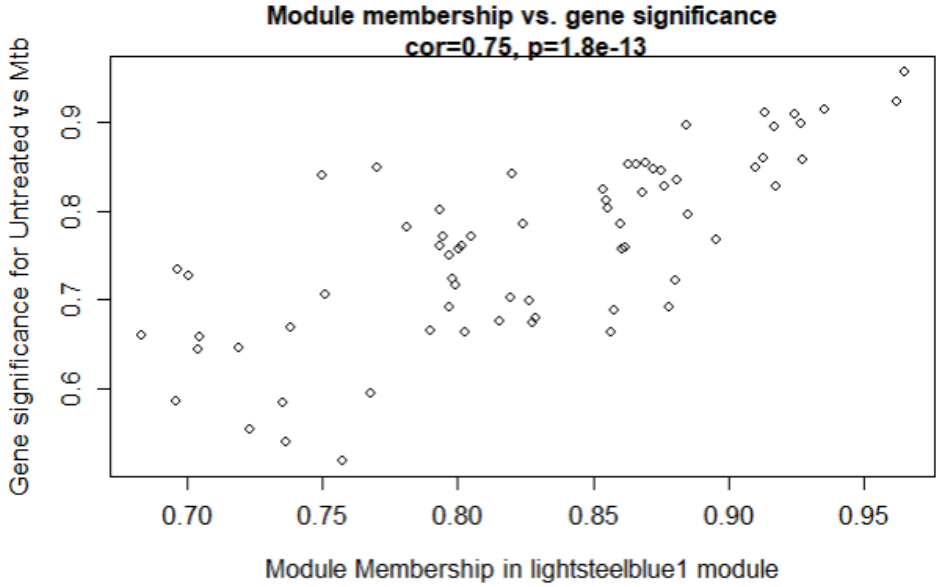

Figure 3-7. Gene significance and module membership are highly correlated in module 41. Scatterplot of the gene significance (y-axis) and module membership (x-axis) of all the genes in module 41 (lightsteelblue1), fit to a linear model to show the correlation (cor = 0.75) and the p-value (1.8e-13).

The relationship between module 25 (orange) and the stimulated samples had higher variation, with Mtb infected MDMs and AMs showing lower expression of this module than iMACs and THP1 (see Figure 3-8). This strong association iMACs and THP1 show with type 1 interferon and negative regulation of viral responses is supported by the enrichment analysis (see Figure 3-5) as well as the high expression of similar genes in the hierarchical clustering heatmap (see Figure 3-4). The correlation between GS and module membership (MM) was lower than module 41 (r = 0.4, p-value = 1.5e-7), with C-X-C motif chemokine ligand 10 (CXCL10), ETS Variant Transcription Factor 7 (ETV7), Signal transducer and activator of transcription 1 and 2 (STAT1/2) and CXCL11, being the genes with the highest MM and GS.

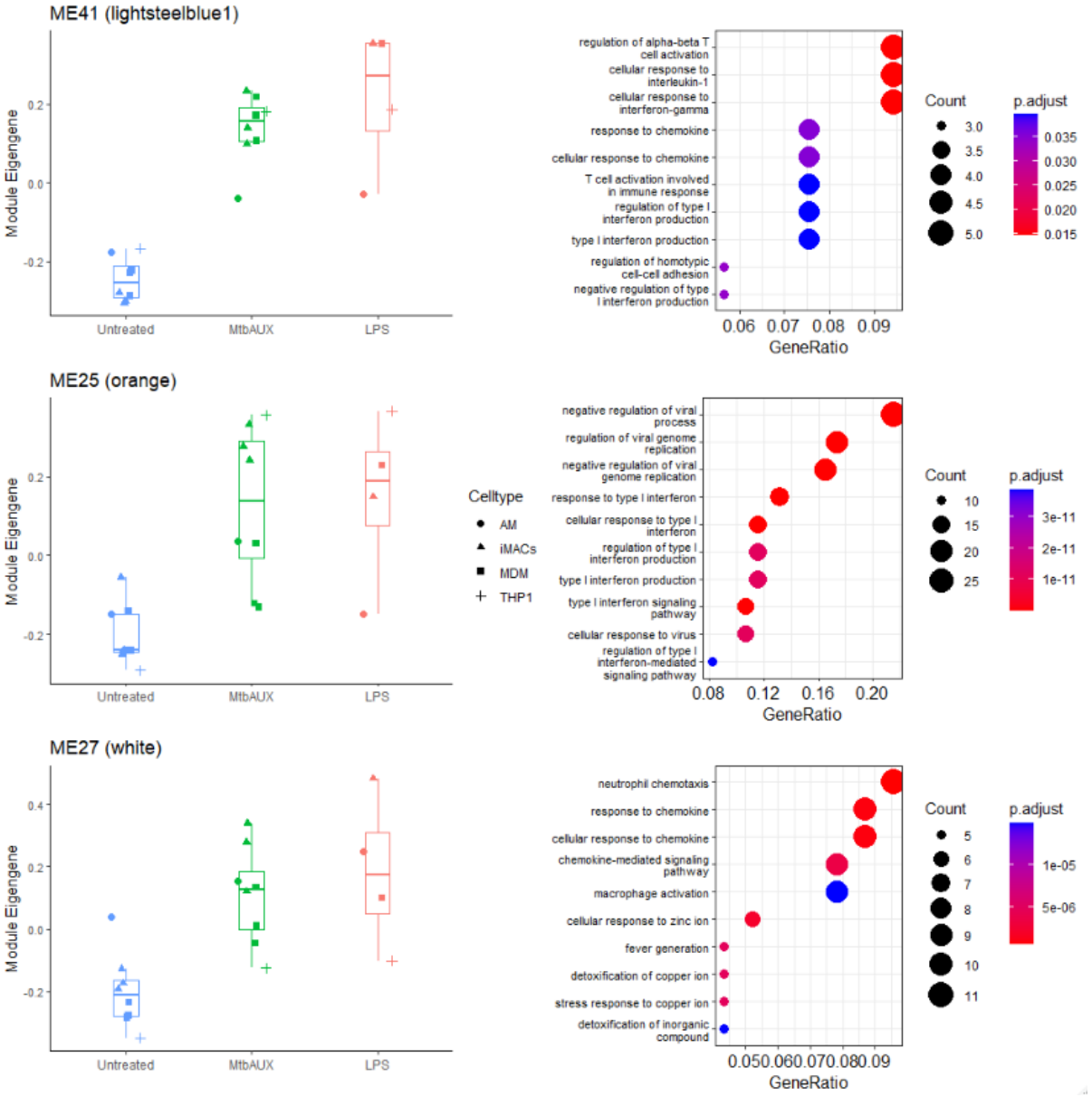

Figure 3-8. iMACs and THP1 display a strong type 1 interferon response. Boxplots of the module eigengene values (measure of collective module gene expression) for the samples grouped by treatment type. GO enrichment of biological processes related to the genes in modules 41, 25 and 27 respectively, with the x-axis displaying the geneRatio (ratio of input genes that are annotated in the given GO term), and the size of the dot indicating the number of genes that conformed to the respective GO term.

Module 27 (orange) is most significantly enriched for genes related to neutrophil chemotaxis, macrophage activation, cellular responses to chemokines and unexpectedly, cellular responses to metal ions such as zinc and copper (see Figure 3-8). The THP1 cells showed a consistently lower expression of this module for all treatment types, although some upregulation can be observed in response to stimuli. Interestingly, untreated AMs display a significantly higher expression of this module in comparison to the other cell types however, the upregulation was not as large as iMACs, which expressed the module 27 genes at the highest level after stimulation.

3.4 Pathway maps provide indications of differing regulation of TB related processes

The differential expression of key receptors, intermediate signaling molecules and pathway products in the tuberculosis KEGG pathway (obtained from the KEGG database March 2022, accession code hsa05152, https://www.genome.jp/entry/pathway+hsa05152) was visualized using the pathview package [106]. This provides an overview of the of key differences between the cells with regards to Mtb infection specific processes, that is useful for selecting what specific immunological events to investigate further.

From these pathway maps, differences can be observed in the differential expression of genes related to antigen presentation and inhibition of apoptosis, as well as in the cell surface receptors and anti-inflammatory cytokine expression. Furthermore, the expression

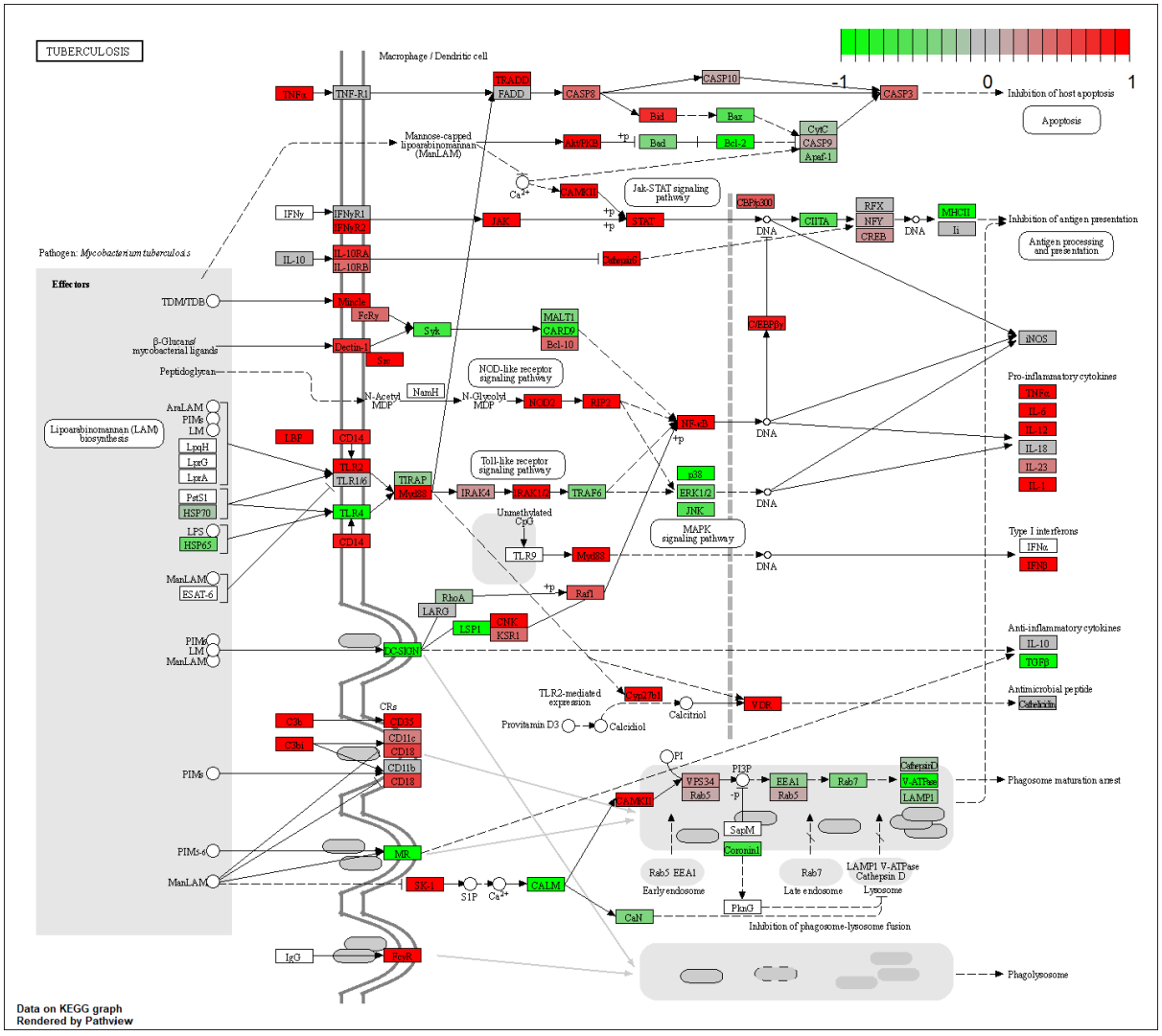

Figure 3-9. Pathway map indicates MHC class 2 and TGFB downregulation in AMs.

The log2 fold change is denoted by the color of the gene boxes from -1 (green) to 1 (red). The boxes represent a single gene (i.e. IL-10) or a group of closely related genes (i.e. MHC class 2 molecules) of which the mean log2 fold change is calculated and displayed. The image (accession code hsa05152) was downloaded from the KEGG database (https://www.genome.jp/entry/pathway+hsa05152) in March 2022.

of pro-inflammatory cytokines and their upstream regulators like NFkB, show a high degree of similarity between cell types (see Figure 3-9, Figure 3-9, Figure 3-11, Figure 3-12).

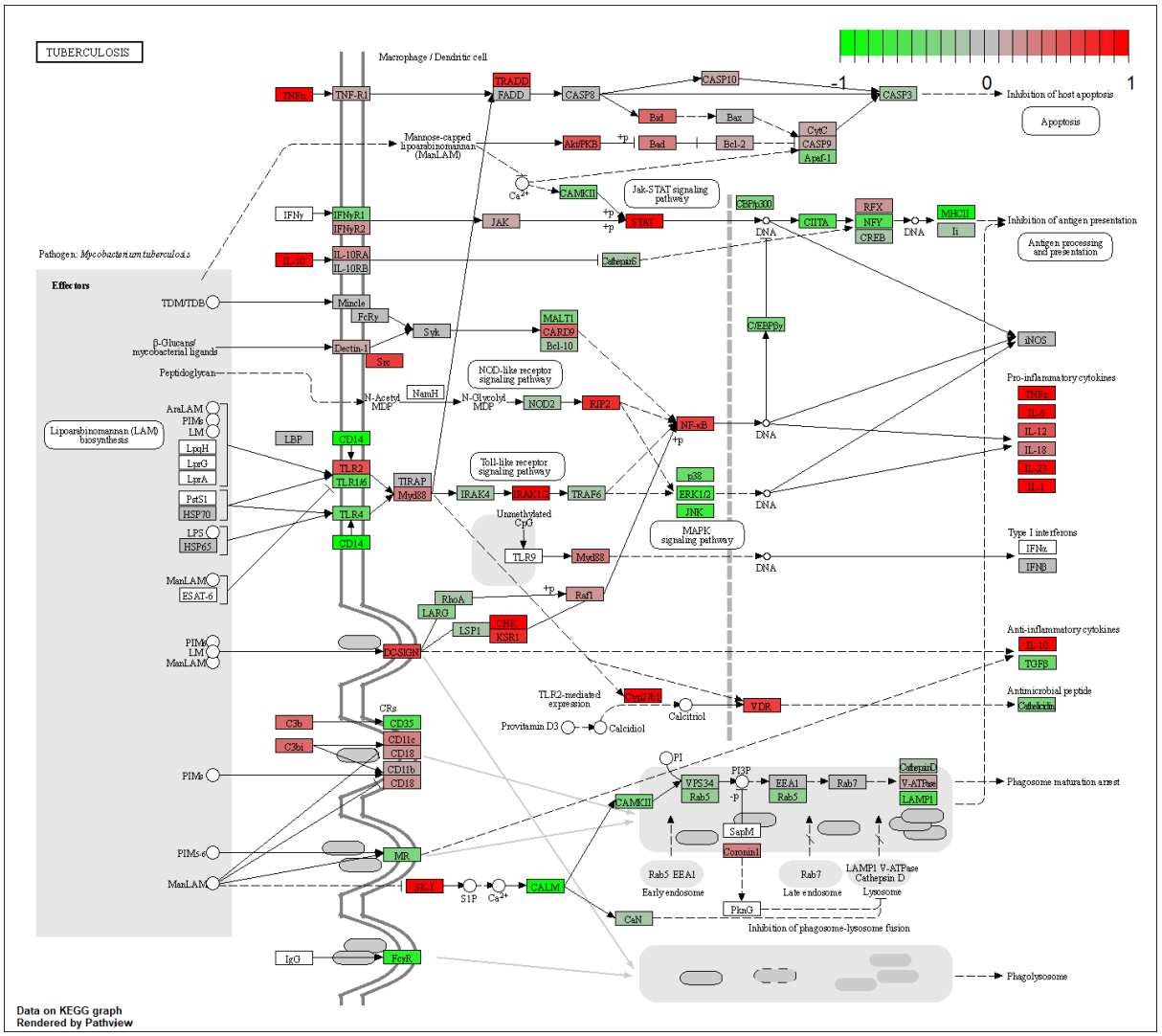

Figure 3-10. Pathway map indicates MHC class 2 downregulation and IL-10 upregulation in iMACs.

The log2 fold change is denoted by the color of the gene boxes from -1 (green) to 1 (red). The boxes represent a single gene (i.e. IL-10) or a group of closely related genes (i.e. MHC class 2 molecules) of which the mean log2 fold change is calculated and displayed. The image (accession code hsa05152) was downloaded from the KEGG database (https://www.genome.jp/entry/pathway+hsa05152) in March 2022.

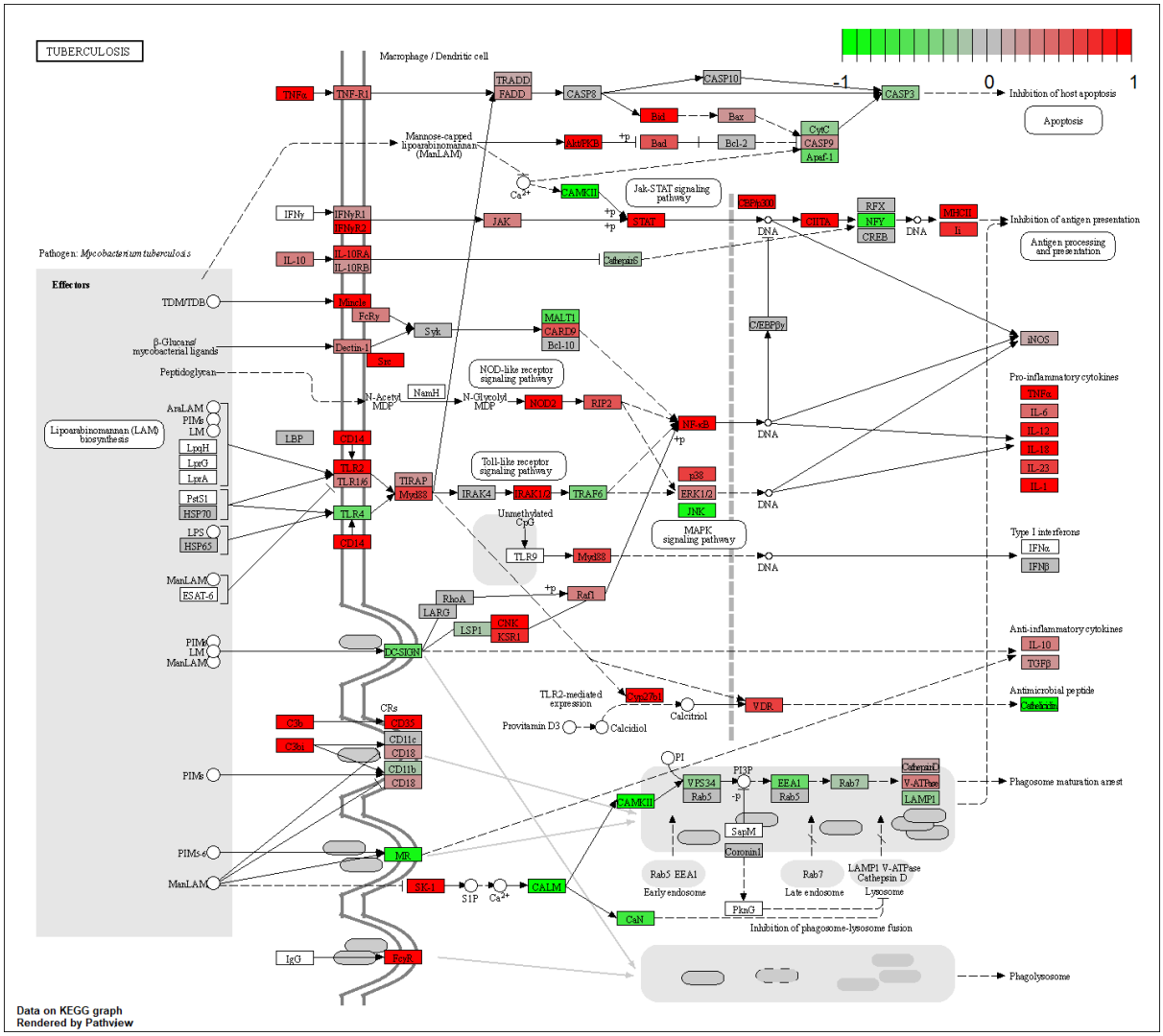

Figure 3-11. Pathway map indicates MHC class 2 upregulation in MDMs.

The log2 fold change is denoted by the color of the gene boxes from -1 (green) to 1 (red). The boxes represent a single gene (i.e. IL-10) or a group of closely related genes (i.e. MHC class 2 molecules) of which the mean log2 fold change is calculated and displayed. The image (accession code hsa05152) was downloaded from the KEGG database (https://www.genome.jp/entry/pathway+hsa05152) in March 2022.

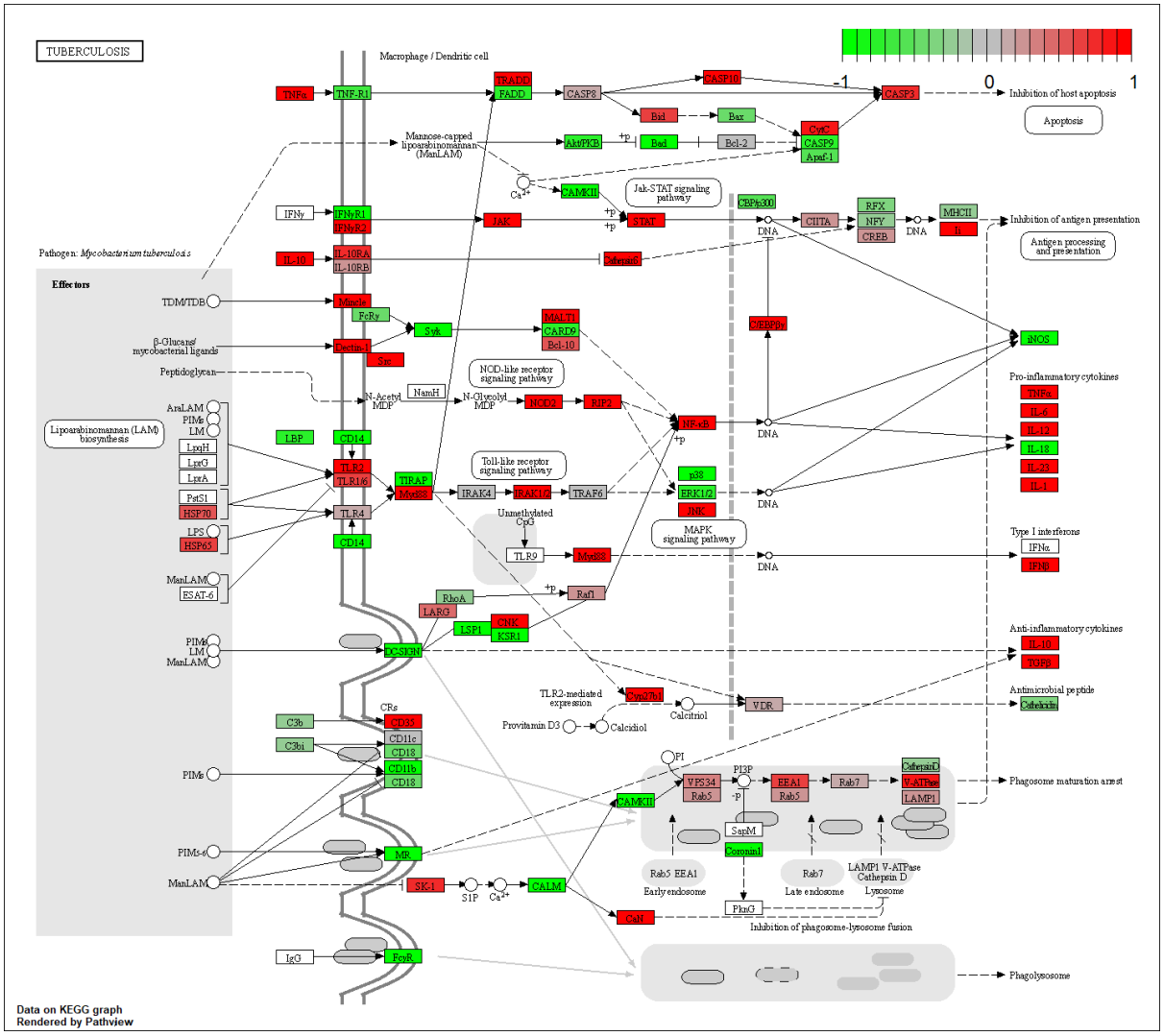

Figure 3-12. Pathway map indicates an upregulation of IFN-beta and anti-inflammatory cytokines in THP1.

The log2 fold change is denoted by the color of the gene boxes from -1 (green) to 1 (red). The boxes represent a single gene (i.e. IL-10) or a group of closely related genes (i.e. MHC class 2 molecules) of which the mean log2 fold change is calculated and displayed. The image (accession code hsa05152) was downloaded from the KEGG database (https://www.genome.jp/entry/pathway+hsa05152) in March 2022.

3.5 iMACs and THP1 have many more differentially expressed genes than AMs and MDMs

To look at the number of differentially expressed genes that were shared between the different cells types a four-way Venn diagram was made. The number of significantly (p-value < 0.05 and -1 > log2FoldChange > 1) differentially expressed protein coding genes varied greatly between the cell types, with iMACs having the most significantly differentially expressed genes (1766) and AMs having the least (205). Only 20 significantly differentially expressed protein coding genes are shared among all four cell types, however, this is largely limited by the low number of SDEGs identified in the AMs and if removed the three remaining cell types share 143 SDEGs. Interestingly, THP1 share the most SDEGs with AMs, contrasting with the highly different expression profiles (see Figure 3-1, Figure 3-2, Figure 3-3).

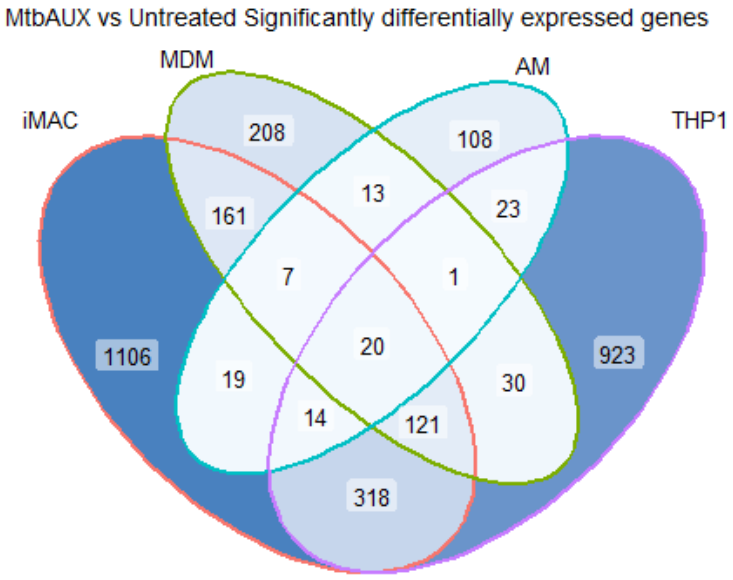

Figure 3-13. Venn diagram shows the high variation in the number of differentially expressed genes between the macrophages. Venn diagram of Mtb vs Untreated significantly differentially expressed genes (-1 > log2FoldChange > 1 and p-value < 0.05) shared between cell types.

3.6 Differential expression of genes related to spesific immune processes

The exploratory analyses provided insights into the differences and similarities in regulation of biological processes involving many genes. The results discussed above, together with a review of the current literature, were used to select specific aspects of the host-pathogen interactions of which to focus on. These specific aspects include the cell surface receptors, inflammatory response, antigen processing and T-cell activation, and cell death pathways. Little evidence of cell death was observed in the exploratory analyses; however, this is a major area of tuberculosis research, an area that the CEMIR research group, the primary benefactors of the author of this thesis, is deeply invested in.

The expression of key genes (selected and curated by the author of the thesis), central to immunological processes important during Mtb infection, were compared by creating heatmaps and corresponding dendrograms generated using hierarchical clustering. This allows the reader to easily see patterns of up and downregulation, compare expression

levels and, using the dendrograms, see patterns of similarity between treatment groups and cell types.

3.6.1 THP1 cells display significant differences in PRR expression

The fate of Mtb inside the cell, as well as the induced inflammatory response, can differ based on what receptor that is responsible of recognizing and internalizing the bacteria [17]. The basal expression, as well as the gene expression changes of these receptors in response to stimuli is therefore compared.

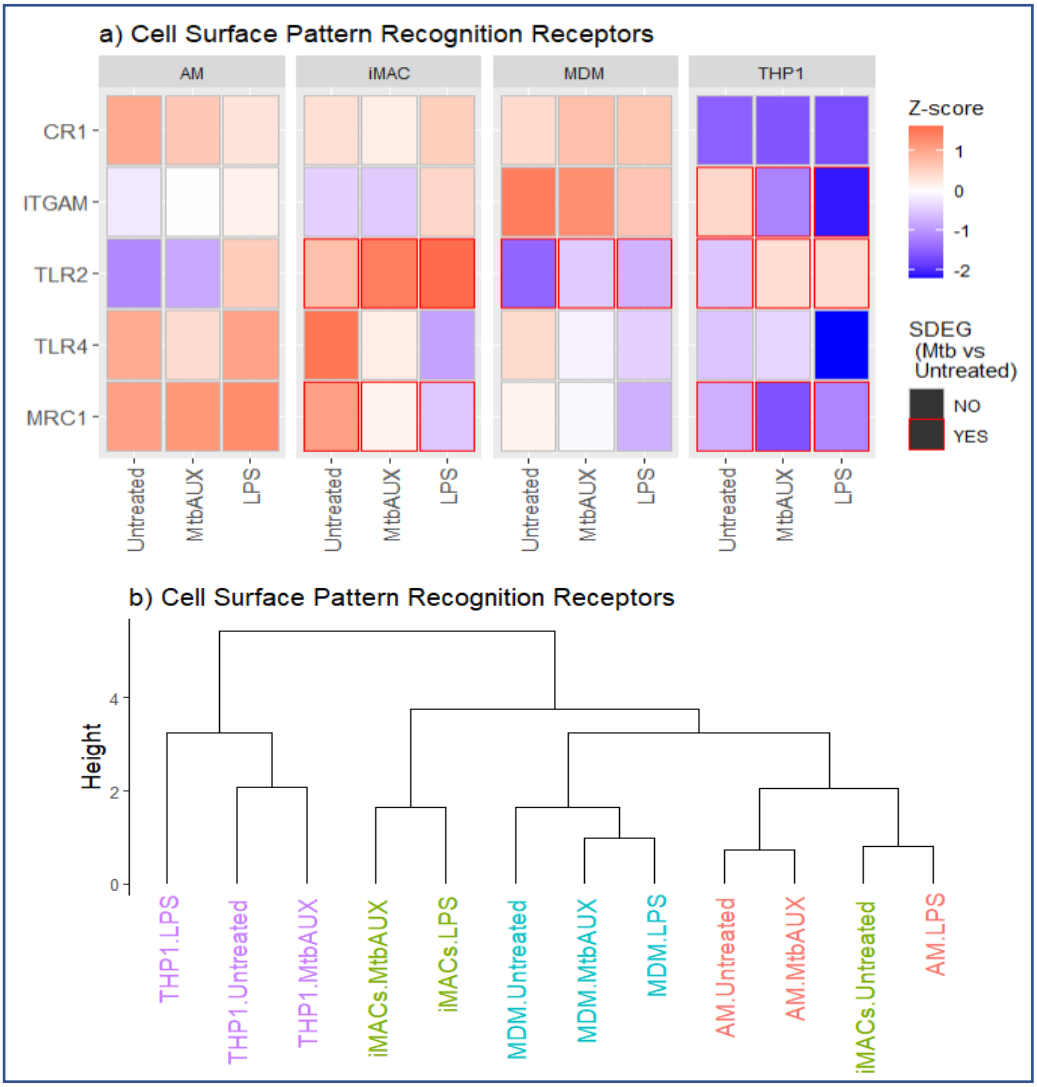

Figure 3-14. THP1 show significant differences in PRR expression.

(a) Heatmap where each row represents a gene, and the columns represent the treatment groups separated by cell type. The z-scores, averaged for cell type-treatment replicates, represent gene-wise relative expression (see equation 1) and are visualized by a continuous color gradient from low (blue) to high (red). Mtb vs Untreated significantly differentially expressed genes (-1 > log2FoldChang > 1 and p-value < 0.05) are annotated by a red outline. (right) Hierarchical clustering dendrogram generated based on the expression correlation of the genes in the heatmap.

The expression of most of the selected cell surface PRRs was similar for untreated AMs, iMACs and MDMs, while the low expression of these receptors in THP1 cells make them a bit of an outlier (see Figure 3-14b). Notable exceptions are the high basal expression of

TLR2 in iMACs and complement receptor 3 (ITGAM) in MDMs. Interestingly, except TLR2 in iMACs, MDMs and THP1, most of the receptors show a downregulating trend after 20 hours of stimuli exposure.

3.6.2 Many similarities in the expression of pro-inflammatory mediators but the MDM response in subdued

The hallmark drivers of the inflammatory response during Mtb infection were compared revealing a high degree of similarity in the upregulation patterns of AMs, iMAC and THP1, with the major difference being the significant upregulation of IL-23 and GM-CSF (CSF2) in AMs. Although all pro-inflammatory cytokines were upregulated after exposure to stimuli, the MDMs showed an unexpectedly subdued response in comparison with the other

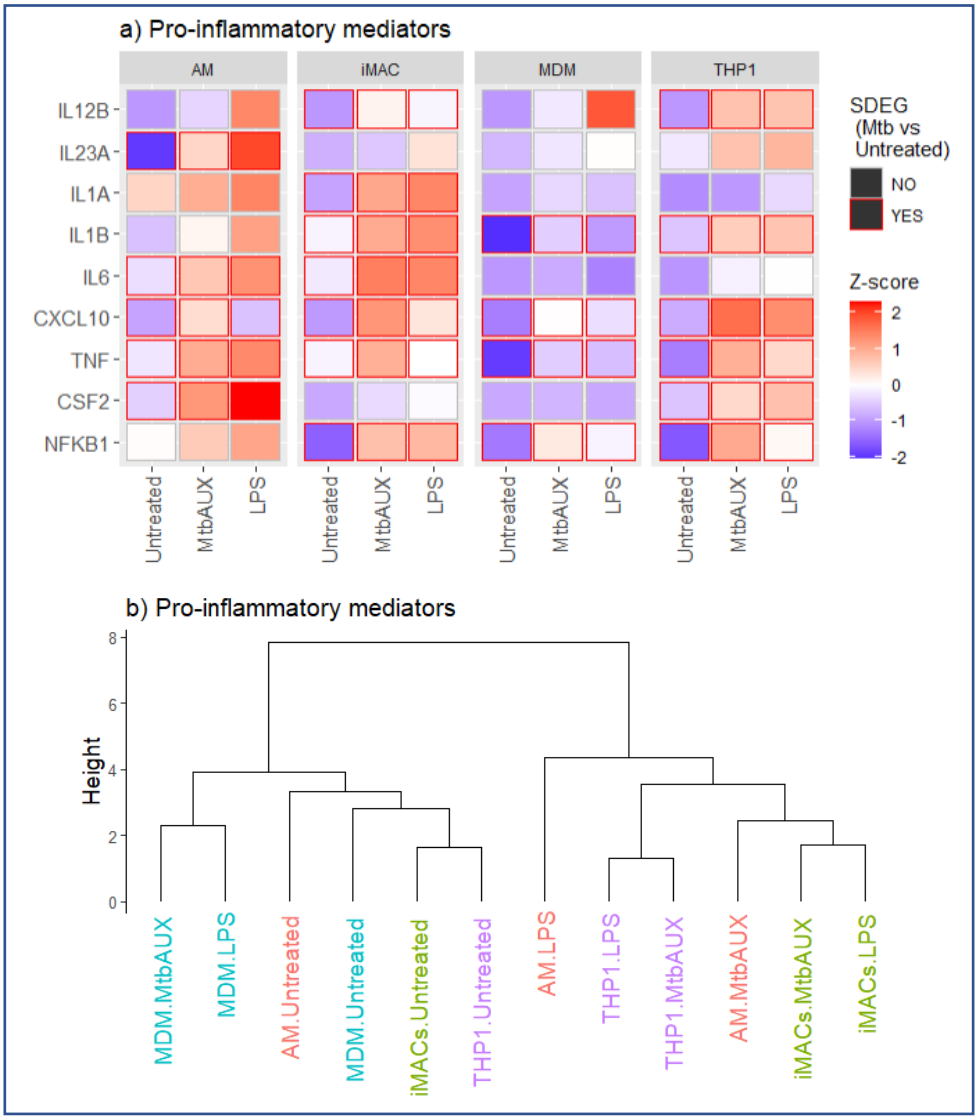

Figure 3-15. Mtb induced gene expression of pro-inflammatory mediators in AMs is most accurately reflected by iMACs.

(a) Heatmap where each row represents a gene, and the columns represent the treatment groups separated by cell type. The z-scores, averaged for cell type-treatment replicates, represent gene-wise relative expression (see equation 1) and are visualized by a continuous color gradient from low (blue) to high (red). Mtb vs Untreated significantly differentially expressed genes (-1 > log2FoldChang > 1 and p-value < 0.05) are annotated by a red outline. (b) Hierarchical clustering dendrogram generated based on the expression correlation of the genes in the heatmap.

cell types. However, TNF, IL-1B and IP-10 (CXCL10), arguably the most important, were significantly upregulated. NFkB was also upregulated in iMACs, MDMs and THP1, and while AMs do show a higher expression of the signaling molecule this was not a significant observation.

The effect of Mtb and LPS stimuli of the gene expression of iMACs, AMs and THP1 is highlighted by the distinct clustering of the samples according to treatment (see Figure 3-15). Interestingly, the dendrogram also shows that iMACs and AMs had the most similar expression of the pro-inflammatory mediators after Mtb infection.

3.6.3 Anti-inflammatory cytokines

The role of anti-inflammatory cytokine production induced by Mtb as well as the anti-inflammatory characteristics of AMs *in vivo* are of great interest when comparing the immune response of the cells, as they have several important down-stream effects that are believed to be promoted by the pathogen.

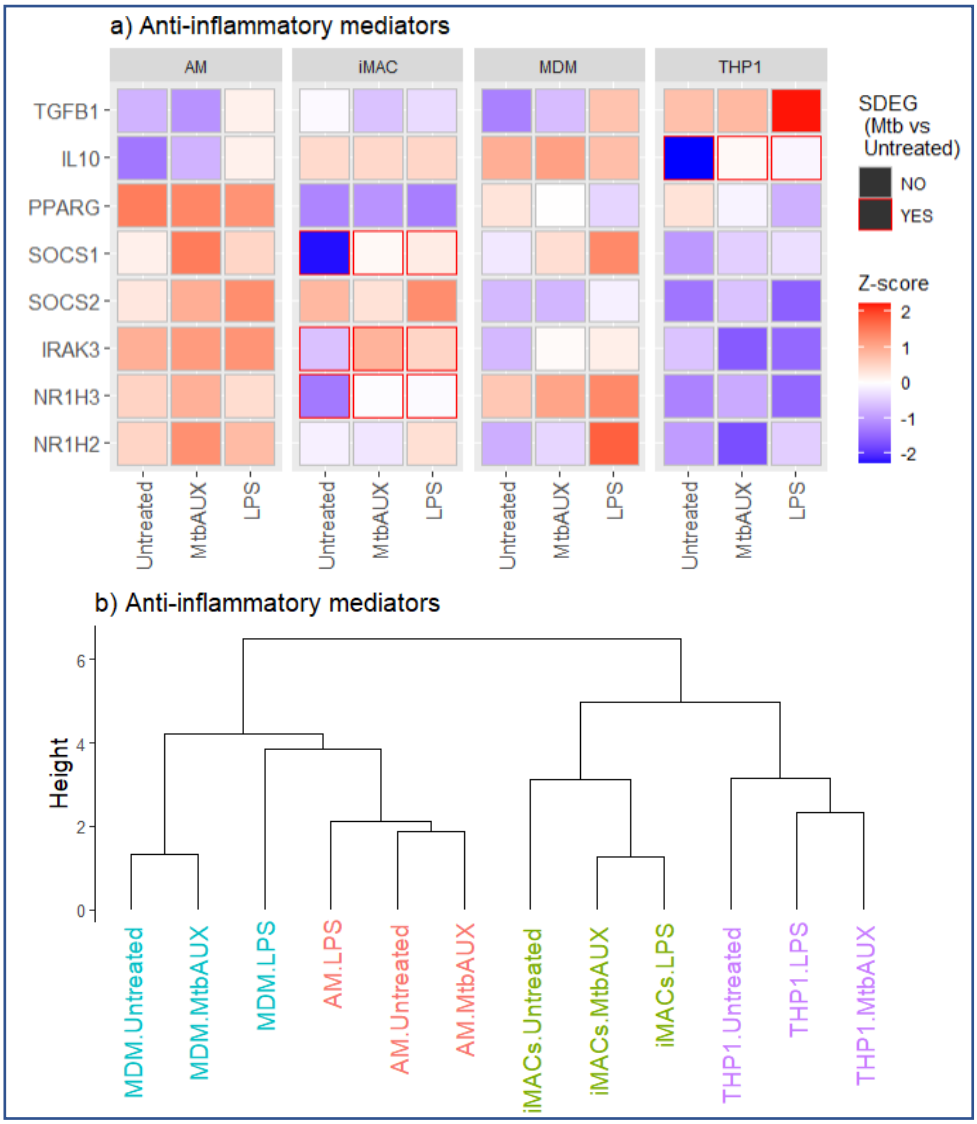

Figure 3-16. Expression of anti-inflammatory cytokines changes little in response to stimuli.

(a) Heatmap where each row represents a gene, and the columns represent the treatment groups separated by cell type. The z-scores, averaged for cell type-treatment replicates, represent gene-wise relative expression (see equation 1) and are visualized by a continuous color gradient from low (blue) to high (red). Mtb vs Untreated significantly differentially expressed genes (-1 > log2FoldChang > 1 and p-value < 0.05) are annotated by a red outline. (right) Hierarchical clustering dendrogram generated based on the expression correlation of the genes in the heatmap.

Except for TGFB and IL-10, AMs show a trend of higher expression of anti-inflammatory mediators than the other cell types. iMACs do show a significant upregulation of several important regulatory proteins such as SOCS1 and IRAK3, as well as the LXR transcription factor NR1H3. However, this is only in response to the stimuli whereas AMs express these factors at a higher level even when unstimulated. Interestingly, IL-10 expression in iMACs and MDMs show little change but much higher expression than AMs and THP1, which was not expected. The dendrogram generated from the gene expression of these anti-inflammatory mediators indicate that there are little treatment related changes in these genes as the samples cluster according to cell type and not treatment group.

3.6.4 IFN-beta is expressed in iMACs and THP1 but not in AMs and MDMs

The differences in type 1 interferon related cellular processes identified by the exploratory analyzes as well as its complex role during bacterial infection prompts an investigation of the expression of type 1 interferon related genes. Therefore, the expression of type 1 interferon response genes, as well as IFN-beta was visualized in a heatmap and, to see similarities between the cell types a dendrogram was created based on the expression of the selected genes.

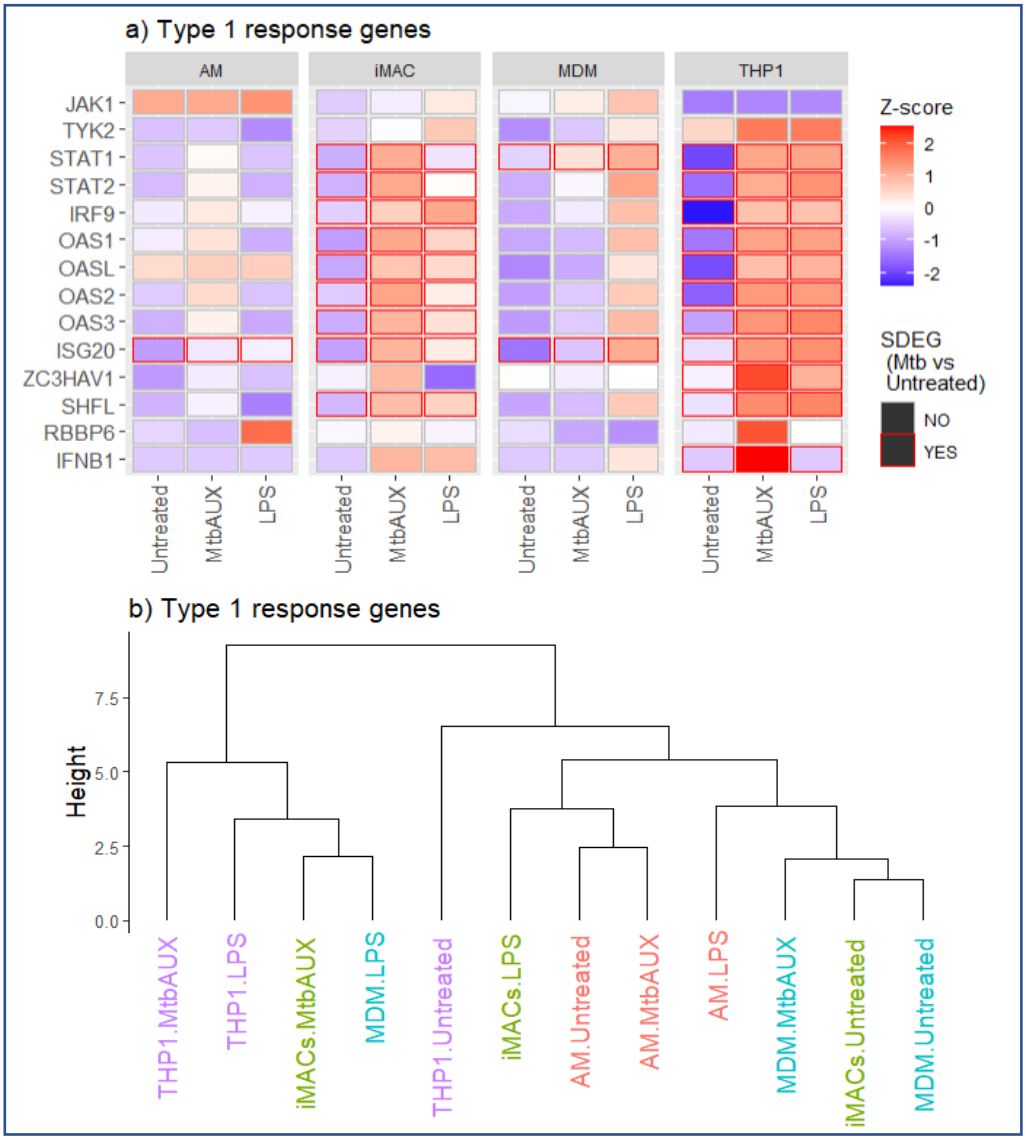

Figure 3-17. iMACs and THP1 show a strong upregulation of type 1 interferon response genes.

(a) Heatmap where each row represents a gene, and the columns represent the treatment groups separated by cell type. The z-scores, averaged for cell type-treatment replicates, represent gene-wise relative expression (see equation 1) and are visualized by a continuous color gradient from low (blue) to high (red). Mtb vs Untreated significantly differentially expressed genes (-1 > log2FoldChang > 1 and p-value < 0.05) are annotated by a red outline. (b) Hierarchical clustering dendrogram generated based on the expression correlation of the genes in the heatmap.

The expression of type 1 interferon response genes differs greatly between AMs/MDMs and iMACs/THP1 and correlates clearly with the presence or absence of IFN-beta.

Interestingly, there is one exception, LPS treated THP1 cells which did not produce IFN-beta, still showed significant upregulation of most of the response genes. The dendrogram generated based on the expression of the selected type 1 interferon response genes forms two clusters according to the presence of IFN-beta expression (except LPS treated THP1). This suggests that the response genes are indeed expressed as a result of IFN-beta production. Interestingly, IFN-alpha was not expressed in any of the samples.

3.6.5 The data suggests that MHC class 2 molecule expression is regulated differently between MDMs and AMs

Mtb's ability to suppress antigen presenting processes in macrophages and other antigen presenting cells is well defined and is believed to occur via several mechanisms, one of which is the downregulation of MHC class 2 molecules. Therefore, the log2 fold change (Mtb vs Untreated) of all the MHC class 2 molecules is visualized to determine whether this downregulating trend is seen in the query cells.

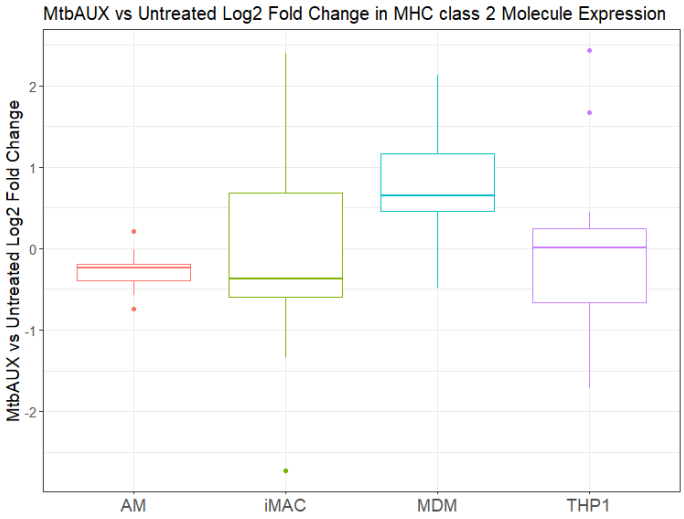

Figure 3-18. The differential expression of MHC class 2 molecules differs between AMs and MDMs. Mtb vs Untreated Log2 fold change in MHC class 2 molecule expression for AMs, iMACs, MDMs and THP1.

The log2 fold change in expression of the 15 MHC class 2 molecule subunits was highly variable for iMACs and THP1 while AMs showed a clear, albeit small, downregulation contrasting the upregulation seen in MDMs of the antigen presenting molecules (see Figure 3-18). The master regulator CIITA, believed to induce MHC class 2 expression was slightly downregulated in the AMs and iMACs (log2 fold change = -0.5, not significant), and upregulated (log2 fold change = 1.13, not significant) in MDMs which correlates with the transcription factor function.

3.6.6 Cell death pathways

3.6.6.1 Mtb challenge affect on the expression of apoptosis inhibiors is more evident in iMACs and THP1 than in MDMs and AMs

The inhibition of apoptosis has been shown to be preferential to Mtb in that necrotic cell death pathways are associated with Mtb immune evasion and dissemination [74]. The expression of apoptosis inhibitors was therefore explored in order to determine if there Mtb induced an upregulation in these inhibitors that might lead to necrotic cell death.

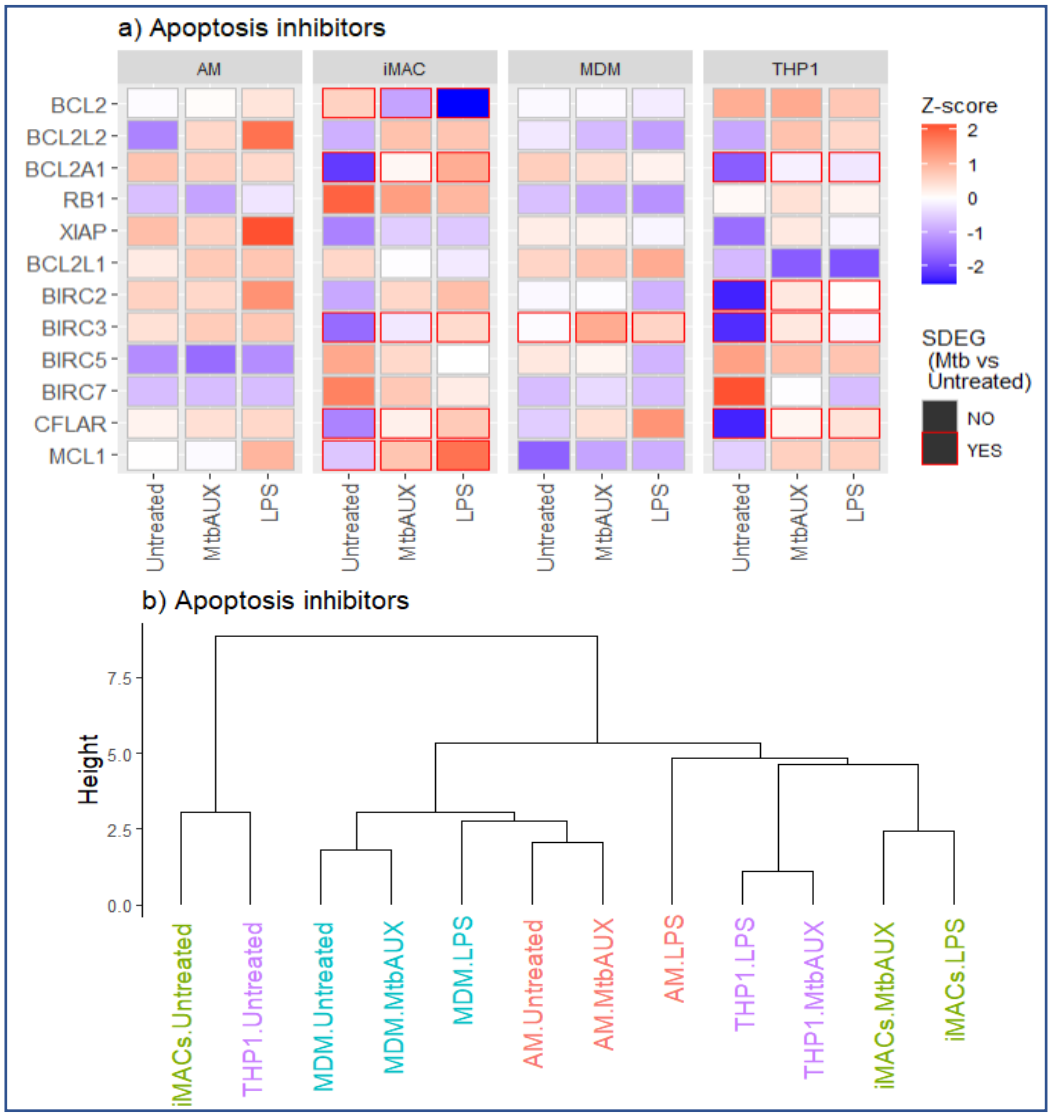

Figure 3-19. iMACs and THP1 show significant upregulation of several apoptosis inhibitor genes.

(a) Heatmap where each row represents a gene, and the columns represent the treatment groups separated by cell type. The z-scores, averaged for cell type-treatment replicates, represent gene-wise relative expression (see **Equation 1**) and are visualized by a continuous color gradient from low (blue) to high (red). Mtb vs Untreated significantly differentially expressed genes (-1 > log2FoldChang > 1 and p-value < 0.05) are annotated by a red outline. (b) Hierarchical clustering dendrogram generated based on the expression correlation of the genes in the heatmap**.**

Several key apoptosis inhibitors were significantly upregulated in iMACs and THP1, while MDMs and AMs showed little change in expression of these genes as a result of Mtb exposure (see figure 21). Interestingly, iMACs also showed a downregulation of the anti-apoptosis protein Bcl-2 which contrasts the general upregulation of pro-survival signals.

3.6.6.2 THP1 regulates necroptosis related gene expresseion differently from the other cell types

To look for differences in the regulation of necroptosis related genes in the sequenced macrophages, the expression of central mediators was visualized. Key to necroptosis activation is the inhibition of apoptosis (discussed above) as well as the expression of necroptosis regulating proteins, the constituents of complex 1 and 2 and effector proteins like MLKL.

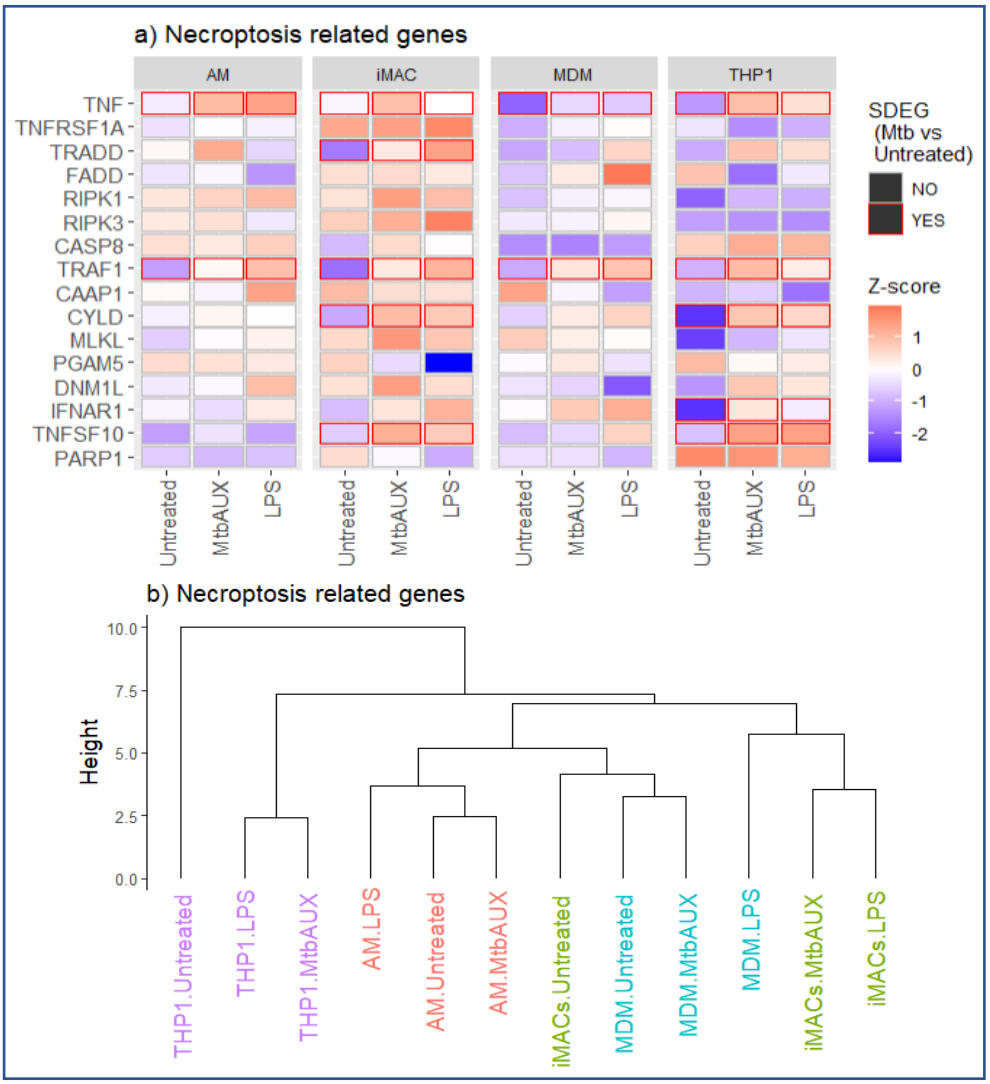

Figure 3-20. Little evidence of Mtb induced upregulation of necroptosis related genes can be observed.

(a) Heatmap where each row represents a gene, and the columns represent the treatment groups separated by cell type. The z-scores, averaged for cell type-treatment replicates, represent gene-wise relative expression (see **Equation 1**) and are visualized by a continuous color gradient from low (blue) to high (red). Mtb vs Untreated significantly differentially expressed genes (-1 > log2Fold-Chang > 1 and p-value < 0.05) are annotated by a red outline. (b) Hierarchical clustering dendrogram generated based on the expression correlation of the genes in the heatmap.

mRNA for the proteins that form Complex 1 and 2 (RIPK1, cFLIP, FADD, CASP8 and TNFR1 (TNFRSF1A)) was detected in all cell types, indicating that the necroptosis required complexes can be formed. Interestingly, iMACs and THP1 show a low basal expression and a tendency to upregulate many of the necroptosis related genes in response to simuli, while AMs and MDM show little differential expression. The iMACs treated with Mtb seem to show a similar expression pattern as MDM and iMACs treated with LPS and these samples therefore cluster together (see figure 22b).

3.6.6.3 THP1 expression of ferroptosis related genes contrasts the other macrophages

The expression of ferroptosis related genes show little differentiation based on the treatment of the cells highlighted by the clustering pattern seen in the dendrogram (see figure 23). Although there were some differentially expressed genes in these do not indicate that ferroptosis is occurring in the cells after 20 hours of stimuli. Interestingly, AMs showed the

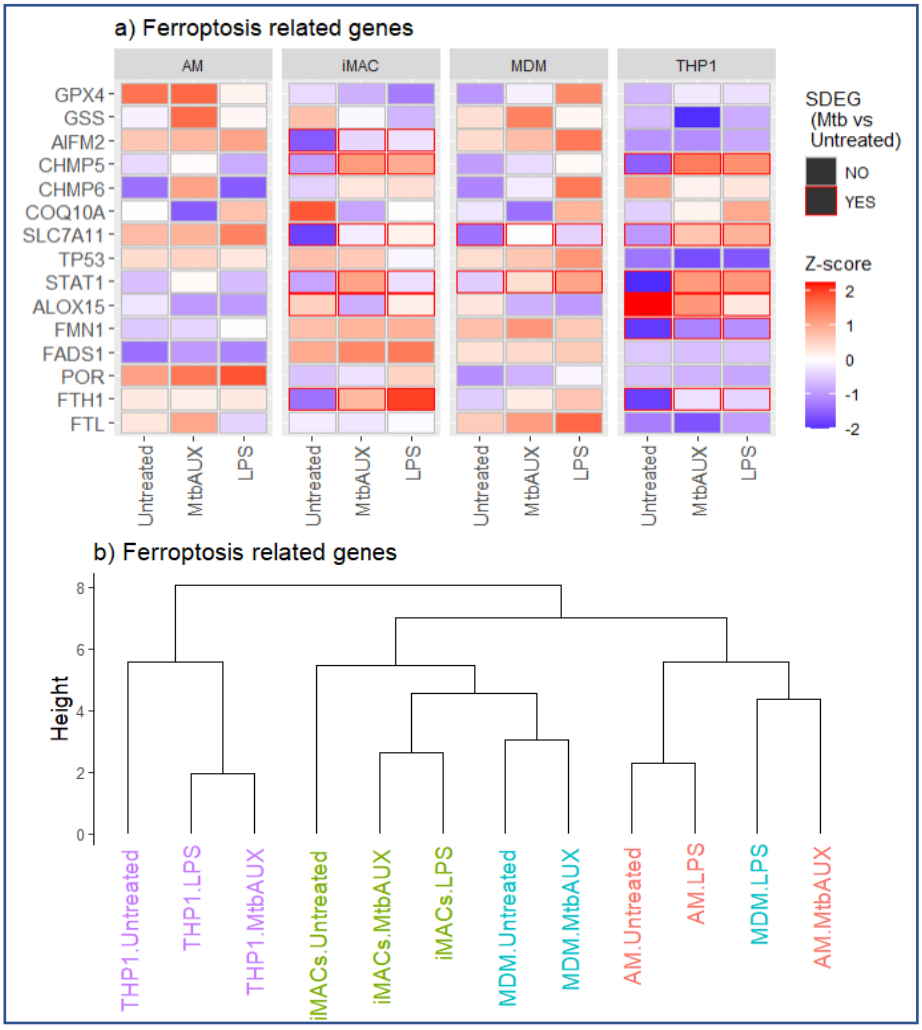

Figure 3-21. Differential expression of ferroptosis related genes indicate that ferroptosis is not occurring. (a) Heatmap where each row represents a gene, and the columns represent the treatment groups separated by cell type. The z-scores, averaged for cell type-treatment replicates, represent gene-wise relative expression (see **Equation 1**) and are visualized by a continuous color gradient from low (blue) to high (red). Mtb vs Untreated significantly differentially expressed genes (-1 > log2FoldChang > 1 and p-value < 0.05) are annotated by a red outline. (b) Hierarchical clustering dendrogram generated based on the expression correlation of the genes in the heatmap.

highest expression of GPX4, and an upregulation (not significant) in GSS, the two main effector proteins responsible for preventing the lipid peroxidation that induces ferroptosis.

3.6.6.4 Little evidence of Mtb induced pyroptosis could be observed in the macrophages

Pyroptosis is a cell death pathway that has only recently been shown to be involved in Mtb infected macrophages [72]. The upregulation of the NLRP3 or AIM2 inflammasome components is believed to be a hallmark of the pyroptosis pathway and should therefore be more easily observed with mRNA sequencing data if the cell death pathway is activated at the time of RNA extraction.

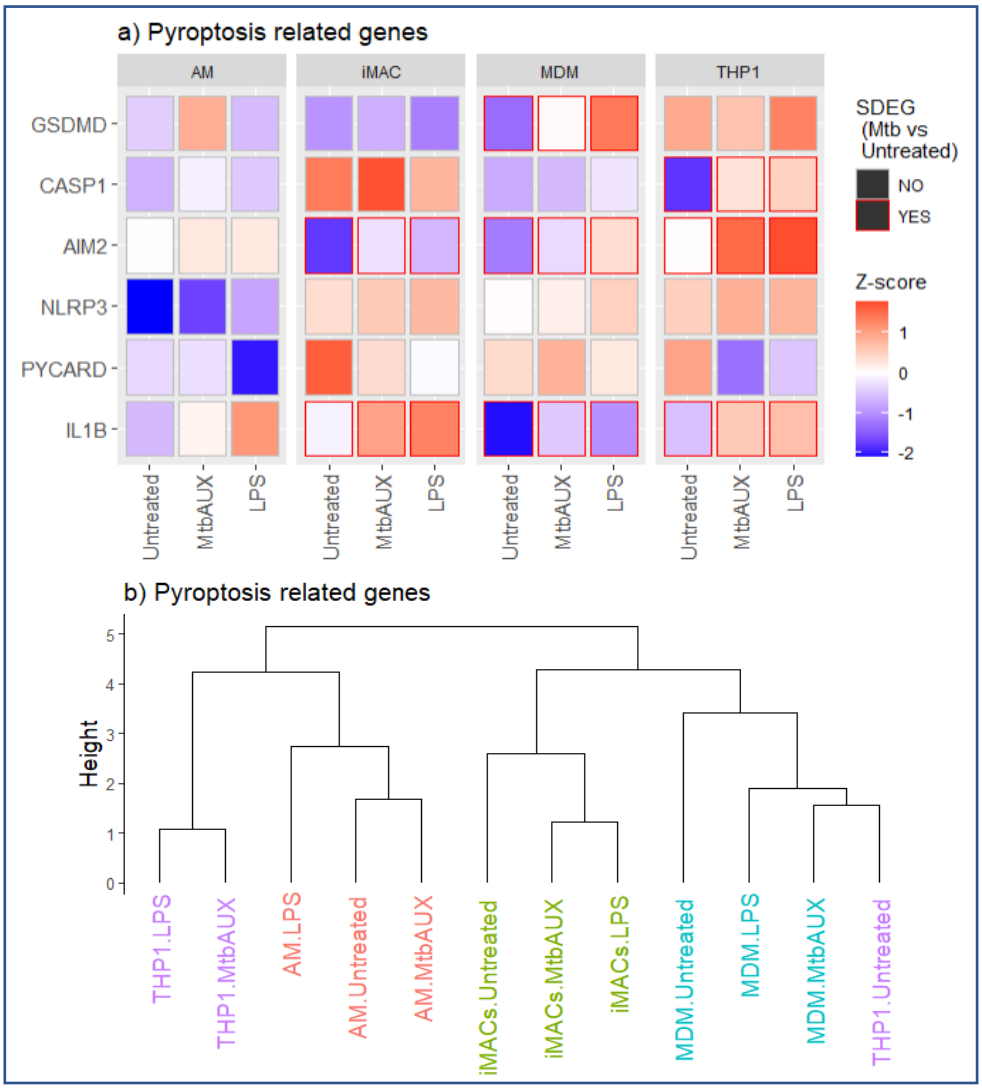

Figure 3-22. AMs expression of pyroptosis related genes differs from the other macrophages.

(a) Heatmap where each row represents a gene, and the columns represent the treatment groups separated by cell type. The z-scores, averaged for cell type-treatment replicates, represent gene-wise relative expression (see **Equation 1**) and are visualized by a continuous color gradient from low (blue) to high (red). Mtb vs Untreated significantly differentially expressed genes (-1 > log2FoldChang > 1 and p-value < 0.05) are annotated by a red outline. (b) Hierarchical clustering dendrogram generated based on the expression correlation of the genes in the heatmap.

Although, IL-1B is upregulated the expression data shows little differential expression of the NLRP3 inflammasome components (see figure 24a). Interestingly, with the exception of AIM2, the AMs seem to express the inflammasome components at a lower level than the other cell types. This is especially prominent in the case of NLRP3, which might indicate a lower chance of NLRP3 mediate pyroptosis activation. AIM2 was significantly upregulated in iMACs, MDMs and THP1, however, iMACs and MDMs also show a very low basal expression of the intracellular DNA recognizing receptor, compared to AMs and THP1. The THP1 cells show the largest change in the expression pattern of the pyroptosis related genes, while the others cluster largely according to cell type indicating that the stimuli had little transcriptional effect on the cells 20 hours post infection.

3.7 Comparison of iMAC gene expression at three timepoints

To get an overview of iMAC mRNA expression over time, the data generated for this thesis was compared with sequencing data obtained from Bernard et al. [2] where iPSC derived macrophages (produced following the same protocol as in this thesis [93]) were challenged with Mtb at two timepoints (2 and 48 hours). This raw count data was filtered and normalized using the same parameters and algorithms used on the sequencing data analyzed in this thesis, providing a pseudo timeline of gene expression across 3 timepoints.

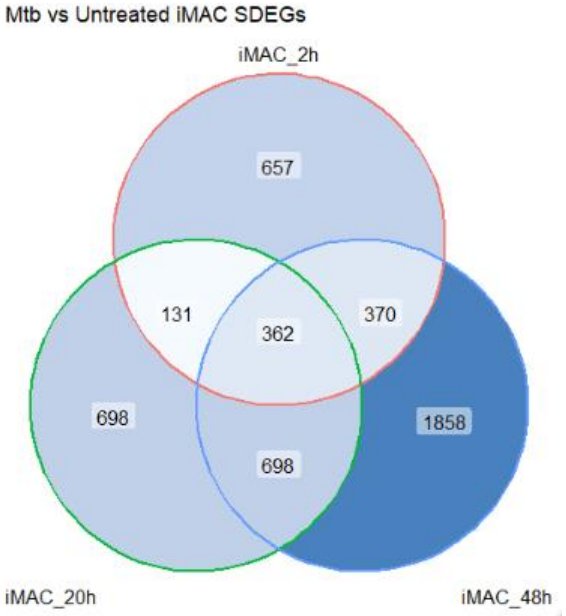

Figure 3-23. Venn diagram of shared significantly differentially expressed genes between iMACs stimulated with Mtb for 2, 20 and 48 hours. Sequencing data for iMAC_2h and iMAC_48 hour samples were obtained from Bernard et al. [2].

The iMACs sequenced for this thesis shared 131 and 698 significantly differentially expressed genes with the iMACs stimulated for 2 and 48 hours respectively. Additionally, 362 genes were shared between all samples. Interestingly, the iMACs exposed to Mtb for 48 hours had a much higher total number of differentially expressed genes (3288) compared to the 20-hour (1889) and 2 (1520) hour stimulated iMACs.

A gene enrichment analysis of the differentially expressed genes identified from the iMACs sequenced by Bernard et al. provides an overview of the changes in the immune response against Mtb in the iMACs over time. The cellular responses to IL-1, IFN-gamma and to some degree chemokines is maintained in the iMACs at all four timepoints, indicating that

there is no change in what drives the inflammatory response during the query timeline. The impact of chemokines (chemotaxis) on the biological processes of the iMACs seem to lessen over time, with many of the relevant terms not being represented at all after 48 hours. The downregulation of chemotaxis related processes suggests that the expression of chemokines was downregulated over time, or that there is a desensitization of chemokine receptors. The negative regulation of viral processes and genome replication does not appear to be induced until after the first two hours but seems, at least in part, to continue until 48 hours post infection. The activation of processes linking the innate to the adaptive immunity such as antigen processing and presentation, as well as T-cell mediated immunity seems to occur sometime between 20-48 hours post infection. The delay in antigen presentation in response to Mtb is well documented in other macrophages [107].

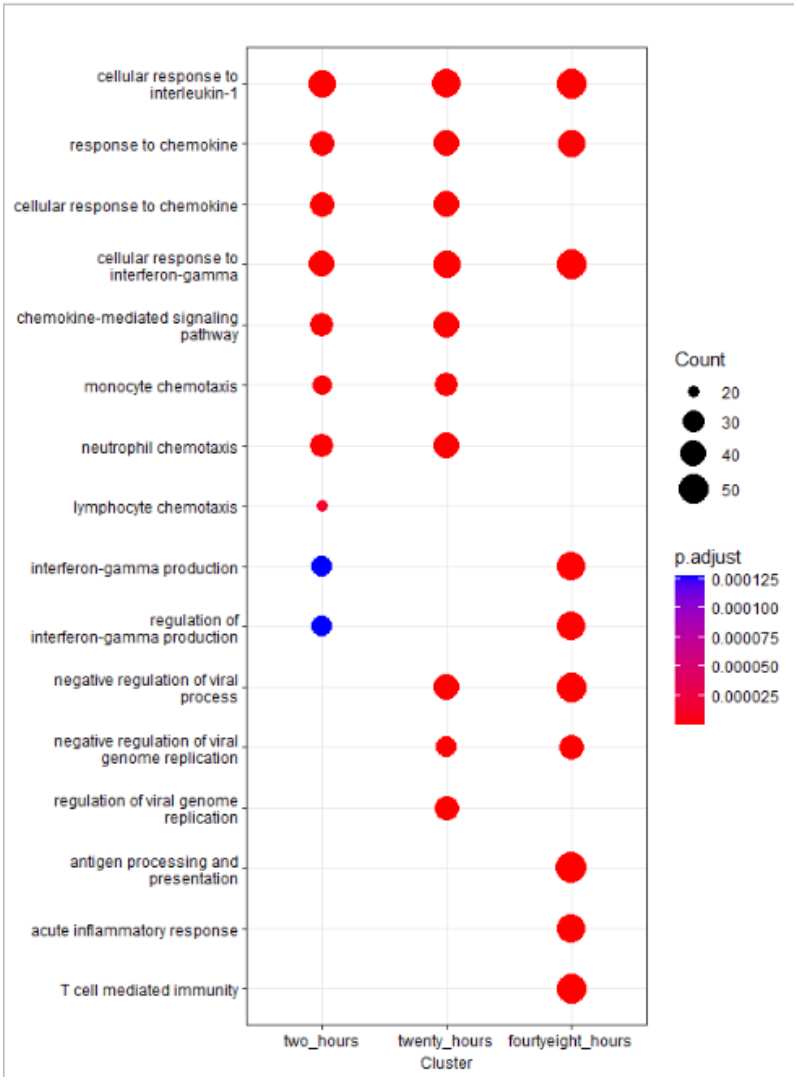

Figure 3-24. GO enrichment comparative dotplot of biological processes in iMACs at 2, 20 and 48 hours. Sequencing data for 2h and 48 hour samples were obtained from Bernard et al. [2]

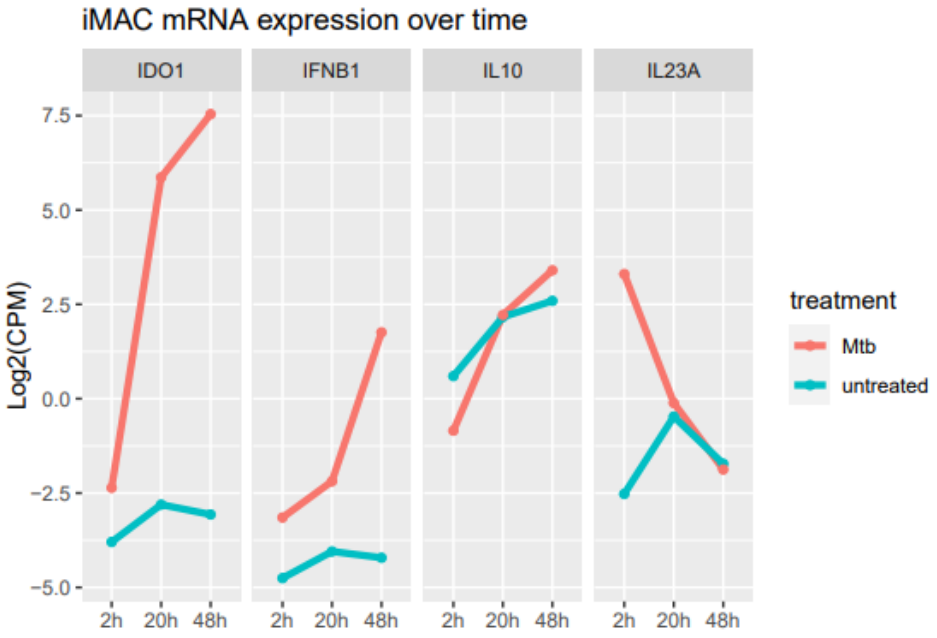

Figure 3-25. Expression patterns trends of IDO1, IFN-beta, IL-10 and IL-23 continue after 20 hours of Mtb exposure. IDO1, IFN-beta, IL-10 and IL-23 average expression in Mtb-challenged and untreated iMACs at 2, 20 and 48 hours. Sequencing data for 2h and 48 hour samples were obtained from Bernard et al. [2]

The expression over time of four genes of interest was visualized to predict the long-term changes in gene expression (see Figure 3-25). All four of these genes show a consistent trend of up- or down- regulation, indicating that the log2 fold change values of these four genes increased with longer exposure to the pathogen.

3.8 Cell death pathway assay suggests ferroptosis and pyroptosis can be activated in iMACs

The explore the inducibility of different cell death pathways in iMACs a wet lab experiment was performed aimed at activating pyroptosis, ferroptosis, necroptosis and apoptosis using specific stimuli. The cells were treated with four different cell death inducers, LPS + Nigericin, RSL-3, Venetoclax and TNF + zVAD. The cells were also treated with several reagents to measure their inhibitory effect on the release of LDH during cell death.

The experiment showed that LPS/Nigericin, RSL-3 and venetoclax were able to cause cell death in iMACs while TNF/zVAD did not show significantly more cell death than the 18-hour negative control. Interestingly, PEG showed consistent inhibition of cell death in all three of the stimuli that worked. This was expected in RSL-3 as PEG 8000 has previously been shown to delay ferroptotic cell death by affecting the osmotic swelling of cells with membrane pores [108]. The inhibition of LDH release in cells stimulated by LPS + nigericin is also somewhat expected as this stimuli is known to activate the oligomerization of the pore forming protein gasdermin D. Glycine also showed an inhibitory effect on the LDH release in RSL-3, which was also expected as its role in the inhibition of necrotic cell death is well described [109]. Interestingly, PEG and glycine both inhibited LDH release in the venetoclax treated cells. The high degree of LDH release, as well as the inhibition by reagents that affect necrotic cell death pathways indicate that the Bcl-2 inhibitor venetoclax did not cause an apoptotic cell death in the iMACs. Unexpectedly, disulfiram had some inhibitory

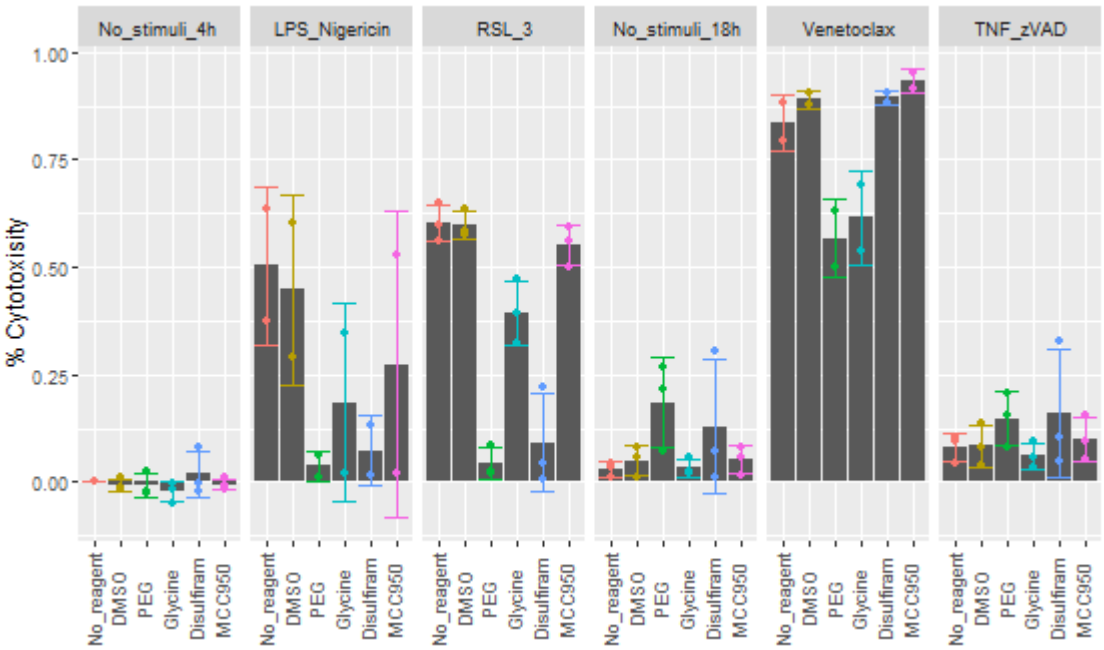

Figure 3-26. ferroptosis, pyroptosis and apoptosis inducers resulted in iMAC cell death. % Cytotoxicity as measured by LDH assay after treatment with cell death stimuli, in the presence of various reagents and inhibitors.

effect of the LDH release in RLS-3 stimulated cells even though its main activity in cell death related pathways is the inhibition of gasdermin d pore formation (pyroptosis) and TNF induced necrosis [110,111].

4 Discussion

In this thesis the main goal was to compare the gene expression of four cell types in response to *Mycobacterium tuberculosis*. This was done in order to evaluate the use of iMACs, as a model system for AMs in comparison to MDMs and THP1 cells. First, the data analysis focused on techniques aimed at characterizing differences in the larger biological processes. Then, by reviewing the current literature on the differing processes identified by the exploratory analyses, key genes were identified, and their expression was compared between cell types and treatment groups.

It is in this order of increasing specificity this thesis has attempted to compare the cells in their response to stimulus. First, by looking how cells relate to each other with relation to their global expression profiles followed by the expression profiles of differentially expressed genes in an exploratory manner. Secondly, evaluating what biological processes the differentially expressed genes are enriched for. Lastly, by looking at the expression of genes related to specific immunological events, such as inflammation, antigen presentation and T-cell activation, and cell death.

4.1 AM state of activation

A major part of this thesis is comparing iMACs, MDMs and THP1 cells to the AMs and it is therefore important to ensure that the measured gene expression of the AM samples reflect the treatment (untreated, MtbAUX and LPS). Although the healthiest possible patients were selected as donors, bronchoalveolar lavage is only performed to diagnose lung related diseases, and as a result none of the donors were completely healthy. This introduces unknown variables such as the state of activation and inflammation the cells were already exposed to prior to extraction. As untreated control cells from two of the donors displayed a stimulated state, they were removed from the analysis in order to identify as many differentially expressed genes as possible. Although the cells from the last donor showed a more distinctive response to the stimuli, the untreated sample still shows some tendency towards an inflamed state. AMs in the alveoli have been shown to display anti-inflammatory characteristics mainly perpetuated by TGFB and a close association with alveolar epithelial cells [22]. However, the silent, quiescent properties described in the literature is not observed in the AMs obtained for this experiment. This is therefore a major weakness of the analysis performed for this thesis and needs to be kept in mind when interpreting the results.

4.2 Differing expression of PRR may lead to contrasting intracellular survival of Mtb

The recognition and phagocytosis of *mycobacterium tuberculosis* is a key event in the AM-pathogen interaction and can influence the phagosome maturation, inflammatory response, and ultimately the fate of the internalized bacteria [112]. TLR 2 has been identified as an important PRR that can bind a range of mycobacterial antigens, which can elicit both pro-inflammatory mediators like TNF, IL-12 and NOS as well as anti-inflammatory responses such as IL-10 and TGFB [113,114]. The C-type lectin MRC1 (CD206) together with

complement receptors CR1 and CR3 have been shown to the main effectors of mycobacterial phagocytosis in AMs and MDMs [17,115]. Interestingly, bacterial entry via the CD206 has been shown limit phagosome-lysosome fusion and is believed to enhance intracellular survival [116]. Therefore, the expression of the PRRs responsible for activation of inflammation as well as bacterial internalization was important to characterize.

The expression of most of the important PRR is similar for iMACs, AMs and MDMs however, THP1 express these receptors at generally lower rate, with the exception of TLR2. This indicates that THP1 cells are influenced by TLR2 signaling than the other cells which might lead to further downstream differences in the inflammatory response. CD206 has previously been shown to be highly expressed in AMs and MDMs [117] which is supported by the data collected in this thesis. iMACs also show high expression of this PRR, but interestingly also downregulates its expression in response to Mtb. This might affect Mtb exploitation of this internalization pathway and lead to more effective phagosome-lysosome fusion in iMACs than in AMs and MDMs. THP1 also show a significant downregulation of CD206 as well as CR3. Together with the low expression of CR1 these factors might add up to affect THP1 cell's ability to phagocytose the bacteria, however, further research is needed to confirm this.

4.3 Major differences in inflammatory mediators

The expression of Mtb related, pro-inflammatory cytokines were compared between cells and treatment groups revealing a high degree of similarity in AMs, iMACs and THP1 while MDMs, although showing an upregulating trend for all cytokines in response to stimuli, showed a distinctly more subdued response. The induction of pro-inflammatory cytokines in response to Mtb has been shown to be largely mediated by TLR recognition of mycobacterial antigens, initiating the NFkB cascade through the adaptor protein MYD88 [28]. The upregulation of NFkB and MYD88 as well as TNF and IL-1 indicate that the same major mediators are driving the inflammatory response in all cell types.

Interestingly, although all cells showed enrichment of IFN-gamma mediated biological processes, no IFN-gamma mRNA was detected in any of the cells. The lack of IFN-gamma mRNA in Mtb infected iMACs, MDMs and AMs has been reported in previous studies [2,118,119]. However, IFN-gamma protein has been shown with ELISA to be present in MDMs and AMs as soon as 4 hours post infection [32], and in MDMs IFN-gamma mRNA was detected at 24 hours with quantitative RT-PCR [118]. Furthermore, Volpe et al. showed that the amount of IFN-gamma mRNA was too low for microarray detection, and that protein levels increased significantly after 3 days in MDMs. This suggests that IFN-gamma mRNA might have been detected in the experiment performed for this thesis with deeper sequencing. Furthermore, the significant upregulation of IFN-gamma induced protein 10 (CXCL10) in all cells as a response to stimuli (see figure 17a), together with the enriched IFN-gamma related biological processes suggests the presence of IFN-gamma protein in the query cells.

However, the upregulated expression of IFN-beta and type 1 interferon related genes in iMACs and THP1 might also affect the expression of IFN-gamma. Studies have shown that type 1 interferons and downstream effectors such as IL-10 have an inhibitory effect on IFN-gamma [120]. The correlation between type 1 interferon related genes and the Mtb stimulated samples (see figure 10) as well as the upregulation of type 1 interferon response genes (see figure 19) was especially prominent in the iMACs and THP1 and correlate somewhat to the observed IL-10 expression. Although studies have shown that the type 1 interferon IFN-beta has some protective functions in Mtb infection [121], the high expression

of type 1 interferon related genes in iMACs and THP1 may result in an altered inflammatory response that may not reflect the AMs at the timepoint that was measured. The production of type 1 interferons can be induced by cytosolic pattern recognition receptors (PRRs) that are activated by bacterial components and DNA such as, nucleotide-binding oligomerization containing protein 2 (NOD2) [122] and cGAS-STING [123]. This might indicate poor phagosome integrity, or that the bacteria escape the phagosome more effectively or at an earlier timepoint in the iMACs and THP1 than in the MDMs and AMs.

Type 1 interferons suppress expression of proinflammatory cytokines and inhibit T-cell responses [124] and correlate with increased severity of TB in mice [125]. Furthermore, type 1 interferons have been shown to cause macrophages switch from the classically activated phenotype (M1) to the more permissively activated phenotype (M2) in the absence of IFN-gamma [126]. The induction of type 1 interferon signaling in AMs as a response to Mtb is well documented [127,128], however, the expression data suggests that this does not occur in the AMs examined in this thesis at the 20 hour timepoint. The contrasting activation of type 1 interferons in iMACs and THP1 may therefore influence the IFN-gamma activation, T-cell interactions and possibly the overall phenotype of the cells that is not reflected in the AMs.

CSF2 has been shown to be upregulated in human AMs in response to virulent Mtb [119] supported by the AMs and THP1 tested in this thesis, however, MDMs and iMACs showed no significant upregulation of CSF2 in response to Mtb. GM-CSF is believed to promote a M1 phenotype in macrophages, which Verreck et al. have shown to express IL-23 in response to mycobacterial stimuli, while M2 macrophages expressed higher levels of IL-10 [129]. In this regard, iMACs and MDMs show M2 characteristics that AMs do not display.

The subdued pro-inflammatory response of the MDMs seen evident from several of the performed analyses (see Figure 3-4, and Figure 3-15). The GO enrichment analysis also showed that a majority of the enriched biological processes were related to cell migration and chemotaxis contrasting iMACs and THP1 (see). As MDMs are usually recruited from the blood stream and activated by other macrophages at the site of infection, they are rarely the first to encounter a pathogen directly without previous stimuli. Thus, the poor inflammatory response might indicate that the PBMC to macrophage differentiation process was not sufficient for proper activation. However, it may also indicate that other cell types are better suited for infection experiments like the one performed for this thesis.

The differences in type 1 interferon responses, as well as CSF2, IL-23 and IL-10 expression between the cells may affect processes such as expression of other inflammatory cytokines, macrophage differentiation as well as downstream interactions with other immune cells. Although AMs cannot be categorized as strictly M1 or M2, the query cells do not reflect certain AM M1 characteristics and further investigation should focus on type 1 interferon responses and the M1/M2 characteristics of iMAC, MDMs and THP1.

4.4 AMs show several unique properties in the regulation of antigen presenting, and T-cell activating genes

The activation of antigen presenting processes in macrophages during Mtb infection is a critical function as it allows macrophages to activate CD4+ Th1 and Th17 cells that are crucial in controlling the pathogen and preventing active TB disease [44,130]. The downregulation of antigen processing and presentation during infection is an important regulatory mechanism preventing excessive inflammation, however, studies have shown that this

regulatory measure is exploited and increased by Mtb in order to prevent CD4+ T-cell recognition of infected macrophages [107].

Studies have shown that Mtb suppresses MHC class 2 antigen presentation by inhibiting antigen loading and processing as well as transcriptional downregulation of MHC class 2 molecules. Transcriptionally, antigen presentation is through to be suppressed through a TLR2 dependent inhibition of CIITA [61], a MHC class 2 master regulator. CIITA is expressed at a much lower level in iMACs and THP1 resulting in an overall low expression of MHC class 2 molecules when compared to AMs and MDMs. Furthermore, the downregulation of CIITA seems to cause some downregulation of MHC class 2 molecules in Mtb stimulated AMs and iMACs, however, this is not reflected in MDMs (see figure 11-13). The downregulation of MHC class 2 molecules through TLR2 is not Mtb specific but has been shown to be more pronounced for pathogens known to reside in intracellular membrane bound compartments for a prolonged period of time [130]. The lack of CIITA and MHC class 2 molecule downregulation in might therefore indicate that the bacteria reside inside the phagosome for a shorter time period or that they are more effectively eliminated in MDMs, than in AMs and iMACs.

Antigen processing and loading onto MHC class 2 molecules is believed be inhibited through interference with Cathepsin S, a cystine protease [131]. This protease generates MHC class 2 molecules that can efficiently load Mtb antigens, and is thought to be inhibited by IL-10 [107]. However, this is not reflected in the gene expression measured in this thesis, as Cathepsin S (CTSS) is not downregulated in any cells and rather is significantly upregulated in iMACs.

The interactions between the macrophages and adaptive immune cells determine the cell fate of the T-cells. Th17 and Th1 cells are the main effector CD4+ cells in tuberculosis, activating the macrophages and neutrophils with IFN-gamma secretion which has been shown to be aN essential in the control of Mtb [132]. This is supported in the mRNA data by the high association between the regulation of alpha-beta (T-cell receptor) T-cell activation and Mtb infection observed in the WGCNA analysis (see figure 10). T-cell receptors (TCR) interact with antigen bound MHC class 1 or 2 molecules, resulting in the activation of the T-cell into either cytotoxic T-cells or helper/regulatory T-cells respectively [133]. The specification of the CD4+ T-cells that interact with MHC class 2 presenting cells depends on cytokines and catabolites secreted by the antigen presenting cell [134,135]. Th1-cell specification is activated through IL-2, IFN-gamma and IL-12 signaling from the antigen presenting cells, where as a Th17 differentiation is mediated by a combination of IL-6, TGFB, and IL-23 [133,136]. Interestingly, none of the Th1 signaling cytokines were detected with mRNA sequencing and AMs were the only cell type to display a significant upregulation of IL-23 and IL-6. It can therefore be speculated that the query cell types are not able to induce a Th17 T-cell differentiation. Furthermore, the major hub gene of the TCR regulatory associated co-expressed gene module (module 41), IDO1 has been shown to promote a T-regulatory differentiation of naïve CD4+ T-cells [135], as well as inhibiting IL-17 production by Th17 cells [132] by producing the tryptophan catabolite kynurenine. IDO1 is significantly upregulated by all well types, however, AMs express this gene as a substantially lower level (3.5 transcripts per million) than iMACs and MDMs (60 transcripts per million), which might affect kynurenine concentration and subsequently affect the T-cell activation.

Several factors indicate that the cells tested in this thesis regulate their antigen presentation processes differently. The differences in MHC class 2 molecule expression, as well as the changes in CIITA expression indicates poor antigen presentation activity in iMACs and

THP1. Furthermore, the cytokines and catabolites produced by the model cell lines indicate that the activation of naïve CD4+ T-cells is likely to fail to induce a Th17 differentiation at the timepoint mRNA was measured in this thesis. The mRNA sequencing data obtained from Bernard et al. also indicates that expression of IL-23 continues to decrease, while IFN-beta and IDO1 mRNA production continues to increase after 20 hours (see figure 27), suggesting that the proposed effects will not dissipate with time.

4.5 Cell death

Determining the activation of various cell death pathways and differentiating them from each other using mRNA sequencing proved difficult and probably inaccurate. The central proteins involved in most of the cell death pathways are regulated by protein-protein interactions such as cleavages, complex formations and phosphorylations leading to little change in the transcriptional profile of the cells. The results therefore reflect little differential expression of cell death effector proteins, and one has to look at less specific genes, indirectly affecting the query pathways, decreasing the resolution of the analysis. Furthermore, the timepoint at which the cells undergo cell death can differ greatly according to cell type and the activated pathway. As the mRNA collected in this thesis was extracted at only one timepoint it is therefore difficult to conclude anything about the activation of cell death with the data available.

However, some inferences can be made based on the presence or absence of certain gene transcripts, as the relative expression of proteins like apoptosis inhibitors, cell death complex components and PRRs indicate whether a certain pathway can or cannot be triggered.

4.5.1 Apoptosis inhibition and necroptosis

Several mycobacterial proteins have been implicated in the inhibition of apoptosis [137,138], however the mechanisms and effects on expression of pro- and anti- apoptotic proteins in the host cell seems to vary greatly with the cell type [139]. iMACs and THP1 cells showed significant upregulation of several anti-apoptotic genes such as cIAP2 (BIRC3) (also upregulated in MDMs and highly expressed in AMs), cFLIP (CFLAR) and Bcl-2 related protein A1 (BCL2A1). The expression of cAIP2, cFLIP and Bcl-2 A1 has been shown to be induced by NFkB signaling [140-142], suggesting that a strong activation of the NFkB cascade is preferential to Mtb in that the cells are pushed towards a necrotic cell death. Furthermore, NFkB is significantly upregulated in all cell types except AMs and may therefore inhibit apoptosis to a stronger degree in iMACs, MDMs and THP1. Further research is therefore needed to interpret what causes the upregulation of NFkB in the query cells and not the AMs, as well as the effects this might have on the cell death pathways that are activated in these cells.

The primary regulator of necroptotic cell death is believed to be TNF-alpha. Similarly to apoptosis, TNF-alpha binds tumor necrosis factor receptor (TNFR) on the cell surface, resulting in the formation of complex 1. Complex 1 consists of a TNFR associated death domain (TRADD), FAS associated death domain (FADD), RIPK1, TNFR associated factors (TRAF) and cellular inhibitor of apoptosis (cAIP1/2). RIPK1 promotes NFkB signaling and cell survival, but can be deubiquitinated by CYLD, forming a new complex of RIPK1, RIPK3, FADD and caspase-8 [81]. At this point, caspase-8 can cleave RIPK1 and RIPK3, leading the cell to apoptosis, however if caspase-8 is inhibited the two RIP-kinases for a RIP complex which will induce mitochondrial ROS release. RIPK3 interacts with the mitochondrial phosphatase PGAM5 which in turn phosphorylates DRP1 which has been shown to trigger ROS production and release [143]. Furthermore, the RIP complex phosphorylates MLKL which can

oligomerize leading to plasma membrane pore formation and subsequently, necroptosis [144]. One study has shown that intracellular pathogens such as *Salmonella enterica* and *Salmonella Typhimurium* cause necroptosis in a TNF independent manner [145]. This is thought to occur through type 1 interferon induced, persistent upregulation of STAT1, STAT2 and IRF9, and direct interaction between type 1 interferon receptor IFNAR inducing phosphorylation and activation of RIPK1.

Although necroptosis largely mediated by non-transcriptional mechanisms, Stutz et al. recently identified several key necroptosis mediators that were differentially regulated in macrophages as a result of Mtb infection. MLKL, TNFR1, cFLIP and ZBP1 were all significantly upregulated while caspase-8, RIPK1 and RIPK3 were not significantly altered [75]. Unexpectedly, they also found that cAIP1 and CYLD were downregulated. The gene expression patterns of the AMs, iMACs and THP1 tested in this thesis support some of the findings proposed by Stutz et al. such as the significant upregulation of ZPB1 and cFLIP (CFLAR) and some upregulation of MLKL TNFR1 (see figure 22), as well as the lack of change in RIPK1 and RIPK3 expression. However, MDMs showed a contrasting pattern of MLKL and ZBP1 downregulation (not significant), as well as a low expression of the complex 1 and 2 components.

Little evidence of necroptosis can be inferred from the gene expression of the cells at the timepoint when mRNA was extracted and further investigation should focus on when the macrophages are likely to undergo necroptosis, as well as establishing if Mtb induced necroptosis can occur in a TNF independent manner, especially in the cell types that showed a strong type 1 interferon response.

4.5.2 Ferroptosis

Ferroptosis is a cell death pathway is characterized by an increase in the intracellular concentration of lipid reactive oxygenated species (ROS) [146]. A recent study has shown that ferroptosis occurs during Mtb infection in bone marrow derived macrophages, and that ferroptosis might have a detrimental effect on the host similar to necrosis. The study showed that Mtb induced ferroptosis was highly associated with reduced levels of glutathione (GSH) and glutathione peroxidase-4 (GPX4) expression.

Ferroptosis occurs as a result of lipid ROS accumulation, usually prevented by GPX4 together with GSH synthase (GSS) [146]. However, GPX4 inhibitors such as RSL3, DP17, and FIN56, all known activators of ferroptosis, act directly on GPX4 or by promoting GPX4 degradation [147]. Amaral et al. did show that GPX4 expressed decreased, however not until 5 days post infection [73], which is supported by the lack of GPX4 (and GSS) downregulation in the cells investigated in this thesis. The amino acid antitransporter SLC7A11/SLC3A2, which transports cystine (involved in GSH production) into the intracellular lumen, has been shown to be transcriptionally inhibited by p53 [148], leading to lipid ROS accumulation. P53 has also been shown to activate ferroptosis through the STAT1-ALOX15 pathway, which leads to lipid peroxidation and higher levels of lipid ROS [149]. However, the mRNA data showed a downregulation of ALOX15 and an upregulation SLC7A11 indicating that p53 activated ferroptosis did not occur.

Although the observed gene expression patterns indicate that ferroptosis does not occur in any of the query cells, the mechanisms by which key proteins such as GPX4 is regulated, means that the mRNA sequencing performed in this thesis is inadequate for determining whether ferroptosis occurs. The cell death experiment showed that inhibiting GPX4 with RSL-3 lead to cell death in iMACs, and long term (> 5 days) experiments measuring GPX4

mRNA as well as intracellular GSH levels should be performed to confirm that ferroptosis can be induced in the cells as a result of Mtb stimuli.

4.5.3 Pyroposis

Pyroptosis is believed to be induced by Mtb through the activation of the NLRP3 inflammasome, together with plasma membrane damage leading to the efflux of K+ from the cell [72]. The first step in NLRP3 activation is thought to be a transcriptional upregulation of the protein itself, together with IL-1B and caspase-1. This upregulation which can be triggered by TLRs or NOD2 recognition of PAMPs or DAMPs, or through the NFkB cascade which is triggered by TNF or IL-1B signaling [150,151]. The mRNA sequencing data of cells measured in this thesis do show a significant upregulation of IL-1B in iMACs, MDMs and THP1 but very little change in NLRP3 and caspase-1 expression. Interestingly, AIM2 upregulation in iMACs, MDMs and THP1 seems to correlate with the IFN-beta, and type 1 interferon response gene expression. This upregulation of AIM2 is strongest in the iMACs and THP1 treated with Mtb and the MDMs treated with LPS and provides further evidence of more Mtb or Mtb-cellular components in the cytosol of the secondary cell lines. Further research is needed to determine the cellular location of Mtb in iMACs and THP1, as well as the possible activation of AIM2 and its role in Mtb induced pyroptosis.

4.6 mRNA sequencing as a tool for immune response characterization

Due to the vast number of post translational modifications and regulatory steps that affect the expression and activity of a protein, mRNA sequencing provides only an indication of the change in processes that occur inside a cell. This limits the scope of conclusions that can be drawn from mRNA sequencing data analysis to cellular processes that are transcriptionally regulated. As the innate immune response is the first line of defense activated when challenged with a pathogen, many of the regulatory mechanisms are mediated by faster protein-protein interactions such as phosphorylation, cleavages and protein degradation.

Protein mass spectrometry (MS) is another high-throughput that measures the protein concentration, the splice variant as well as post-translational modifications, and can therefore provide more information to go along with the changes is protein production. This method might therefore be more useful when characterizing immunological processes that are regulated through non-transcriptional mechanisms, such as cell death.

Another major issue with the mRNA sequencing performed for this thesis is that only a single timepoint was measured. Other timepoints of mRNA extraction could have been added, but due to the number of cell types and conditions, this would be very expensive and produce a vast amount of data that is unpractical to handle. This could be solved by experimentally verifying the mRNA or protein concentrations of proteins of interest at other timepoints with techniques such as RT-PCR or ELISA respectively.

A fallacy of the mRNA sequencing performed for this thesis was the lack of replicates for LPS stimulated samples and THP1 samples. In addition, more replicates for AMs should have been included to account for the possible pre-activation that was observed in two of the samples. A benchmark study has shown that a minimum of six biological replicates are recommended but that 12 was preferrable to accurately identify all differentially expressed genes [152]. The study also showed that DESeq2 performed best for analysis of low replicate data and should therefore have been used in place of limma for this thesis.

However, limma, edgeR and DESeq were all shown to have low false discovery rates with few replicates[98], indicating that the algorithm choice for this thesis lead to lower sensitivity and false negatives, rather than false positives.

One advantage of high-throughput techniques like mRNA sequencing is its ability to gather data on almost all mRNA transcripts available in the cell. As a result, inferences can be made about the biological processes that are affected in a cell, not by knowing the activation state or concentration of specific proteins, but by the sheer number of process related genes whose gene expression is altered.

Inferences can also be made based on the presence or absence of certain mRNA transcripts. Many genes are cell type specific, and their respective mRNA can be completely absent based on the cell that is measured. This is useful when comparing cell types as the lack of mRNA from certain genes will affect the related cellular processes exhibited by that cell.

In conclusion, other high throughput tools that provide more information than mRNA, as well as experimental techniques that could be used in conjunction with mRNA sequencing, would create a more complete picture of the host cell response and differences in immunological processes displayed by the query cells tested in this thesis. However, as a limited project, that aims to characterize the broad cellular processes, and indicate where further, more specific research is needed, mRNA provides a simple method of cell comparison.

4.7 Future prospects

This thesis provides an overview of differences in gene expression between the cell types in response to Mtb, however, in order to verify the findings of these computational observations, more specific *in vitro* experiments are needed. Here several characteristics of the iMACs that would benefit from further experimental investigations are proposed.

Further investigation into the phagocytosis of Mtb by the different cell types could lead to a better understanding of what model cell lines that are best suited for *in vitro* experiments regarding the internalization of the bacteria. The changes in expression of central receptors CD206 and TLR2 seen in iMACs and THP1 was in sharp contrast to AMs and MDMs and may affect important downstream processes. Experiments that explore the differences in bacterial uptake as well as the importance of the specific receptors on downstream effects like intracellular survival and inflammatory responses are therefore recommended. This would provide insight, not only on the characteristics of the model cell lines, but also on the early host-pathogen interactions that have been shown to be vital to Mtb infection control.

The characterization of type 1 and 2 interferon expression over time is also a recommended aspect of interest as interferons play a major role during both innate and adaptive Mtb immunity. The difference in the type 1 interferon response observed between iMACs/THP1 and AMs (as well as MDMs to some degree) could result in a major difference in the regulation of their cellular Mtb response. Simple qPCR and ELISA experiments that span several timepoints could be used to observe the timeline of IFN production. Subsequently, this resolve whether a similar type 1 interferon response seen in iMACs and THP1, occurs in MDMs and AMs at all or just at a different timepoint. Furthermore, this could verify the early, but low level, production of IFN-gamma that is speculated to occur in all the query cells tested in this thesis, but which was not detected by mRNA sequencing.

Further experiments regarding the activation of different cell death pathways are also recommended as mRNA sequencing was unable offer any definitive conclusions to this aspect. Furthermore, the cell death experiment performed in this thesis needs to be optimized and Mtb added to the list of stimuli as this would allow a quantification of what cell death pathways that were activated as a result of the bacteria. If data on the gene expression profiles of macrophage cell death is wanted, initial experiments to determine the timepoint when most cell death is occurring would be needed. This could be determined by treating cells with cell death stimuli (see Table 2-2) or Mtb and using microscopy, in conjunction with DRAQ7 or LDH assays at different timepoints to determine percentage of cell death.

4.8 Conclusion

The aim of this thesis was to characterize and compare the early Mtb immune response of iMACs, AMs, MDMs and THP1 cells based on the mRNA gene expression. Of the four, two primary (AMs and MDMs) and one secondary cell line (THP1) are well established model systems used frequently in tuberculosis research. The last cell type, an iPSC derived macrophage, is a recent addition, and as such its interactions and response to Mtb needs to be well characterized and defined for future reference.

In order to achieve the aim of this thesis, a data analysis workflow, starting with exploratory techniques looking at larger biological processes and ending with a comparison of expression at a single gene level, was implemented. This was done to provide both a larger overview of similarities and differences between cell lines at the time of mRNA extraction, as well as to hypothesize about the downstream effect of the differential expression of key genes.
Main findings presented in this thesis:

- Basal expression of cell surface receptors in AMs is reflected most accurately in iMACs.
- THP1 had a highly contrasting expression profile of the cell surface receptors.
- The expression of pro-inflammatory mediators in AMs infected with Mtb was most accurately reflected by iMACs.
- MDMs displayed a poor Mtb induced inflammatory response.
- The strong type 1 interferon response seen in iMACs and THP1 was not reflected in MDMs and AMs.
    - This might be an indication of differences in the intracellular location of the bacteria or phagosome integrity.
    - This might also affect downstream inflammatory processes as well as T-cell activation.
- iMACs and AMs are possibly more susceptible to Mtb induced MHC class 2 downregulation than MDMs.
- The expression of T-cell differentiation factors indicate that AMs are more likely to induce a Th17 cell fate than iMACs, THP1 and MDMs.
- Evidence supporting the activation of specific cell death pathways could not be inferred from the mRNA sequencing data at 20 hours post infection.
    - iMAC expression of cell death related genes were more similar to AMs and MDMs than that of THP1, with the exception of pyroptosis.

This thesis presents strong evidence that iMACs is a viable model cell that can be a useful tool in tuberculosis research. Importantly, the mRNA expression data strongly indicates that iMACs are more suited to emulate AMs, than THP1, while offering many of the same

advantages such as homogeneity and reproducibility. Furthermore, the iMACs can be further manipulated to better display wanted characteristics, making them a valuable tool that this thesis has shown to be worthwhile investing in.

Model systems never reflect *in vivo* conditions perfectly and translating observations from cell culture experimental conditions to real life interactions is impossible without making many assumptions. However, to understand a system as complex as the immune system and host-pathogen interactions, variables need to be removed and conditions simplified. Using cells that most accurately reflect *in vivo* conditions is therefore vital but, in the case of Mtb infection of the unique niche of the alveoli, extremely difficult. The establishment of a new model cell line like iMACs could improve our understanding of the body's early interactions with Mtb, and in a world where this pathogen has claimed countless lives over the millennia, this is sorely needed. In light of the emerging threat of drug resistant tuberculosis, continuing to improve the quality of TB research, should be a priority for all, not only for the developing countries most heavily burdened with this disease, and as recent events have shown, money does not make one immune to the threat of microorganisms.

5 References

1. Lopez-Yrigoyen M, May A, Ventura T, et al. Production and characterization of human macrophages from pluripotent stem cells. *JoVE (Journal of Visualized Experiments)*. 2020;(158):e61038.
2. Bernard EM, Fearns A, Bussi C, et al. M. tuberculosis infection of human iPSC-derived macrophages reveals complex membrane dynamics during xenophagy evasion. *Journal of cell science*. 2021;134(5):jcs252973.
3. World Health Organization. Global tuberculosis report 2021. 2021. *Google Scholar*. 2022:57.
4. Pai M, Behr MA, Dowdy D, et al. Tuberculosis. *Nature Reviews Disease Primers*. 2016/10/27 2016;2(1):16076. doi:10.1038/nrdp.2016.76
5. Ramakrishnan L. Revisiting the role of the granuloma in tuberculosis. *Nature Reviews Immunology*. 2012;12(5):352-366.
6. Jasmer RM, Nahid P, Hopewell PC. Latent tuberculosis infection. *New England Journal of Medicine*. 2002;347(23):1860-1866.
7. Ai J-W, Ruan Q-L, Liu Q-H, Zhang W-H. Updates on the risk factors for latent tuberculosis reactivation and their managements. *Emerging microbes & infections*. 2016;5(1):1-8.
8. Pfyffer GE. Mycobacterium: general characteristics, laboratory detection, and staining procedures. *Manual of clinical microbiology*. 2015:536-569.
9. Suárez I, Fünger SM, Kröger S, Rademacher J, Fätkenheuer G, Rybniker J. The Diagnosis and Treatment of Tuberculosis. *Deutsches Aerzteblatt International*. 2019;116(43)
10. Shah NS, Wright A, Bai G-H, et al. Worldwide emergence of extensively drug-resistant tuberculosis. *Emerging infectious diseases*. 2007;13(3):380.
11. Upshur R, Singh J, Ford N. Apocalypse or redemption: responding to extensively drug-resistant tuberculosis. *Bulletin of the World Health Organization*. 2009;87(6):481-483.
12. Nellums LB, Rustage K, Hargreaves S, Friedland JS. Multidrug-resistant tuberculosis treatment adherence in migrants: a systematic review and meta-analysis. *BMC medicine*. 2018;16(1):1-11.
13. Barreto ML, Pereira SM, Ferreira AA. BCG vaccine: efficacy and indications for vaccination and revaccination. *Jornal de pediatria*. 2006;82:s45-s54.
14. Tait DR, Hatherill M, Van Der Meeren O, et al. Final analysis of a trial of M72/AS01E vaccine to prevent tuberculosis. *New England Journal of Medicine*. 2019;381(25):2429-2439.
15. Leemans JC, Juffermans NP, Florquin S, et al. Depletion of alveolar macrophages exerts protective effects in pulmonary tuberculosis in mice. *The journal of immunology*. 2001;166(7):4604-4611.
16. Mitsi E, Kamng'ona R, Rylance J, et al. Human alveolar macrophages predominately express combined classical M1 and M2 surface markers in steady state. *Respiratory research*. 2018;19(1):1-4.
17. Rajaram MV, Ni B, Dodd CE, Schlesinger LS. Macrophage immunoregulatory pathways in tuberculosis. Elsevier; 2014:471-485.
18. Murray PJ, Allen JE, Biswas SK, et al. Macrophage activation and polarization: nomenclature and experimental guidelines. *Immunity*. 2014;41(1):14-20.
19. Genin M, Clement F, Fattaccioli A, Raes M, Michiels C. M1 and M2 macrophages derived from THP-1 cells differentially modulate the response of cancer cells to etoposide. *BMC cancer*. 2015;15(1):1-14.

20. Ginhoux F, Guilliams M. Tissue-resident macrophage ontogeny and homeostasis. *Immunity*. 2016;44(3):439-449.
21. Holt PG. Inhibitory activity of unstimulated alveolar macrophages on T-lymphocyte blastogenic response. *American Review of Respiratory Disease*. 1978;118(4):791-793.
22. Lambrecht BN. Alveolar macrophage in the driver's seat. *Immunity*. 2006;24(4):366-368.
23. Hmama Z, Peña-Díaz S, Joseph S, Av-Gay Y. Immunoevasion and immunosuppression of the macrophage by M ycobacterium tuberculosis. *Immunological reviews*. 2015;264(1):220-232.
24. Ernst JD. The immunological life cycle of tuberculosis. *Nature Reviews Immunology*. 2012;12(8):581-591.
25. Dorhoi A, Desel C, Yeremeev V, et al. The adaptor molecule CARD9 is essential for tuberculosis control. *Journal of Experimental Medicine*. 2010;207(4):777-792.
26. Hölscher C, Reiling N, Schaible UE, et al. Containment of aerogenic Mycobacterium tuberculosis infection in mice does not require MyD88 adaptor function for TLR2,-4 and-9. *European journal of immunology*. 2008;38(3):680-694.
27. Drennan MB, Nicolle D, Quesniaux VJ, et al. Toll-like receptor 2-deficient mice succumb to Mycobacterium tuberculosis infection. *The American journal of pathology*. 2004;164(1):49-57.
28. Hussell T, Bell TJ. Alveolar macrophages: plasticity in a tissue-specific context. *Nature reviews immunology*. 2014;14(2):81-93.
29. Yu K, Mitchell C, Xing Y, Magliozzo R, Bloom B, Chan J. Toxicity of nitrogen oxides and related oxidants on mycobacteria: M. tuberculosis is resistant to peroxynitrite anion. *Tubercle and Lung Disease*. 1999;79(4):191-198.
30. Sasindran SJ, Torrelles JB. Mycobacterium Tuberculosis Infection and Inflammation: what is Beneficial for the Host and for the Bacterium? *Frontiers in microbiology*. 2011;2:2.
31. Cavalcanti YVN, Brelaz MCA, Neves JKdAL, Ferraz JC, Pereira VRA. Role of TNF-alpha, IFN-gamma, and IL-10 in the development of pulmonary tuberculosis. *Pulmonary medicine*. 2012;2012
32. Fenton MJ, Vermeulen MW, Kim S, Burdick M, Strieter RM, Kornfeld H. Induction of gamma interferon production in human alveolar macrophages by Mycobacterium tuberculosis. *Infection and immunity*. 1997;65(12):5149-5156.
33. Chan ED, Chan J, Schluger NW. What is the role of nitric oxide in murine and human host defense against tuberculosis? Current knowledge. *American journal of respiratory cell and molecular biology*. 2001;25(5):606-612.
34. Rajaram MV, Brooks MN, Morris JD, Torrelles JB, Azad AK, Schlesinger LS. Mycobacterium tuberculosis activates human macrophage peroxisome proliferator-activated receptor γ linking mannose receptor recognition to regulation of immune responses. *The Journal of Immunology*. 2010;185(2):929-942.
35. Daynes RA, Jones DC. Emerging roles of PPARs in inflammation and immunity. *Nature Reviews Immunology*. 2002;2(10):748-759.
36. Gong J-H, Zhang M, Modlin RL, et al. Interleukin-10 downregulates Mycobacterium tuberculosis-induced Th1 responses and CTLA-4 expression. *Infection and immunity*. 1996;64(3):913-918.
37. Li L, Elliott JF, Mosmann TR. IL-10 inhibits cytokine production, vascular leakage, and swelling during T helper 1 cell-induced delayed-type hypersensitivity. *The Journal of Immunology*. 1994;153(9):3967-3978.
38. O'Leary Sn, O'Sullivan MP, Keane J. IL-10 blocks phagosome maturation in Mycobacterium tuberculosis–infected human macrophages. *American journal of respiratory cell and molecular biology*. 2011;45(1):172-180.
39. Schottelius AJ, Mayo MW, Sartor RB, Baldwin AS. Interleukin-10 signaling blocks inhibitor of κB kinase activity and nuclear factor κB DNA binding. *Journal of Biological Chemistry*. 1999;274(45):31868-31874.

40. Chen Z-m, O'Shaughnessy MJ, Gramaglia I, et al. IL-10 and TGF-β induce alloreactive CD4+ CD25−T cells to acquire regulatory cell function. *Blood*. 2003;101(12):5076-5083.
41. Mayer-Barber KD, Andrade BB, Barber DL, et al. Innate and adaptive interferons suppress IL-1α and IL-1β production by distinct pulmonary myeloid subsets during Mycobacterium tuberculosis infection. *Immunity*. 2011;35(6):1023-1034.
42. Stanley SA, Johndrow JE, Manzanillo P, Cox JS. The Type I IFN response to infection with Mycobacterium tuberculosis requires ESX-1-mediated secretion and contributes to pathogenesis. *The Journal of Immunology*. 2007;178(5):3143-3152.
43. Berry MP, Graham CM, McNab FW, et al. An interferon-inducible neutrophil-driven blood transcriptional signature in human tuberculosis. *Nature*. 2010;466(7309):973-977.
44. Lyadova I, Panteleev A. Th1 and Th17 cells in tuberculosis: protection, pathology, and biomarkers. *Mediators of inflammation*. 2015;2015
45. Blauenfeldt T, Petrone L, Del Nonno F, et al. Interplay of DDP4 and IP-10 as a potential mechanism for cell recruitment to tuberculosis lesions. *Frontiers in immunology*. 2018;9:1456.
46. Weiss G, Schaible UE. Macrophage defense mechanisms against intracellular bacteria. *Immunological reviews*. 2015;264(1):182-203.
47. Witowski J, Pawlaczyk K, Breborowicz A, et al. IL-17 stimulates intraperitoneal neutrophil infiltration through the release of GROα chemokine from mesothelial cells. *The Journal of Immunology*. 2000;165(10):5814-5821.
48. Crowle AJ, Dahl R, Ross E, May MH. Evidence that vesicles containing living, virulent Mycobacterium tuberculosis or Mycobacterium avium in cultured human macrophages are not acidic. *Infection and immunity*. 1991;59(5):1823-1831.
49. Armstrong J, Hart PDA. Response of cultured macrophages to Mycobacterium tuberculosis, with observations on fusion of lysosomes with phagosomes. *The Journal of experimental medicine*. 1971;134(3):713-740.
50. Myrvik QN, Leake E, Wright M. Disruption of phagosomal membranes of normal alveolar macrophages by the H37Rv strain of Mycobacterium tuberculosis. A correlate of virulence. *The American review of respiratory disease*. 1984;129(2):322-328.
51. Gallegos AM, Pamer EG, Glickman MS. Delayed protection by ESAT-6–specific effector CD4+ T cells after airborne M. tuberculosis infection. *The Journal of experimental medicine*. 2008;205(10):2359-2368.
52. Bussi C, Gutierrez MG. Mycobacterium tuberculosis infection of host cells in space and time. *FEMS Microbiology Reviews*. 2019;43(4):341-361.
53. Bach H, Papavinasasundaram KG, Wong D, Hmama Z, Av-Gay Y. Mycobacterium tuberculosis virulence is mediated by PtpA dephosphorylation of human vacuolar protein sorting 33B. *Cell host & microbe*. 2008;3(5):316-322.
54. Vergne I, Chua J, Lee H-H, Lucas M, Belisle J, Deretic V. Mechanism of phagolysosome biogenesis block by viable Mycobacterium tuberculosis. *Proceedings of the National Academy of Sciences*. 2005;102(11):4033-4038.
55. Wong D, Bach H, Sun J, Hmama Z, Av-Gay Y. Mycobacterium tuberculosis protein tyrosine phosphatase (PtpA) excludes host vacuolar-H+−ATPase to inhibit phagosome acidification. *Proceedings of the National Academy of Sciences*. 2011;108(48):19371-19376.
56. Queval CJ, Song O-R, Carralot J-P, et al. Mycobacterium tuberculosis controls phagosomal acidification by targeting CISH-mediated signaling. *Cell reports*. 2017;20(13):3188-3198.
57. Houben D, Demangel C, Van Ingen J, et al. ESX-1-mediated translocation to the cytosol controls virulence of mycobacteria. *Cellular microbiology*. 2012;14(8):1287-1298.
58. Ivashkiv LB, Donlin LT. Regulation of type I interferon responses. *Nature Reviews Immunology*. 2014;14(1):36-49.
59. Reiley WW, Calayag MD, Wittmer ST, et al. ESAT-6-specific CD4 T cell responses to aerosol Mycobacterium tuberculosis infection are initiated in the mediastinal lymph nodes. *Proceedings of the National Academy of Sciences*. 2008;105(31):10961-10966.

60. Ho AW, Prabhu N, Betts RJ, et al. Lung CD103+ dendritic cells efficiently transport influenza virus to the lymph node and load viral antigen onto MHC class I for presentation to CD8 T cells. *The Journal of Immunology*. 2011;187(11):6011-6021.
61. Noss EH, Pai RK, Sellati TJ, et al. Toll-like receptor 2-dependent inhibition of macrophage class II MHC expression and antigen processing by 19-kDa lipoprotein of Mycobacterium tuberculosis. *The Journal of immunology*. 2001;167(2):910-918.
62. Fortune SM, Solache A, Jaeger A, et al. Mycobacterium tuberculosis inhibits macrophage responses to IFN-γ through myeloid differentiation factor 88-dependent and-independent mechanisms. *The Journal of Immunology*. 2004;172(10):6272-6280.
63. Chelen CJ, Fang Y, Freeman GJ, et al. Human alveolar macrophages present antigen ineffectively due to defective expression of B7 costimulatory cell surface molecules. *The Journal of clinical investigation*. 1995;95(3):1415-1421.
64. Urdahl K, Shafiani S, Ernst J. Initiation and regulation of T-cell responses in tuberculosis. *Mucosal immunology*. 2011;4(3):288-293.
65. Moraco AH, Kornfeld H. Cell death and autophagy in tuberculosis. Elsevier; 2014:497-511.
66. Lee J, Hartman M, Kornfeld H. Macrophage apoptosis in tuberculosis. *Yonsei medical journal*. 2009;50(1):1-11.
67. Kornfeld H, Mancino G, Colizzi V. The role of macrophage cell death in tuberculosis. *Cell Death & Differentiation*. 1999;6(1):71-78.
68. Fratazzi C, Arbeit RD, Carini C, Remold HG. Programmed cell death of Mycobacterium avium serovar 4-infected human macrophages prevents the mycobacteria from spreading and induces mycobacterial growth inhibition by freshly added, uninfected macrophages. *The Journal of Immunology*. 1997;158(9):4320-4327.
69. Schaible UE, Winau F, Sieling PA, et al. Apoptosis facilitates antigen presentation to T lymphocytes through MHC-I and CD1 in tuberculosis. *Nature medicine*. 2003;9(8):1039-1046.
70. Behar S, Martin C, Booty M, et al. Apoptosis is an innate defense function of macrophages against Mycobacterium tuberculosis. *Mucosal immunology*. 2011;4(3):279-287.
71. Hinchey J, Lee S, Jeon BY, et al. Enhanced priming of adaptive immunity by a proapoptotic mutant of Mycobacterium tuberculosis. *The Journal of clinical investigation*. 2007;117(8):2279-2288.
72. Beckwith KS, Beckwith MS, Ullmann S, et al. Plasma membrane damage causes NLRP3 activation and pyroptosis during Mycobacterium tuberculosis infection. *Nature communications*. 2020;11(1):1-18.
73. Amaral EP, Costa DL, Namasivayam S, et al. A major role for ferroptosis in Mycobacterium tuberculosis–induced cell death and tissue necrosis. *Journal of Experimental Medicine*. 2019;216(3):556-570.
74. Pajuelo D, Gonzalez-Juarbe N, Tak U, Sun J, Orihuela CJ, Niederweis M. NAD+ depletion triggers macrophage necroptosis, a cell death pathway exploited by Mycobacterium tuberculosis. *Cell reports*. 2018;24(2):429-440.
75. Stutz MD, Ojaimi S, Allison C, et al. Necroptotic signaling is primed in Mycobacterium tuberculosis-infected macrophages, but its pathophysiological consequence in disease is restricted. *Cell Death & Differentiation*. 2018;25(5):951-965.
76. Murphy JM, Czabotar PE, Hildebrand JM, et al. The pseudokinase MLKL mediates necroptosis via a molecular switch mechanism. *Immunity*. 2013;39(3):443-453.
77. Pechkovsky D, Zalutskaya O, Ivanov G, Misuno N. Calprotectin (MRP8/14 protein complex) release during mycobacterial infection in vitro and in vivo. *FEMS Immunology & Medical Microbiology*. 2000;29(1):27-33.
78. Dragset MS, Poce G, Alfonso S, et al. A novel antimycobacterial compound acts as an intracellular iron chelator. *Antimicrobial agents and chemotherapy*. 2015;59(4):2256-2264.
79. Dixon SJ, Stockwell BR. The role of iron and reactive oxygen species in cell death. *Nature chemical biology*. 2014;10(1):9-17.

80. Hornung V, Ablasser A, Charrel-Dennis M, et al. AIM2 recognizes cytosolic dsDNA and forms a caspase-1-activating inflammasome with ASC. *Nature*. 2009;458(7237):514-518.
81. Robinson N, Ganesan R, Hegedűs C, Kovács K, Kufer TA, Virág L. Programmed necrotic cell death of macrophages: Focus on pyroptosis, necroptosis, and parthanatos. *Redox biology*. 2019;26:101239.
82. Muñoz-Planillo R, Kuffa P, Martínez-Colón G, Smith BL, Rajendiran TM, Núñez G. K+ efflux is the common trigger of NLRP3 inflammasome activation by bacterial toxins and particulate matter. *Immunity*. 2013;38(6):1142-1153.
83. Hornung V, Bauernfeind F, Halle A, et al. Silica crystals and aluminum salts activate the NALP3 inflammasome through phagosomal destabilization. *Nature immunology*. 2008;9(8):847-856.
84. Zhou R, Yazdi AS, Menu P, Tschopp J. A role for mitochondria in NLRP3 inflammasome activation. *Nature*. 2011;469(7329):221-225.
85. Shi J, Zhao Y, Wang K, et al. Cleavage of GSDMD by inflammatory caspases determines pyroptotic cell death. *Nature*. 2015;526(7575):660-665.
86. Welin A, Eklund D, Stendahl O, Lerm M. Human macrophages infected with a high burden of ESAT-6-expressing M. tuberculosis undergo caspase-1-and cathepsin B-independent necrosis. *PloS one*. 2011;6(5):e20302.
87. Tobin DM, Roca FJ, Oh SF, et al. Host genotype-specific therapies can optimize the inflammatory response to mycobacterial infections. *Cell*. 2012;148(3):434-446.
88. Dorhoi A, Kaufmann SH. Pathology and immune reactivity: understanding multidimensionality in pulmonary tuberculosis. Springer; 2016:153-166.
89. Arora G, Misra R, Sajid A. Model systems for pulmonary infectious diseases: paradigms of anthrax and tuberculosis. *Current Topics in Medicinal Chemistry*. 2017;17(18):2077-2099.
90. Jung J-Y, Madan-Lala R, Georgieva M, et al. The intracellular environment of human macrophages that produce nitric oxide promotes growth of mycobacteria. *Infection and immunity*. 2013;81(9):3198-3209.
91. Schroder K, Irvine KM, Taylor MS, et al. Conservation and divergence in Toll-like receptor 4-regulated gene expression in primary human versus mouse macrophages. *Proceedings of the National Academy of Sciences*. 2012;109(16):E944-E953.
92. Maxwell KG, Millman JR. Applications of iPSC-derived beta cells from patients with diabetes. *Cell Reports Medicine*. 2021;2(4):100238.
93. Wilgenburg Bv, Browne C, Vowles J, Cowley SA. Efficient, long term production of monocyte-derived macrophages from human pluripotent stem cells under partly-defined and fully-defined conditions. *PloS one*. 2013;8(8):e71098.
94. Patro R, Duggal G, Kingsford C. Salmon: accurate, versatile and ultrafast quantification from RNA-seq data using lightweight-alignment. 2015;
95. Soneson C, Love MI, Robinson MD. Differential analyses for RNA-seq: transcript-level estimates improve gene-level inferences. *F1000Research*. 2015;4
96. R Core Team. R: A language and environment for statistical computing. 2013;
97. Chen Y, Lun AT, Smyth GK. From reads to genes to pathways: differential expression analysis of RNA-Seq experiments using Rsubread and the edgeR quasi-likelihood pipeline. *F1000Research*. 2016;5
98. Dillies M-A, Rau A, Aubert J, et al. A comprehensive evaluation of normalization methods for Illumina high-throughput RNA sequencing data analysis. *Briefings in bioinformatics*. 2013;14(6):671-683.
99. Robinson MD, McCarthy DJ, Smyth GK. edgeR: a Bioconductor package for differential expression analysis of digital gene expression data. *Bioinformatics*. 2010;26(1):139-140.
100. Robinson MD, Oshlack A. A scaling normalization method for differential expression analysis of RNA-seq data. *Genome biology*. 2010;11(3):1-9.
101. Wu T, Hu E, Xu S, et al. clusterProfiler 4.0: A universal enrichment tool for interpreting omics data. *The Innovation*. 2021;2(3):100141.
102. Gu Z, Eils R, Schlesner M. Complex heatmaps reveal patterns and correlations in multidimensional genomic data. *Bioinformatics*. 2016;32(18):2847-2849.

103. Ritchie ME, Phipson B, Wu D, et al. limma powers differential expression analyses for RNA-sequencing and microarray studies. *Nucleic acids research*. 2015;43(7):e47-e47.
104. Langfelder P, Horvath S. WGCNA: an R package for weighted correlation network analysis. *BMC bioinformatics*. 2008;9(1):1-13.
105. Yu G. enrichplot: visualization of functional enrichment result. R package version 1.14. 2, 2022. 2021.
106. Luo W, Brouwer C. Pathview: an R/Bioconductor package for pathway-based data integration and visualization. *Bioinformatics*. 2013;29(14):1830-1831.
107. Baena A, Porcelli SA. Evasion and subversion of antigen presentation by Mycobacterium tuberculosis. *Tissue antigens*. 2009;74(3):189-204.
108. Pedrera L, Espiritu RA, Ros U, et al. Ferroptotic pores induce Ca2+ fluxes and ESCRT-III activation to modulate cell death kinetics. *Cell Death & Differentiation*. 2021;28(5):1644-1657.
109. Weinberg JM, Bienholz A, Venkatachalam M. The role of glycine in regulated cell death. *Cellular and Molecular Life Sciences*. 2016;73(11):2285-2308.
110. Zhao A, Wu Z-Q, Pollack M, Rollwagen FM, Hirszel P, Zhou X. Disulfiram inhibits TNF-α-induced cell death. *Cytokine*. 2000;12(9):1356-1367.
111. Hu JJ, Liu X, Xia S, et al. FDA-approved disulfiram inhibits pyroptosis by blocking gasdermin D pore formation. *Nature immunology*. 2020;21(7):736-745.
112. Yamamoto M, Takeda K, Akira S. TIR domain-containing adaptors define the specificity of TLR signaling. *Molecular immunology*. 2004;40(12):861-868.
113. Brightbill HD, Libraty DH, Krutzik SR, et al. Host defense mechanisms triggered by microbial lipoproteins through toll-like receptors. *Science*. 1999;285(5428):732-736.
114. Drage MG, Pecora ND, Hise AG, et al. TLR2 and its co-receptors determine responses of macrophages and dendritic cells to lipoproteins of Mycobacterium tuberculosis. *Cellular immunology*. 2009;258(1):29-37.
115. Schlesinger L, Bellinger-Kawahara C, Payne N, Horwitz M. Phagocytosis of Mycobacterium tuberculosis is mediated by human monocyte complement receptors and complement component C3. *The Journal of Immunology*. 1990;144(7):2771-2780.
116. Kang PB, Azad AK, Torrelles JB, et al. The human macrophage mannose receptor directs Mycobacterium tuberculosis lipoarabinomannan-mediated phagosome biogenesis. *The Journal of experimental medicine*. 2005;202(7):987-999.
117. Wileman TE, Lennartz MR, Stahl PD. Identification of the macrophage mannose receptor as a 175-kDa membrane protein. *Proceedings of the National Academy of Sciences*. 1986;83(8):2501-2505.
118. Volpe E, Cappelli G, Grassi M, et al. Gene expression profiling of human macrophages at late time of infection with Mycobacterium tuberculosis. *Immunology*. 2006;118(4):449-460.
119. Silver RF, Walrath J, Lee H, et al. Human alveolar macrophage gene responses to Mycobacterium tuberculosis strains H37Ra and H37Rv. *American journal of respiratory cell and molecular biology*. 2009;40(4):491-504.
120. Teles RM, Graeber TG, Krutzik SR, et al. Type I interferon suppresses type II interferon–triggered human anti-mycobacterial responses. *Science*. 2013;339(6126):1448-1453.
121. Divangahi M, King IL, Pernet E. Alveolar macrophages and type I IFN in airway homeostasis and immunity. *Trends in immunology*. 2015;36(5):307-314.
122. Pandey AK, Yang Y, Jiang Z, et al. NOD2, RIP2 and IRF5 play a critical role in the type I interferon response to Mycobacterium tuberculosis. *PLoS pathogens*. 2009;5(7):e1000500.
123. Collins AC, Cai H, Li T, et al. Cyclic GMP-AMP synthase is an innate immune DNA sensor for Mycobacterium tuberculosis. *Cell host & microbe*. 2015;17(6):820-828.
124. Manca C, Tsenova L, Freeman S, et al. Hypervirulent M. tuberculosis W/Beijing strains upregulate type I IFNs and increase expression of negative regulators of the Jak-Stat pathway. *Journal of Interferon & Cytokine Research*. 2005;25(11):694-701.

125. Dorhoi A, Yeremeev V, Nouailles G, et al. Type I IFN signaling triggers immunopathology in tuberculosis-susceptible mice by modulating lung phagocyte dynamics. *European journal of immunology*. 2014;44(8):2380-2393.
126. Moreira-Teixeira L, Sousa J, McNab FW, et al. Type I IFN inhibits alternative macrophage activation during Mycobacterium tuberculosis infection and leads to enhanced protection in the absence of IFN-γ signaling. *The Journal of Immunology*. 2016;197(12):4714-4726.
127. Mayer-Barber KD, Andrade BB, Oland SD, et al. Host-directed therapy of tuberculosis based on interleukin-1 and type I interferon crosstalk. *Nature*. 2014;511(7507):99-103.
128. Ng CT, Mendoza JL, Garcia KC, Oldstone MB. Alpha and beta type 1 interferon signaling: passage for diverse biologic outcomes. *Cell*. 2016;164(3):349-352.
129. Verreck FA, de Boer T, Langenberg DM, et al. Human IL-23-producing type 1 macrophages promote but IL-10-producing type 2 macrophages subvert immunity to (myco) bacteria. *Proceedings of the National Academy of Sciences*. 2004;101(13):4560-4565.
130. Harding CV, Boom WH. Regulation of antigen presentation by Mycobacterium tuberculosis: a role for Toll-like receptors. *Nature Reviews Microbiology*. 2010;8(4):296-307.
131. Hestvik ALK, Hmama Z, Av-Gay Y. Mycobacterial manipulation of the host cell. *FEMS microbiology reviews*. 2005;29(5):1041-1050.
132. Desvignes L, Ernst JD. Interferon-γ-responsive nonhematopoietic cells regulate the immune response to Mycobacterium tuberculosis. *Immunity*. 2009;31(6):974-985.
133. Zhu J, Yamane H, Paul WE. Differentiation of effector CD4 T cell populations. *Annual review of immunology*. 2009;28:445-489.
134. Apetoh L, Quintana FJ, Pot C, et al. The aryl hydrocarbon receptor interacts with c-Maf to promote the differentiation of type 1 regulatory T cells induced by IL-27. *Nature immunology*. 2010;11(9):854-861.
135. Dorhoi A, Kaufmann SH. Perspectives on host adaptation in response to Mycobacterium tuberculosis: modulation of inflammation. Elsevier; 2014:533-542.
136. Aggarwal S, Ghilardi N, Xie M-H, de Sauvage FJ, Gurney AL. Interleukin-23 promotes a distinct CD4 T cell activation state characterized by the production of interleukin-17. *Journal of Biological Chemistry*. 2003;278(3):1910-1914.
137. Velmurugan K, Chen B, Miller JL, et al. Mycobacterium tuberculosis nuoG is a virulence gene that inhibits apoptosis of infected host cells. *PLoS pathogens*. 2007;3(7):e110.
138. Wang Q, Liu S, Tang Y, Liu Q, Yao Y. MPT64 protein from Mycobacterium tuberculosis inhibits apoptosis of macrophages through NF-kB-miRNA21-Bcl-2 pathway. *PloS one*. 2014;9(7):e100949.
139. Danelishvili L, McGarvey J, Li Yj, Bermudez LE. Mycobacterium tuberculosis infection causes different levels of apoptosis and necrosis in human macrophages and alveolar epithelial cells. *Cellular microbiology*. 2003;5(9):649-660.
140. Conte D, Holcik M, Lefebvre CA, et al. Inhibitor of apoptosis protein cIAP2 is essential for lipopolysaccharide-induced macrophage survival. *Molecular and cellular biology*. 2006;26(2):699-708.
141. Micheau O, Lens S, Gaide O, Alevizopoulos K, Tschopp Jr. NF-κB signals induce the expression of c-FLIP. *Molecular and cellular biology*. 2001;21(16):5299-5305.
142. Wang C-Y, Guttridge DC, Mayo MW, Baldwin Jr AS. NF-κB induces expression of the Bcl-2 homologue A1/Bfl-1 to preferentially suppress chemotherapy-induced apoptosis. *Molecular and cellular biology*. 1999;19(9):5923-5929.
143. Suen D-F, Norris KL, Youle RJ. Mitochondrial dynamics and apoptosis. *Genes & development*. 2008;22(12):1577-1590.
144. Newton K. RIPK1 and RIPK3: critical regulators of inflammation and cell death. *Trends in cell biology*. 2015;25(6):347-353.
145. Robinson N, McComb S, Mulligan R, Dudani R, Krishnan L, Sad S. Type I interferon induces necroptosis in macrophages during infection with Salmonella enterica serovar Typhimurium. *Nature immunology*. 2012;13(10):954-962.

146. Tang D, Kroemer G. Ferroptosis. *Current Biology*. 2020;30(21):R1292-R1297.
147. Li J, Cao F, Yin H-l, et al. Ferroptosis: past, present and future. *Cell death & disease*. 2020;11(2):1-13.
148. Jiang L, Hickman JH, Wang S-J, Gu W. Dynamic roles of p53-mediated metabolic activities in ROS-induced stress responses. *Cell cycle*. 2015;14(18):2881-2885.
149. Ou Y, Wang S-J, Li D, Chu B, Gu W. Activation of SAT1 engages polyamine metabolism with p53-mediated ferroptotic responses. *Proceedings of the National Academy of Sciences*. 2016;113(44):E6806-E6812.
150. Xing Y, Yao X, Li H, et al. Cutting edge: TRAF6 mediates TLR/IL-1R signaling–induced nontranscriptional priming of the NLRP3 inflammasome. *The Journal of Immunology*. 2017;199(5):1561-1566.
151. Bauernfeind FG, Horvath G, Stutz A, et al. Cutting edge: NF-κB activating pattern recognition and cytokine receptors license NLRP3 inflammasome activation by regulating NLRP3 expression. *The Journal of Immunology*. 2009;183(2):787-791.
152. Schurch NJ, Schofield P, Gierliński M, et al. How many biological replicates are needed in an RNA-seq experiment and which differential expression tool should you use? *Rna*. 2016;22(6):839-851.

6 Appendix

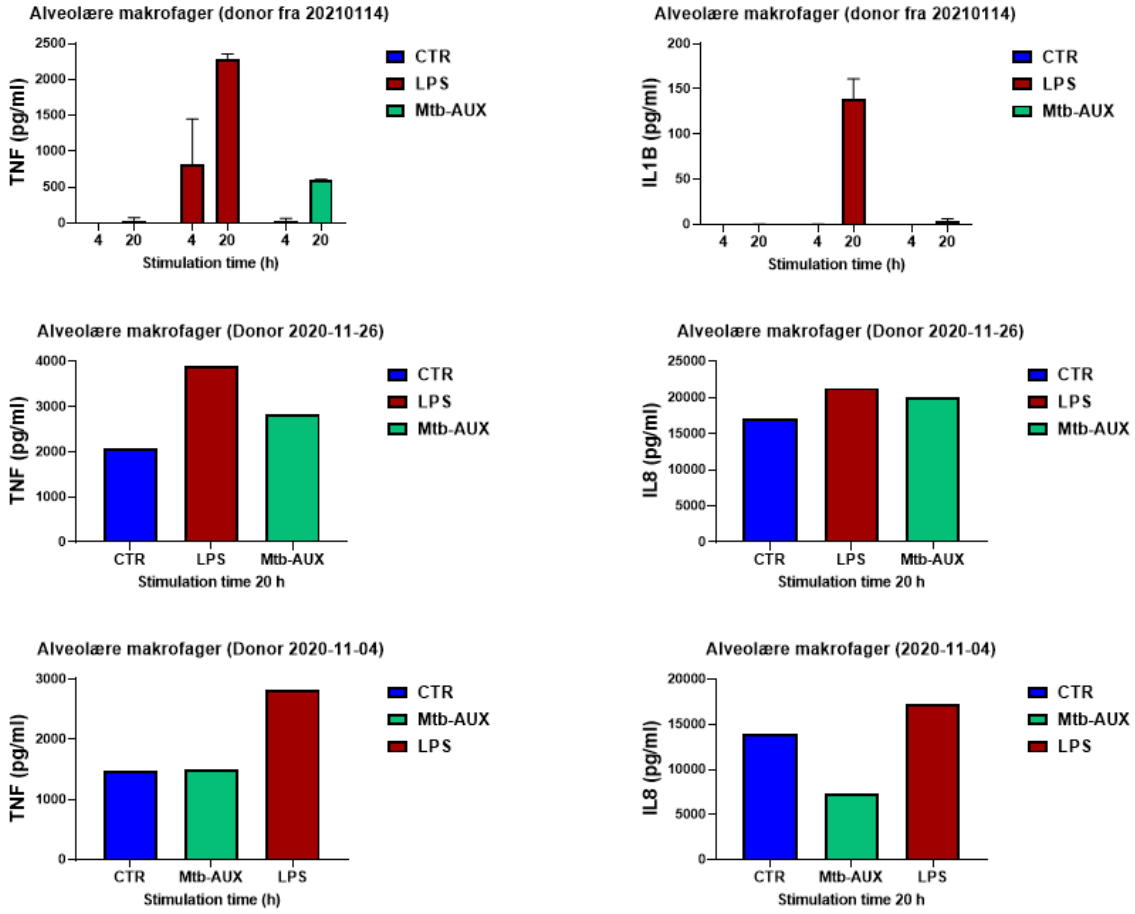

Appendix Figure 1. Donor 2020-11-26 and 2020-11-04 show high expression of TNF and IL-8 in control samples.

TNF, IL-1b and IL8 ELISA was performed by Dr. Marit Bugge on alveolar macrophages from the three donors used to perform the RNA sequencing infection experiment for this thesis.

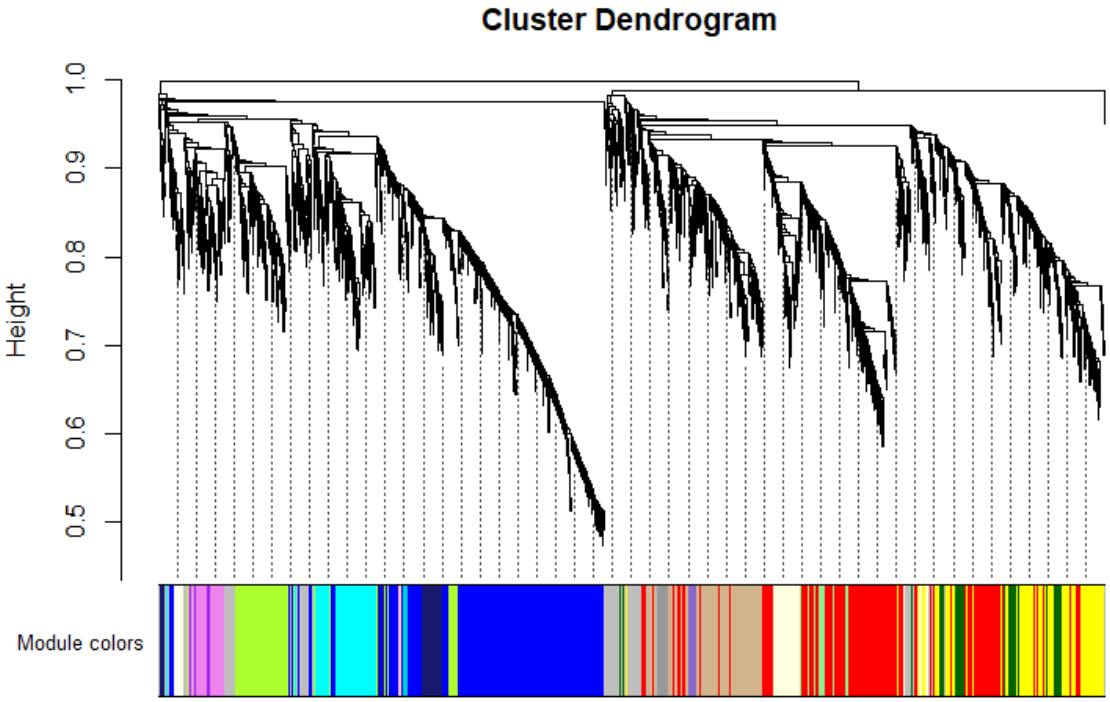

Appendix Figure 2. Hierarchical clustering of WGCNA identified modules.

WGCNA was performed on the mRNA expression data of untreated, Mtb-infected and LPS treated iMACs, MDMs, AMs and THP1 cells to identify 50 modules of co-expressed genes.

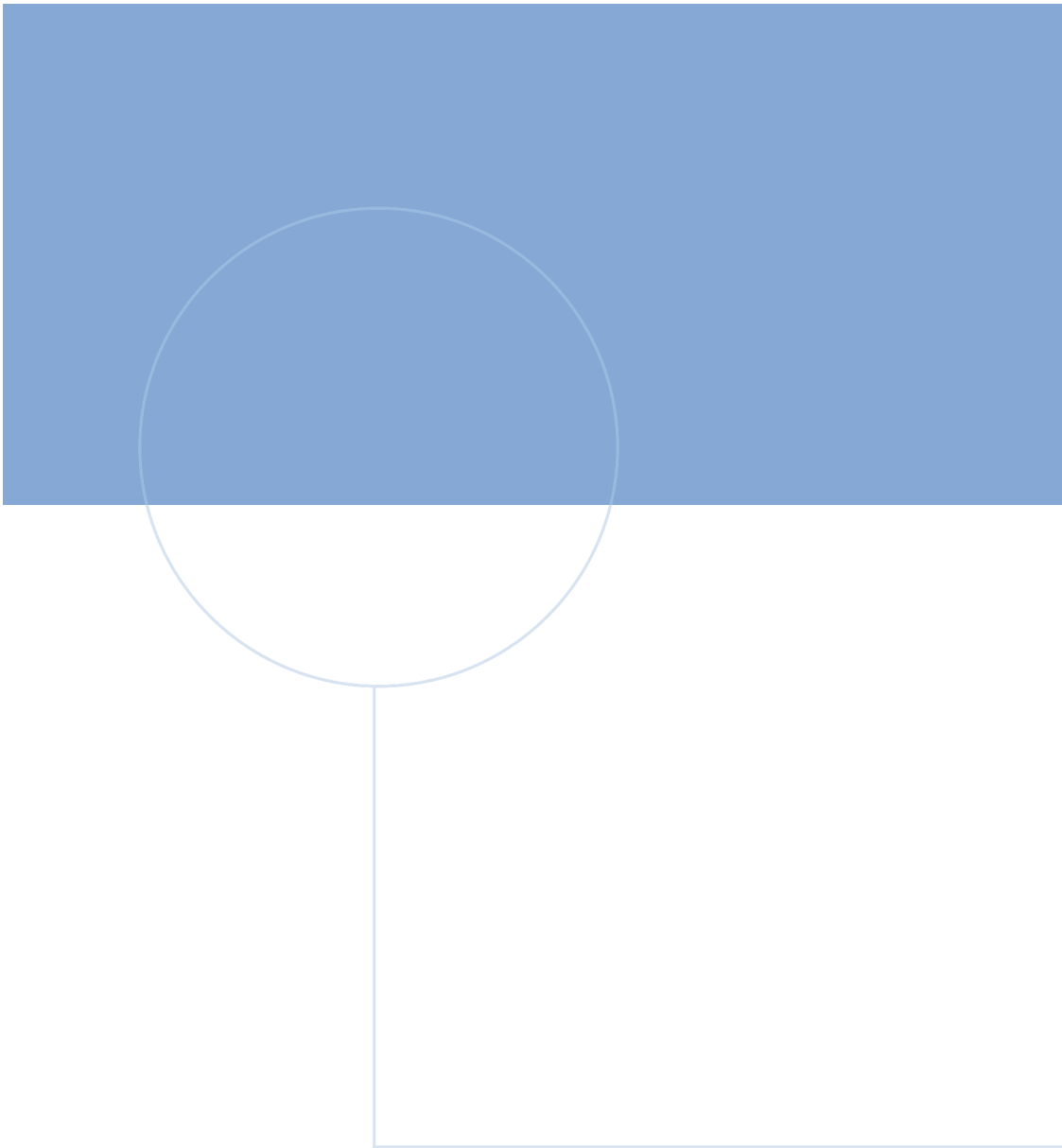

NTNU

Norwegian University of
Science and Technology